JET–R(99)13

THE SCIENCE OF JET

John Wesson

FOREWORD

The idea of writing an account of the achievements of JET in a coherent way for a wider readership arose a few years ago when it became clear that JET as a Joint Undertaking would end in 1999. I was convinced that such a book, if well written, would serve an important purpose not only for JET but for the European Fusion Community at large. I was therefore extremely pleased when John Wesson agreed to attempt this difficult task immediately following his retirement, while the JET history was still fresh in his mind. I am delighted that John has been able to complete the book in time for the farewell celebrations of the Joint Undertaking and that his account makes such interesting reading.

The JET Project truly deserves to be remembered and honoured in this way. It is fair to say that JET has been one of the most successful joint ventures in Europe, not only from a scientific point of view but also as one of the most efficient organisations in Big Science. Here I would like to record our debt to the founding fathers of JET: Donato Palumbo, the then Director of Fusion in the European Commission, who used his great perseverance and immense diplomatic skill to steer this large project through all obstacles to its approval in 1978. Hans-Otto Wüster, the first Director of JET, who successfully set up the complex administrative, scientific and engineering structure of the project and fostered such a splendid team spirit among its staff. And finally his successor as Director, Paul-Henri Rebut, who must be remembered both for his vision and drive in the design and construction of this great machine and for his contributions to its scientific success. They have all shown themselves to be men of great foresight, courage and dedication.

JET has been a major step en route to a fusion reactor, linking the specialised medium size tokamaks of the 70's and 80's to the Next Step (ITER) which calls for a plasma dominated by alpha particle effects and maintained for 1000 seconds or steady state. With its D-shaped plasma cross-section, which later was combined with a divertor, its plasma volume of 100 cubic metres, its plasma current of several mega-amperes and its tritium and remote handling capabilities, the JET machine broke completely new ground. As a result JET was able to take fusion research a large step forward, bringing us to the point where the physics can be extrapolated to a reactor with confidence.

On a personal note I should add that I have felt truly privileged to be associated with scientists and engineers from all over Europe working like a big close-knit family towards the common goal of making the dream of controlled fusion become reality. Working with this team of dedicated and able staff, both as physicist and Director, has certainly been the culmination of my professional career.

I hope that this book will communicate to many people inside and outside fusion some of the scientific excitement that we experienced in bringing about the great success of this unique European Joint Undertaking.

M. Keilhacker

November 1999

PREFACE

Can we produce useful power from the fusion of the nuclei of the light elements?.This question has driven a massive international research effort which has now provided sufficient understanding a allow the design of a fusion reactor. The research carried out on JET, the Joint European Torus, which is the world's largest fusion experiment, has received worldwide acclaim.Its success is the result of the devotion of the scientists and engineers involved, their efforts.being repaid by the excitement which comes from working at the frontiers of knowledge with an excellent experimental facility which allows the discovery of new results.

Following the pattern of modern science, new results from the JET experiments were quickly made available to other researchers at regular meetings and conferences. The more important of the research papers finally appearing as articles in the scientific journals. Through this process the results from JET are scattered over a variety of conference proceedings and embedded in many bound volumes of journals. The purpose of the present book is to bring together the contributions of those involved and to give a coherent account of the scientific achievements from JET.

During the writing I have been asked many times, "for what type of reader is the book intended?" It is not simple to answer this question because I have in mind different types of readers.Firstly, I would like JET scientists themselves to find some satisfaction from seeing the "JET story" put together. Then I would hope that newcomers to the subject will find it useful to learn what has gone before. And finally it would be rewarding if the book found a wider readership both inside and outside the fusion community.

In an attempt to fulfil this broad ambition the book starts with a simple introduction to fusion research and progressively introduces the concepts required for an appreciation of the scientific advances coming from JET. Thus the technical level increases with successive chapters.After the introductory chapters we come to the early JET experiments, and these lead to the core aspects of the research - stability, plasma confinement, interaction between the plasma and the neighbouring material surfaces, and basic physics. In the penultimate chapter we reach the high point - the production of the thermonuclear power. The final chapter then gives an overview and assessment of the JET research, and measures the achievements against the aims declared at the outset of the undertaking.

I do not know how it will appear to the reader but, as one who has been involved in the research from the early days, I am very impressed by the progress made. Personally, I have found encouragement in the confidence and dynamism of my colleagues and have been full of admiration for the remarkable technical developments, the outstanding improvements in diagnostic techniques, and the theoretical advances inspired by the experimental results, all of which have contributed to the success of JET.My hope now is that fusion research will continue with the same imaginative commitment.

I must record my indebtedness to my colleagues. No matter what aspects of the work I was dealing with, I was always able to turn to very helpful and knowledgeable experts in the JET project to answer my questions. Many colleagues have read parts of the manuscript and detected my errors.I would particularly like to mention those who read the whole draft and have given me their advice - Roy Bickerton, Rob Felton, Alan Gibson, Chris Gowers, MartinK eilhacker, MerviMantsinen, Phil Morgan and Paul Thomas. I must thank Lynda Lee for her patience and care in typing the manuscript, and RogerBasto w for his help in preparing the large number of figures. Finally, I am very much indebted to Stuart Morris for the skill and commitment he has put into preparing the manuscript for printing.

JET, Oxfordshire, England

November 1999 JOHN WESSON

CONTENTS

UNITS

The system of units used is m.k.s. Following the convention generally accepted in the subject, temperatures are written either in joules or in eV (or keV). Thus in place of the conventional kT° (where k is Boltzmann's constant and T° is in degrees Kelvin) we write T (joules), so that T°= T (joules)/1.381 $\times$ 10^{-23}. The temperature in electron-volts is defined by the potential difference in volts through which an electron must fall to acquire an energy T, that is T(eV)=T(joules)/e w here e is the electronic charge. Thus T(eV) = T(joules)/1.602 $\times$ 10^{-19}. Whenever the temperature given is in eV this is explicitly stated.

1. BRINGING THE SUN TO EARTH

JET came into operation in 1983, its purpose being to make a substantial step in the search for a means of obtaining power from nuclear fusion. It had been preceded by a world-wide exploration of the subject which began in the late 1940s. However, the story starts a century earlier with the problem of understanding the sun.

Mankind had always recognised that it owed its survival to the continuous supply of heat and light inexplicably provided by the sun, but the mystery of this provision deepened with the discovery of the law of the conservation of energy. This law meant that the energy radiated by the sun had to be accounted for in terms of an energy source. What could it be?

It is easy to calculate the magnitude of the problem. The power received at the earth is 1.4kilowatts per square metre. Since the sun radiates uniformly in all directions we can calculate the total power emitted by the sun by multiplying this figure by the area of a spherearound the sun, passing through the earth. The radius of this sphere is the distance ofthe ear th from the sun, 150 million kilometres, and so the area of our sphere ($4\pi r^2$) is 2.8×10^{23} square metres. Multiplying by 1.4 kilowatts per square metre gives the total power, 4×10^{23} kilowatts. When we recall that a typical electricity generating plant produces around 10^6 kilowatts we recognise that the magnitude of the sunÕs output is difficult to conceive.

In the nineteenth century physicists must have been very concerned about the need to provide an answer to this very obvious problem. The only sources of energy they had to call on were chemical energy and gravitational energy. Let us look at these in turn.

In the case of chemical energy it is easy to take a typical fuel, coal say, and imagine it to burn in an oxygen atmosphere. Coal and oxygen have a calorific value of about 10 megajoules per kilogram, and since the mass of the sun was known from its gravitational attraction to be 2×10^{30} kilograms, the maximum energy available from such a source would be 2×10^{31} megajoules. How long would this last at the observed power output of the sun? Dividing the energy by the power output of 4×10^{20} megawatts gives a time of 5×10^{10} seconds, which is about 1,600 years. The biologists believed that evolutionary timescales implied that the earth had existed in essentially the same state for hundreds of millions of years, and the geologists thought the age of the earth was likely to be measured in billions of years. A few thousand years would not do.

The idea of gravitational collapse is that in a contraction of the sun each spherical shell within the sun would move inward under the gravitational force of the mass enclosed by the shell. The work done by this force is then available as heat. If the total power released by such a contraction is equated to the sunÕs heat output it gives a required rate of contraction. This calculation was carried out by Lord Kelvin and by Helmholtz. The problem was that when the contraction was extrapolated back in time, it only provided the requisite power for tens of millions

of years. Furthermore, going back for such a time, the sun would have been so large it would have enveloped the earth. Again this was in conflict with the evidence of the earthÕs antiquity. As the years passed the problem of the sunÕs energy source remained unsolved.

With the development of relativity and nuclear physics in the first two decades of the twentieth century the necessary tools for constructing a satisfactory theory became available, and they were used by Sir Arthur Eddington to guide the thinking toward a solution of the problem. In the 1920s Eddington came to see the sun, and similar stars, as a sphere of hot gas mainly composed of hydrogen. The temperature necessary for the pressure of the gas to balance the inward gravitational forces was around 15 million degrees Kelvin. Eddington conjectured that under these conditions it would be possible for hydrogen nuclei to fuse together, and that if they formed a helium nucleus energy would be released. By that time it was realised that a helium nucleus has less mass than four hydrogen atoms, and relativity predicts that the mass loss Δm would be converted into an energy $E = \Delta mc^2$, where c is the velocity of light.

Although uncertainties remained Eddington was basically correct. His ideas were given a firm theoretical basis by Hans Bethe who, in 1939, showed that various nuclear processes were possible, depending on the precise conditions. In the sun the dominant process starts from hydrogen nuclei, which are simply protons, and proceeds in three stages. In the first stage two protons fuse, releasing a positron and forming a deuteron. This is an extremely slow process, but once the deuteron is formed it lasts only a few seconds before a further proton is added to form the light isotope of helium, He^3. The He^3 nuclei then wait on average for about a million years before two of them fuse to form He^4 with the release of two protrons.

The total energy released in this sequence of reactions is 6×10^8 megajoules per kilogram of hydrogen. This is about 60 million times the energy per kilogram available from chemical fuels.

The realisation that the fusion of light elements could release nuclear energy provided the basis for inventive minds to search for a practical way of producing power.

> A star is drawing on some vast reservoir of energy by means unknown to us. This reservoir can scarcely be other than the sub-atomic energy which, it is known, exists abundantly in all matter; we sometimes dream that man will one day learn how to release it and use it for his service. The store is well-nigh inexhaustible, if only it could be tapped. There is sufficient in the Sun to maintain its output of heat for 15 billion years.
>
> The nucleus of the helium atom, consists of 4 hydrogen atoms bound with 2 electrons. But Aston has further shown conclusively that the mass of the helium atom is less than the sum of the masses of the 4 hydrogen atoms which enter into it. There is a loss of mass in the synthesis amounting to about 1 part in 120, the atomic weight of hydrogen being 1.008 and that of helium just 4. .É We can therefore at once calculate the quantity of energy liberated when helium is made out of hydrogen. If 5 per cent of a starÕs mass consists initially of hydrogen atoms, which are gradually being combined to form more complex elements, the total heat liberated will more than suffice for our demands, and we need look no further for the source of a starÕs energy.
>
> If, indeed, the sub-atomic energy in the stars is being freely used to maintain their great furnaces, it seems to bring a little nearer to fulfillment our dream of controlling this latent power for the well-being of the human raceÑor for its suicide.

Extracts from Eddington's remarkable lecture to the British Association for the Advancement of Science in 1920.

Fusion Reactions

In a practical system the reactions could not proceed at the leisurely rate of those in the sun, where the protons have a one in a million chance of reacting in ten thousand years. However, this problem is readily solved by starting with deuterium, either alone or in a mixture with the heavier hydrogen isotope, tritium.

With deuterium alone there are two fusion reactions, which occur at essentially the same rate. They are

$$D + D \rightarrow He^3 + n + 3.3 \text{ MeV}$$

and

$$D + D \rightarrow T + H + 4.0 \text{ MeV}$$

where D denotes a deuteron, T a triton, H a proton, and n a neutron. The energies given are the total energies released, this energy being the kinetic energy of the reaction products.

With a deuterium-tritium mixture the following reaction also occurs

$$D + T \rightarrow He^4 + n + 17.6 \text{ MeV} ,$$

the He^4 isotope of helium being an α-particle.

The D-T reactions have a much larger cross-section than those for D-D, and so a D-T mixture offers an easier route to power production than pure deuterium.

Even with deuterons and tritons the cross-section for fusion only becomes large enough to be useful at high energies. If the required nuclear reactions were to be generated through the thermal motions of the nuclei, so-called thermonuclear fusion, it would be necessary to achieve extremely high temperatures, probably 100 million degrees K. How this could be done was not clear.

In the sun the high temperature particles are held together by the gravitational force arising from the sunÕs mass. In the absence of gravity the particles would fly apart with their thermal velocities. In a terrestrial vessel particles at the required temperature would escape to the wall in microseconds.

How could these difficulties be overcome?

Plasmas and Magnetic Fields

If the temperature of a gas is raised above about 10,000K virtually all of the atoms become ionised, with electrons becoming separated from their nuclei. The resulting ions and electrons then form two intermixed fluids. However, the electrostatic attraction between their positive and negative charges is so strong that only small charge imbalances are allowed. The result is that the ionised gas remains almost neutral throughout. This constitutes a fourth state of matter called a plasma. We shall see later that a plasma has some of the properties of other states of matter, but also exhibits a wide range of unique features. Fusion research has been largely aimed at understanding very high temperature plasmas, and the subsequent chapters will relate the discoveries that have been made.

We now return to the problem of confining what we can now call the plasma, without the gravitational field available to the sun. Whereas an uncharged atom is unaffected by a magnetic field, the negatively charged electrons and the positively charged nuclei forming the plasma are subject to a magnetic force called the Lorenz force. The Lorenz force turns the motion perpendicular to the magnetic field into a circular motion around a magnetic field line as illustrated in Figure 1.1. This property of a magnetic field provided a crucial step in the early thinking about confining the particles, leaving only the motion along the magnetic field lines to be controlled.

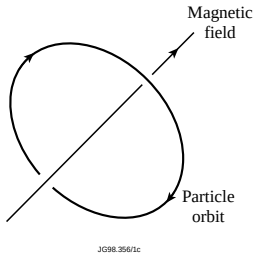

Figure 1.1. In the presence of a magnetic field the motion of a charged particle perpendicular to the field takes the form of a circular orbit.

Early Days

The earliest practical proposals were made by Peter Thonemann and Sir George Thomson. They both had the idea of avoiding ends to the confinement vessel by making it toroidal, or doughnut shaped. The vessel would be filled with hydrogen at a very low pressure and this gas would be converted to a hot plasma by passing an electric current through it around the torus. The magnetic field associated with this current would hold the charged particles away from the walls. In fact the plasma current crossing its own magnetic field would produce an inward force which would ÒpinchÓ the plasma toward the centre of the toroidal tube as illustrated in Figure 1.2.

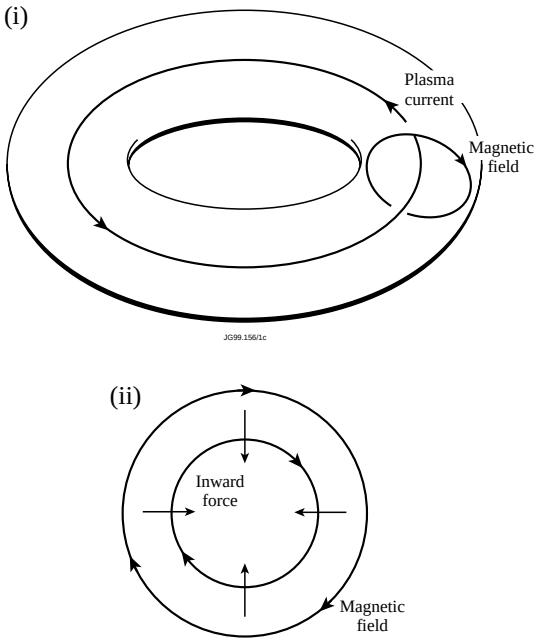

Figure 1.2. The first part shows the direction of the magnetic field associated with the toroidal current passing through the plasma. The current is actually distributed over the plasma cross-section and, being perpendicular to its own magnetic field, produces a radially inward force. This force is illustrated in the second part of the the figure which shows a cross-section of the plasma, the plasma current now being in the direction into the paper.

Experiments of this type were carried out by Alan Ware as a student of Thomson at Imperial College in the late 1940s. His torus had a diameter of 25cm and bore of 3cm, with currents up to 13,000 amps. Later, with Cousins, he observed the pinch effect in a somewhat larger torus with 27,000 amps. Similar experiments in which the plasma was made the secondary winding of a transformer were carried out by Thonemann at the Clarendon Laboratory.

These investigations, which marked the start of fusion research, soon led to an expanded program of research in the United Kingdom with substantial teams of scientists and engineers being formed at Harwell and at the Research Laboratory of the Associated Electrical Industries at Aldermaston. Experiments were also started in the United States.

An important early experiment was carried out at Harwell by Carruthers and Davenport. The toroidal discharges which they produced lasted only for about 100 microseconds, but the torus was made of glass and this allowed them to photograph the plasma. Photographs of one such discharge are reproduced in Figure 1.3. They show how the plasma loses its initial symmetric form, and develops ÒkinksÓ. This result implied that the plasma was unstable, and is the first hint of a problem which was to form one of the main streams of fusion research. In almost all subsequent experiments instability would constrain and limit the achievable plasma conditions.

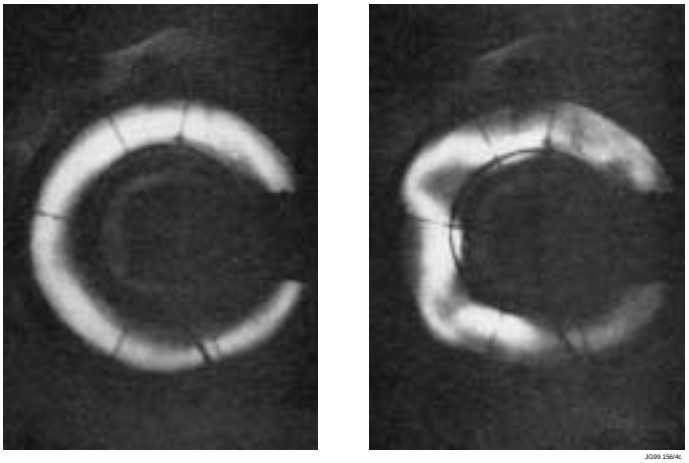

Figure 1.3. Photographs from early pinch experiments showing how the discharge initially forms a symmetric toroidal ring, but then develops a kink instability.

New Ideas

In the 1950s there was a proliferation of designs for confining plasmas with magnetic fields. The early toroidal pinches led to larger experiments including ZETA with a plasma of 50cm minor radius carrying currents of up to a million amps. These pinches were found to be much more stable when a toroidal magnetic field was added.

A related configuration was the stellarator, suggested by Lyman Spitzer, in which the helical form of the magnetic field was achieved by currents in external windings rather than that in the plasma. Another toroidal configuration, the Levitron, had a toroidal current-carrying conductor inside the plasma. Then there were open ended devices including the mirror machine, so-called because the plasma particles were prevented from leaving along the magnetic field through the open ends by reflecting from regions of higher magnetic field.

The ÒtokamakÓ was proposed by Sakharov and Tamm and developed in the Soviet Union. It is a close relative of the toroidal pinch configuration, differing from it by having a larger toroidal magnetic field, and it is to this tokamak family that JET belongs.

A Bleak Period

In the late 1950s the ZETA experiment was operated with a deuterium plasma in an attempt to produce fusion reactions between the deuterons. In one of the two types of D-D reaction neutrons are produced. Being unaffected by the magnetic field, such neutrons could be detected outside the plasma vessel. In fact ZETA produced neutrons, but it was shown by studying the neutrons that they had been predominantly produced by accelerated deuterons, and not through the thermal motions of heated deuterons as had been intended. The precise explanation of the mechanism

has never come to light, but the non-thermonuclear origin of the neutrons certainly cast a shadow over the results.

A wide variety of configurations was explored in the 1960s, but the outcome was not encouraging. Each confinement system was found to be subject to instabilities, which either destroyed the configuration or led to a deterioration of the plasma confinement.

It is probable that the gloom of this period was not really justified. The expectation had been of rapid progress and it took some time to adjust to the longer timescale required to reach a thermonuclear reactor.

The way forward was shown by the tokamak experiments. Having a higher toroidal magnetic field for a given plasma current, this configuration precludes the worst instabilities of the pinch, and allows a comparatively quiescent plasma. In addition, the interaction of the plasma with the wall was carefully controlled. By the late 1960s the Soviet tokamak programme, under the guidance of Lev Artsimovitch, had started to produce impressive results, including the achievement of temperatures around 10 million K.

We shall return to the development of tokamaks, and the JET experiment, shortly but first we need to take a little time to look at some basic plasma physics.

Bibliography

It was clear to the pioneers that there were difficult problems to be solved if useful thermonuclear power was to be achieved. The required temperature alone seemed formidable. In 1949 Gamow and Critchfield, in their book on the Atomic Nucleus and Nuclear Energy Sources, expressed the opinion that ÒIt goes without saying that the problem of obtaining such high temperatures [10 million degrees] on earth is of almost unsurpassable technical difficultyÓ (page 268).

The early history of scientific developments is rarely straightforward, and fusion research is no different. Reasonable claims to early contributions can be made by a number of people. However, the first reported directly relevant experiment seems to be that by Cousins and Ware at Imperial College. Their paper, which reports toroidal experiments with evidence of the pinch effect, is in the Proceedings of the Physical Society, B64, 159 (1951). The photographs of instabilities by Carruthers and Davenport shown in Figure 1.3 are from the Proceedings of the Physical Society B70, 49 (1957).

Until 1958 the main experimental work was secret. The opening up of the subject in January of that year was marked by the publication in Nature of the experimental work by several groups, most notably that working on ZETA. In the following year a United Nations Conference in Geneva brought together a large variety of Òstate of the artÓ developments from several countries. These are published in the Proceedings of the Second United Nations Conference of the Peaceful Uses of Atomic Energy, Volumes 31 and 32 (1959). From then onwards international collaboration was to be an outstanding feature of fusion research.

2. SOME PLASMA PHYSICS

As already described, if a gas is heated sufficiently the force binding the electrons in the atoms is overcome and electrons are separated from the atom. The remaining atom is deficient in electrons and forms a positive ion. For any species of atom there will be a plasma temperature above which all the atoms have lost an electron, and the gas is then said to be fully ionised. In the case of the hydrogen isotopes, hydrogen, deuterium and tritium, the atom has only one electron, and consequently they become fully ionised at a comparatively low temperature.

The plasma can be thought of in two basic ways, both of which are useful. In the first we can ask how individual electrons and ions behave. In particular it is of great importance that their motion is dominated by the effect of a magnetic field. The second way is to regard the electrons and ions as forming fluids. The electron and ion fluids then have their separate temperatures and pressures. They also have other properties familiar from normal gases, such as viscosity and thermal conductivity. It is sometimes convenient to think of the electrons and ions as jointly forming a single fluid and, in particular, the single fluid model provides the simplest approach to analysing stability.

Before looking at the specific properties of the plasma it is useful to obtain some feel for the magnitudes involved with the plasmas of interest.

The plasma densities are most easily appreciated by a comparison with the density of molecules in the atmosphere. This is about 3×10^{25} molecules per cubic metre. The plasmas we shall discuss will have electron and ion densities of a few times 10^{19} per cubic metre. That is, the densities are about one millionth of the atmospheric density. The mass density is correspondingly small. Whereas a cubic metre of air weighs roughly a kilogram, a typical JET plasma, with a volume of 100 cubic metres, weighs only as much as a postage stamp.

The required temperatures on the other hand are impressively high, higher than at the centre of the sun. They need to be high because the rate at which the desired fusion reactions occur is very low at low temperatures. The target temperature for a fusion reactor is in the range 100-200 million degrees. At such temperatures the reaction rate for a deuterium - tritium mixture is 40,000 times higher than at “only” 10 million degrees.

The temperature of the plasma is just a simple way of describing the average kinetic energy of the particles. Knowing the temperature we can straightforwardly calculate the thermal energy, $^1/_2\ mv^2$, of the particles. Electrons and ions at the same temperature have the same energy but, because the electrons have a much smaller mass, this corresponds to a much higher velocity for the electrons. At 100 million degrees deuterons have a thermal velocity of 600 kilometres per second, and electrons have a velocity 40,000 kilometres per second, more than one tenth of the speed of light.

It is traditional and convenient to give plasma temperatures in electron volts, eV, or kilo-electron volts, keV. The electron volt is defined as the energy an electron would receive in

falling through an electric potential of one volt. The conversion is given by 1eV = 11,600 K, and for present purposes it is adequate to think of 100 million degrees as 10 keV. From here on we shall use the eV notation.

The Effect of a Magnetic Field

The behaviour of charged particles in a magnetic field is fundamental to our subject. In a uniform magnetic field the motion of a charged particle has two parts. Firstly, it has a circular motion perpendicular to the magnetic field, the radius of the circle being called the Larmor radius. This radius increases with the energy of the particle and decreases with the strength of the magnetic field. For a typical ion in a JET plasma the Larmor radius is a few millimetres. For an electron the Larmor radius is smaller by the square root of the electron-ion mass ratio and is typically a tenth of a millimetre. Because of the opposite signs of their charges the electrons and ions circulate in opposite directions.

The other part of the motion is that along the magnetic field. In a uniform magnetic field the charged particle's motion parallel to the field is unaffected by the field, and the particles' "parallel velocity" is constant. When the two parts of the motion are combined we have a helical trajectory as shown in Figure 2.1.

If the magnetic field becomes stronger as we move along the field line the particle sees a force in the direction away from the stronger field, and if the increase in the magnetic field is sufficiently large this force can reflect the particle back along its path. For this reason the force is called the "mirror force". This effect is illustrated in Figure 2.2 where the increase in the magnetic field is apparent from the convergence of the magnetic field lines.

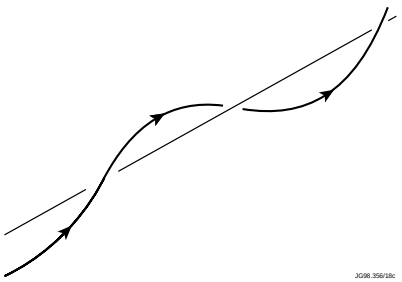

Figure 2.1. The charged particles follow a helical trajectory with its axis along the magnetic field.

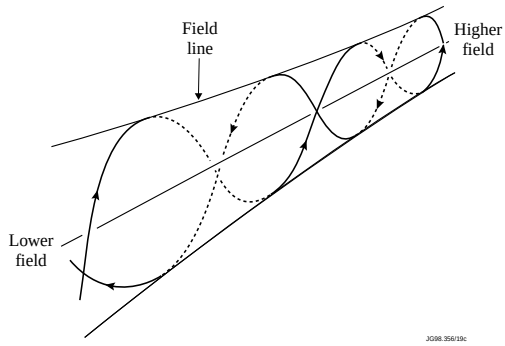

Figure 2.2. The particles are reflected from regions of higher magnetic field.

Pressure Balance

Because the mass of the plasma we are interested in is so tiny, its inertia usually plays little role in the plasma's behaviour. This means that the forces must balance throughout the plasma, any

imbalance being removed by a rapid adjustment.

In a steady equilibrium, the two forces which balance are the gradient of the plasma pressure and the magnetic force which arises from the current crossing the magnetic field. This magnetic force is just that which drives an electric motor. The magnetic force is perpendicular to both the current and the magnetic field, and consequently its component along the magnetic field is zero. This means that there can be no plasma pressure force along the magnetic field, and consequently the plasma adjusts to have a constant pressure along each field line.

The magnetic force can also be thought of as a magnetic pressure. In the simple case of straight magnetic field lines a magnetic field of strength B has a pressure $B^2/2\mu_o$ where μ_o is a constant equal to $4\pi \times 10^{-7}$ in Standard International units. A gradient in $B^2/2\mu_o$ has the same effect as a gradient in plasma pressure. However, the magnetic force is more subtle because, in addition to the simple $B^2/2\mu_o$ pressure, any curvature of the magnetic field lines contributes an extra force in the direction of the centre of curvature, and this must be included in the force balance.

Collisions

Many properties of the plasma are governed by collisions between particles. For example the electrical conductivity is determined by the collisions between electrons and ions as the electrons drift through the ion fluid to produce an electric current.

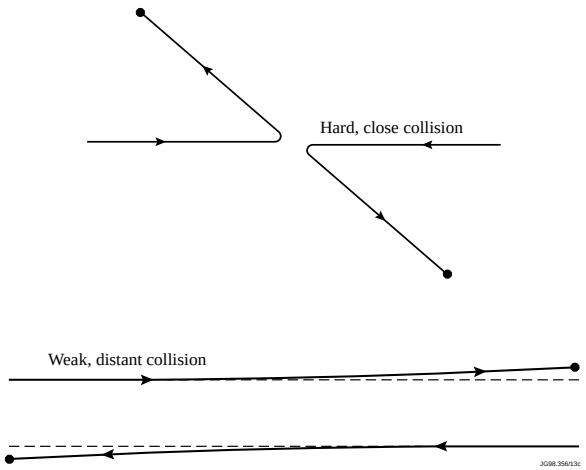

Figure 2.3. Comparing a hard collision with a weak, distant collision. Although the scattering is small in weak collisions, they generally dominate because of their larger number.

However, collisions in a plasma do not conform to the simple picture we might have based on the collisions of billiard balls, or those between the molecules of a normal gas. The basic reason is that in these two cases the collision occurs when the balls or molecules make contact,

but the particles of a plasma collide with distant particles. The force between the plasma particles is the Coulomb force between electric charges. This force falls off comparatively slowly with distance, in fact with the inverse square of the distance between the particles. As a result of this long range interaction any given particle is colliding simultaneously with a large number of other particles. In a plasma such as that in JET each particle is simultaneously "in collision" with millions of other particles.

Because of this special feature, collisions in a plasma are described by the cumulative effect of all the separate collisions. It turns out that the contribution of the weak, but more numerous, distant collisions outweighs that of the hard collisions which result from close encounters. The two types of collision are illustrated in Figure 2.3.

An effective collision time can be defined for each particle species as the time for the multiple collisions to produce a deflection through a large angle. The collision times depend sensitively on the plasma temperature, but taking a typical JET plasma the collision time of the electrons is a few hundred microseconds, and of the ions is tens of milliseconds. The distance travelled in this time gives a mean free path of tens of kilometres for both ions and electrons.

Bibliography

Before fusion research, plasma physics was largely concerned with partially ionised, low temperature plasmas such as those found in arcs and sparks. An influential introduction to the new subject was Spitzer's small book on the Physics of Fully Ionised Gases, Interscience, New York (1956). Since then many books have appeared, a recent and comprehensive one being that by Goldston and Rutherford, Introduction to Plasma Physics, Institute of Physics Publishing (1995). A more mathematical account of the subject is Miyamato's Plasma Physics for Nuclear Fusion, MIT Press (1989).

3. TOKAMAKS

The tokamak was first developed in the Soviet Union in the early 1960s, the name “tokamak” being formed from the Russian words **to**roidalnaya **ka**mera and **ma**gnitnaya **k**atushka meaning “toroidal chamber” and “magnetic coil”.

The advantage of toroidal, as opposed to linear, geometry is obvious from the avoidance of “ends”. The simplest magnetic field in a torus would be a purely toroidal magnetic field in which all the field lines form circles passing round the torus. However, a plasma placed in such a field cannot come to an equilibrium force balance. The pressure of a toroidal plasma would cause it to expand and the toroidal magnetic field is unable to provide a balancing force. The result would be a very rapid loss of the whole plasma.

In the tokamak this difficulty is overcome by passing a toroidal current through the plasma itself. This current produces a poloidal magnetic field, whose field lines pass the “short way” round the plasma, as shown in Figure 3.1. This encircling magnetic field is able to hold the plasma in place and to provide an equilibrium force balance. The way in which the toroidal and poloidal magnetic fields combine is illustrated in Figure 3.2, the resulting field lines taking a helical path around the torus.

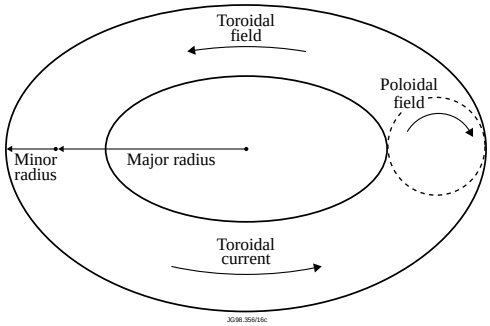

Figure 3.1. The currents and fields in a tokamak plasma.

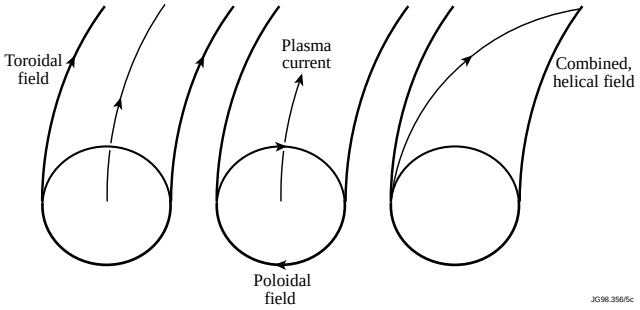

Figure3.2. The tokamakÕs toroidal magnetic field combines with the poloidal field of the plasma current to produce a magnetic field with helical field lines.

With a plasma in toroidally axisymmetric equilibrium the path of a magnetic field line maps out a toroidal surface. Every field line remains within its “magnetic surface” and these surfaces form a nested set. The current lines also lie in the magnetic surfaces, and the plasma pressure is constant on each surface.

All magnetic fields have an associated current, and the toroidal magnetic field in tokamaks is produced by currents in coils linking the torus, as shown in Figure 3.3. The field is produced using many toroidal field coils, to produce as uniform a field as possible. The magnitude of the toroidal field is typically a few Teslas, which is more than 10,000 times the strength of the earth’s magnetic field.

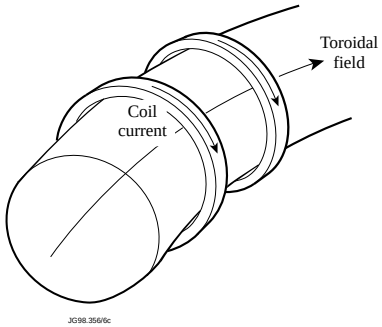

Figure 3.3. Coils linking the torus produce the toroidal magnetic field.

In the early Soviet experiments the heating of the plasma was achieved through the ohmic heating generated by the plasma current. This is the familiar I^2R heating, where I is the current and R the resistance. In plasmas the resistivity is principally dependent on the temperature of the electrons, being proportional to $1/T_e^{3/2}$. The ohmic heating is, therefore, very strong at low temperatures but becomes less effective at higher temperatures. In the early tokamak experiments a typical ohmic heating power would be 10kW.

There was initially some reluctance to accept the superiority of the tokamak as compared to other confinement devices, but the potential of the tokamak became clear when temperatures, first of several hundred eV, and later over 1keV were obtained. By 1970 there was a readiness to pursue this line, and a world wide tokamak programme soon developed. It should be noted, however, that although the successes were welcome there were hints of serious difficulties to come. Two particularly significant problems were the recognition that the confinement of the plasma is not as good as basic theory predicted, and the appearance of violent instabilities, called disruptions, which limited the operating conditions.

Confinement

The important role of confinement can be seen by considering the energy balance in a fusion

reactor. The particles in a reacting plasma have been heated to a high temperature. This requires an input of energy which is wasted for ions which are lost before they undergo an energy producing fusion reaction. We see, therefore, that the confinement must be sufficiently good that a large enough fraction of the ions react before their energy is lost. This leads to a simple criterion, first derived by Lawson, that the product $n\tau$ of the density n and confinement time τ must be greater than 6×10^{19} m^{-3} s.

We shall see later that the subject of plasma confinement in tokamaks is full of mysteries. For the present we shall just look at the fundamental model of confinement in which the losses are due solely to collisions between the particles. This represents the minimum loss rate and provides a basic level of confinement for comparison with experiment.

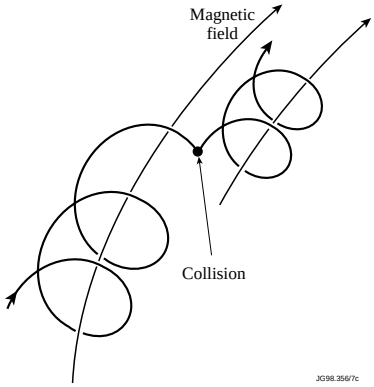

Figure 3.4. Schematic drawing showing how a collision causes the particleÕs orbit to be displaced by approximately a Larmor radius.

In the simplest model the diffusion of particles across the magnetic field is due to collisions. As illustrated in Figure 3.4, a collision allows the gyrating particle to move to another field line about a Larmor radius away. These collisions are equally likely to give an inward or outward step, and the result is a random walk. The resulting flow is outward because the particle density is higher at the centre.

Although it is easy to picture the energy loss as arising from the loss of the particles carrying the energy, the reality is that the energy is mainly lost by the random transfer of energy from particle to particle as a result of collisions. This is the familiar process of thermal conduction. The magnetic field provides the insulation, and the heat is driven across the plasma by the temperature gradient between the hot central plasma and the colder plasma at the edge.

This simple model requires one elaboration. There is a subset of the particles which, in addition to their Larmor motion, move in a broader orbit, and are therefore subject to a higher loss rate. This subset, called trapped particles, dominates the overall collisional losses.

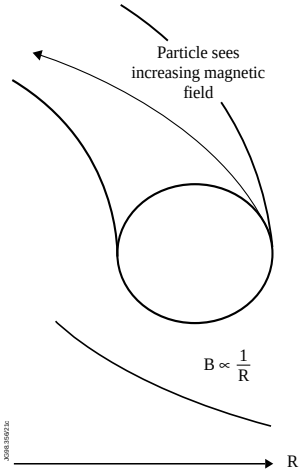

Figure 3.5. The toroidal magnetic field falls off as 1/R , where R is the distance from the major axis. So, as the particle moves along the magnetic field from the outboard side it sees an increasing magnetic field. This produces a Òmirror forceÓ on the particles, and the more slowly moving ones are reflected.

The particle trapping arises from the variation of the strength of the magnetic field seen by the particles as they follow their spiral orbits along the field. A straightforward consequence of Ampères law is that the toroidal magnetic field will fall off with the distance , R, from the major axis of the torus, the field being proportional to 1/R as illustrated in Figure 3.5. This means that a particle starting on the outboard side of the plasma and following the helical magnetic field line will encounter an increasing magnetic field as R decreases. The result is that the particle sees a retarding mirror force as described in Chapter 2. Particles moving slowly along the field are reflected and then, when they attempt to traverse the torus in the opposite direction, they are reflected back again. These are the trapped particles. Until they suffer a collision they bounce backward and forward around the outboard side of the plasma.

The orbit of trapped particles is illustrated in Figure 3.6 which shows the projection of the orbit onto a poloidal plane. Because of its shape it is called a banana orbit. The width of the orbit is greater than the Larmor radius and this results in an enhanced loss rate as the particles are displaced by collisions.

The collisional diffusion of the untrapped particles which circulate freely around the torus is called “classical”. The enhanced diffusion of the trapped particles is called “neo-classical”. When the two are added together the contribution of the trapped particles dominates.

The requirement of electrical neutrality within the plasma means that electrons and ions have equal diffusion rates. There is no such restriction for thermal conduction and the ions have a larger conductivity than the electrons, the ratio being roughly the square root of the ratio of their masses. The result is that, neoclassically, the dominant energy loss process arises from the

thermal conductivity of the ions. The underlying reason for this is their larger banana orbit, which allows a larger step in the thermal diffusion.

The above account is purely theoretical and only sets the scene for the many unexpected developments which we shall encounter later. As with most aspects of plasma physics the plasma seems capable of more complex behaviour than theory predicts.

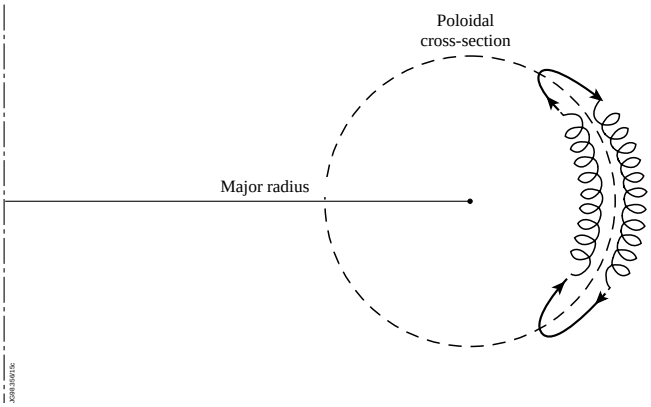

Figure 3.6. A reflected particle returns along the magnetic field until it is reflected back again. Such particles ÒbounceÓ repeatedly and as a result they are trapped on the outboard side of the plasma. The trapped orbit projected onto the poloidal plane, as shown, has the shape of a banana - giving the orbits their name.

Instabilities

The pioneers of tokamak theory were well aware of the possibility that the plasma would be subject to instabilities, and the experimentalists soon discovered such instabilities. Despite this, the success of tokamaks is due largely to the fact that there are parts of operating space which are free from destructive instabilities. However, the early workers could not have foreseen the complexity and subtlety of the stability problem. We shall see that some aspects have come to be understood theoretically, but others have been tantalisingly inexplicable.

A simple model of instability is that of the inverted pendulum, illustrated in Figure 3.7. In its exactly vertical position the pendulum is in equilibrium, but even the smallest displacement will cause the pendulum to fall. This is because, for any finite angle of displacement, there is a component of the gravitational force which acts along the path of the pendulum's head. The result is that gravitational potential energy is released and converted into kinetic energy.

These features of instability also govern the basic stability of tokamak plasmas. Again the question is whether small perturbations about an equilibrium would grow, and this in turn depends on whether there is accessible free energy for the instability. For tokamak plasmas, however, the calculation of stability can be very complex. Firstly, the plasma is three dimensional and rather

complicated, and then we have to consider *all* possible perturbations of the plasma equilibrium. Furthermore, it turns out that there are many types of potential instability. We shall not delve into this complexity. When we return to the subject we shall be content to identify the main sources of instability and to see the significance of the stability limits in constraining the achievable plasma parameters.

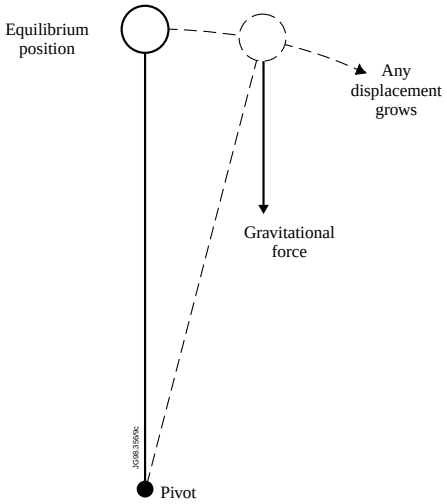

Figure 3.7. An inverted pendulum is unstable. For any displacement from the equilibrium position the gravitational force has a component in the direction of the displacement, causing it to grow.

The Early Tokamaks

The Soviet tokamak programme in the 1960s led to the device T-3. This had a major radius of 1m, a minor radius of 12cm and a plasma current of about 60kA. The electron temperature estimated from the resistance of the plasma was around 100eV, but later measurements using the perturbation of the magnetic field due to the plasma pressure indicated that the temperature was much higher. This was confirmed by measurements based on the scattering of laser light by the plasma electrons, showing that electron temperatures of around 1,000eV were achieved.

On the crucial subject of confinement, the results from T3 indicated that the energy loss through the ions was of the magnitude expected from the neoclassical theory of collisional losses. On the other hand the electron loss, which should have been small in comparison, was in fact dominant. This meant that the electron thermal conduction was larger than predicted by two orders of magnitude.

In addition, these tokamak plasmas were vulnerable to a gross instability, now called a disruption, which was so strong that the plasma current could not be maintained and the discharge was brought to an untimely end. An early example of this is shown in Figure 3.8.

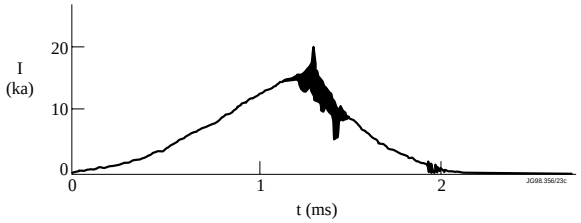

Figure 3.8. Trace of the plasma current showing the collapse brought about by a plasma disruption, from a paper by Gorbunov and Razumova in 1963.

Recognising the potential of tokamaks, the scientists at Princeton Plasma Physics Laboratory converted a toroidal device called a stellarator into a tokamak in 1970. The experiments on this "Stellarator Tokamak", called ST, confirmed that high temperatures were achievable. However, they also uncovered a new instability which became recognised as a regular feature in all subsequent tokamak experiments. It was found that the central electron temperature underwent a repeated and regular collapse. Each rapid collapse was followed by a slow recovery, giving the time traces a sawtooth pattern from which this instability has become known as the sawtooth instability. The original soft X-ray traces showing this behaviour are shown in Figure 3.9.

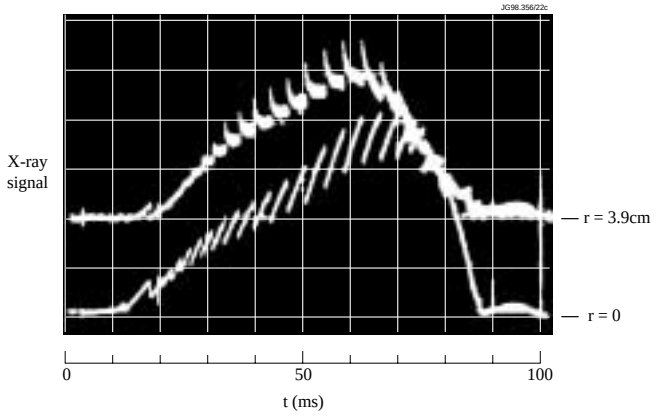

Figure 3.9. Time traces of soft X-rays from ST tokamak, given in the paper by von Goeler, Stodiek and Sauthoff. The emission from the axis (r=0) shows a sudden collapse followed by a slow rise, giving the trace its sawtooth form. This relaxation instability throws energy to the outer region where an inverted sawtooth is observed (r=3.9cm).

The French were quick off the mark, and designed and built the world's most advanced tokamak. In the summer of 1973 TFR (Tokamak de Fontenay-aux-Roses) was providing its first results. The plasma had a major radius of 1m and a minor radius of 20cm, with a design plasma current of 400kA. With ohmic heating alone electron temperatures of 2-3keV were achieved and record confinement times of around 20ms were obtained.

These early tokamaks provided much needed encouragement for the fusion programme and their success opened up a plausible path to a reactor. It was clearly desirable to make a large step in that direction, and in Europe it was agreed that this could be most readily achieved by a collaborative project. With this aim in mind a team was set up to design a Joint European Torus - JET. The decision as to how large the step should be could not be based purely on established scientific principles, since they did not exist. However, one simple calculation could be made. If the experiment was to succeed in producing a significant amount of fusion power, the energy of the α-particles produced could only be retained within the plasma if their orbits in the magnetic field were smaller than the width of the plasma. The condition for this depends only on the plasma current, and the required current is around 3MA. A current of this size was therefore envisaged, but it would be up to the JET design team to identify the important goals and to propose the device which was best able to achieve them.

Bibliography

The earliest theoretical work related to tokamaks was carried out by Sakharov and Tamm in 1951, and is recorded in Volume 1 of Plasma Physics and Controlled Fusion, published by Pergamon Press in 1961. An account of the exploratory tokamak experiments is given by Artsimovitch in his book Controlled Thermonuclear Reactions (published in English in 1964 by Oliver and Boyd) and later in a review, Tokamak Devices, in Nuclear Fusion, 12, 215 (1972).

An introductory account of tokamaks was provided by Wesson's book, Tokamaks (Clarendon Press), in 1987. A substantially expanded second edition of this book was published in 1997. A more theoretical treatment is White's Theory of Tokamak Plasmas (North-Holland 1989), and in 1992 Kadomtsev published his insightful book Tokamak Plasma: A Complex Physical System (IOP Publishing).

4. JET - QUITE A STEP

What was known

Let us first get a feel for the magnitude of the step to the proposed JET tokamak by comparing its physical size to that of the largest tokamak then existing, that is TFR. The plasma volume in TFR was less than $1m^3$. The volume for JET turned out to be over $100m^3$. Measured in these terms, therefore, the step was more than a factor of 100. Whereas the minor radius in TFR could be spanned by one hand, the JET vacuum vessel would be twice the height of a man, so that it would easily be possible to stand inside. Along with the increase in physical size the plasma current, a crucial parameter, would be increased by an order of magnitude.

The scientific framework for making design decisions was very shaky. Perhaps the foremost issue was how to reach thermonuclear conditions. The fundamental uncertainty was the confinement properties of the hotter plasmas that would be required. The only base from which to work was that of previous experiments with ohmic heating. In these experiments the anomalous loss through electron thermal conduction was dominant, and the loss through the ion channel was thought to be close to the minimum value as given by neoclassical transport resulting simply from collisions. It was plausible, at least, that at higher temperatures the ion heat loss would remain neoclassical. In that case theory predicts a lowering of the ion thermal conductivity with increasing temperature. The question would then be that of the electron heat loss. In the absence of experimental information it was natural to look to theory. Unfortunately there was no accepted theory. Then, as now, there were fashionable ideas, but the remarkable truth is that theory has never satisfactorily got to grips with anomalous transport.

Thus, little could be said with confidence and this, of course, was part of the justification for the JET experiment. It was necessary to discover the rules governing confinement in plasmas closer to reactor conditions.

There were other important uncertainties. Perhaps the most fundamental was the question of the so-called β-limit. β is essentially a measure of the ratio of the plasma energy to the energy of the magnetic field. This ratio appears naturally in the theory of magnetohdrodynamic (mhd) instabilities, and it was natural, therefore, to expect that these instabilities would impose a limit on the achievable value of β. This would mean that for a given magnetic field, the plasma energy could not exceed a critical value. When the JET design team started its work the question of a β-limit arose, and the absence of any theoretical calculation of the limit provoked the design team to instigate calculations which were ultimately to lead to the establishment of a sound understanding of the β-limit.

Another subject surrounded by mystery was “disruptions”. It was known that increasing the plasma density too far would cause a fatal disruption of the plasma. The same happened if, for a given toroidal magnetic field, the plasma current was increased to too high a value. Since

high density was to be desired for a high thermonuclear reaction rate, and since larger currents were expected to improve confinement, the disruption problem was crucial. However, disruptions were not understood, and even the pattern of their occurrence was somewhat unclear. It did seem, however, that the limit to the plasma current was related to the so-called safety factor, written as q. This is essentially the ratio of the toroidal and poloidal magnetic fields divided by the ratio of the major and minor radii of the plasma, R/a. That is, $q = (B_T/B_p)/(R/a)$.

Faced with these uncertainties the JET team had to come up with a design. The plasma current was chosen to be 3.8MA, sufficient to confine α-particles, with the possibility of extending this to 4.8MA. The toroidal field is limited by the force it imparts to the toroidal field coils linking the plasma. The JET design implied a conservative view of the acceptable force, and allowed a toroidal magnetic field at the centre of the plasma of 2.8T with a possible extension to 3.5T.

The Geometry

The remaining key decision was the geometry. Should the plasma be circular or elongated, and what should be the aspect ratio, R/a. While there are physics issues involved, these decisions appear to have been made with more practical considerations in mind.

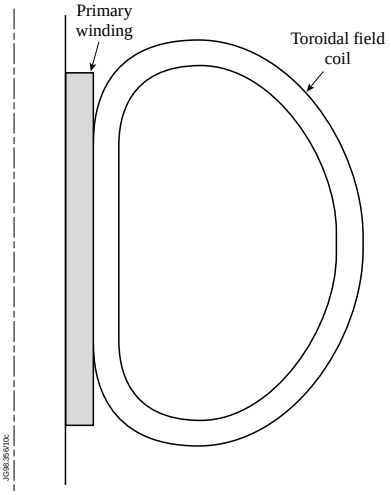

Figure 4.1. The D-shaped design of the toroidal field coils. The magnetic force toward the central axis is carried on the primary winding, and the shape was chosen to eliminate bending forces.

Because the magnetic field inside the toroidal field coils falls off with major radius as 1/R, there is a larger magnetic force on the inboard side of the coils than on the outboard side. In the JET design the resultant force toward the central axis is borne by the primary winding of the transformer as shown in Figure 4.1. The unsupported part of the toroidal field coil would in

general be subject to bending and tensile stresses. However, if we imagine that the coil were free to adjust its shape and balance the magnetic pressure at each position, the bending forces would be reduced to zero. This principle was adopted for JET and as a result the coil is D-shaped, the weaker magnetic field at the outside requiring a smaller curvature to provide a balancing force from the tensile stress. The vacuum vessel was then designed to use the space inside the coils and this gave a height-width ratio of 1.6.

The aspect-ratio was decided on the basis of minimising the cost. With a range of assumptions the optimum value of R/a was found to be between 2 and 3, and the chosen value was 2.4.

The Size

The values of the parameters given above now allow us to see how the physical size of JET was determined. It seemed from earlier experiments that a safety factor, q, of about 3 was needed to provide an adequate margin of stability. With the geometric ratios given above, and a toroidal field of 3T, this requirement on q means that the poloidal magnetic field, B_p , should not be greater than 0.5T. The size of the plasma then follows from Ampère's law, which relates the total current to B_p and the minor radius. For a given plasma current, too small a plasma gives too high a B_p and too small a safety factor. With the given geometry, and the value B_p=0.5T , a current of 4MA requires a minor radius, a, of just over 1m. With the geometric ratios chosen for JET, R/a = 2.4 and b/a = 1.6, the conveniently rounded dimensions R=3m and b = 2m give a satisfactory minor radius, a = 1.25m, and these were the plasma dimensions chosen for the JET design. Figure 4.2 shows the shape and size of the JET plasma and for comparison also gives the size of the TFR plasma.

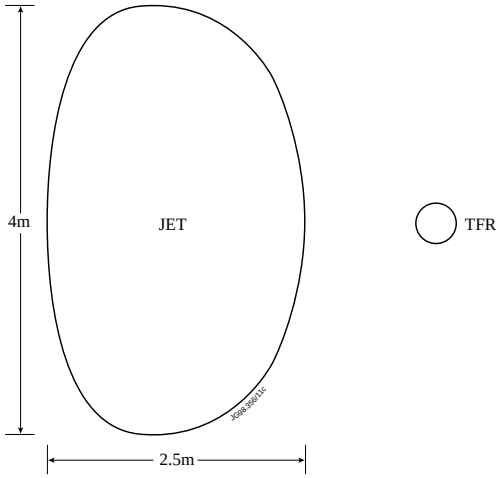

Figure 4.2. Designed shape and size of the JET plasma. The size of the world's most advanced tokamak at that time, TFR, is shown for comparison.

Heating the Plasma

When tokamak plasmas are formed by driving a toroidal current there is initially a substantial amount of ohmic heating. However, because the resistance of the plasma falls with increasing temperature, the ohmic heating is to some extent self-limiting. At the temperatures required for thermonuclear plasmas, the ohmic heating in JET would be negligible.

The design team was therefore faced with the problem of how to heat the plasma. Experiments in other tokamaks had shown the feasibility of various heating schemes, albeit in smaller devices and at powers much less than would be necessary for JET.

The heating of plasmas by injecting high energy beams was already an established technique. Hydrogen ions of a chosen isotope are produced in a specially designed ion source. These ions are then accelerated to the required energy in an electric field. Because charged particles are unable to cross the magnetic field it is necessary to neutralise the ions by passing the beam through a neutral hydrogen gas. In a collision process called charge-exchange, electrons are transferred from the neutral atoms of the gas to the ions of the beam. This turns the beam ions into neutral atoms, still with their high energy, and allows them to cross the magnetic field and penetrate the plasma. The neutral beam particles are finally stopped when they become ionised by the plasma electrons. They are then held by the magnetic field and transfer their energy to the plasma particles as they are slowed by collisions.

Another technique which was available was that of heating the plasma with high frequency electromagnetic waves generated at antennae mounted on the inside of the vacuum vessel. For historical reasons this is called Radio-Frequency heating, always referred to as R.F. heating. The basic mechanism is that the rapidly oscillating electric field of the electromagnetic wave resonates with the cyclotron motion of the plasma particles and accelerates them to higher energy. A variety of schemes can be used, and either the ions or the electrons can be heated depending on the frequency of the chosen heating scheme.

A further method which was seriously considered by the design team was compressional heating. Just as gas can be heated by the work done in compressing it, so can a plasma.

How much Heating?

The question of how much heating would be needed to reach interesting temperatures could not be answered. The fundamental uncertainty was the energy confinement. The energy confinement time in TFR was 20 milliseconds at a temperature of about 1keV. It was reasonable to expect that the confinement time would depend on the size of the plasma and on the magnitude of the current and applied magnetic field, but these dependencies were unknown. The confinement would also depend on the density and temperature of the plasma, and these, of course, would depend on the confinement itself.

In this situation it was not clear what could be regarded as a reasonable goal. If the

expectations were put too high they would lead to disappointment. Rather than review the wide range of unconvincing conjectures made at the time, let us first obtain some feel for the expectations by making the simple assumption that the energy loss process is thermal conduction, and neglect the dependence of the conductivity on all of the variables listed above apart from size.

Thermal conduction is a diffusive process, and its characteristic time is proportional to the square of the linear dimensions. In our case this means that we can take the energy confinement time to be proportional to the area of the minor cross-section of the plasma. In TFR this was $0.13m^2$ and in JET it would be almost $8m^2$. The 20 millisecond energy confinement time of TFR then gives a confinement in JET of $0.02 \times (8/0.13)s = 1.2s$.

The degree of uncertainty is easily seen by imagining that the thermal conductivity might vary with temperature as $T^{1/2}$ or $T^{-1/2}$. Neither of these dependencies is dramatic, but in extrapolating from the 1keV temperatures of the early experiments to a possible 10keV in JET the range of predicted values for the confinement time would be 0.4s to 4s, covering an order of magnitude.

A possible goal for the JET experiment was the achievement of break-even conditions, in which the thermonuclear power would be equal to the heating power supplied. However, calculation of the necessary heating enhances the uncertainties associated with confinement because the heating power, P, required for break-even depends on the square of the energy confinement time, with $P \propto 1/\tau_E^2$.

For a confinement time of 4 seconds the power required for break-even would be only a few megawatts but for a confinement time of 0.4 seconds the requirement would be at the unrealistic level of hundreds of megawatts. The design team decided pragmatically to begin with 3MW of heating and to increase this in stages to 10MW and 25MW.

Stability

When the design team started their work the understanding of the stability of tokamaks was in a very rudimentary state. The major questions to be addressed concerned the mhd stability of the plasma. Mhd stands for magnetohydrodynamics, and this name describes the model of the plasma in which it is treated as a fluid. The fluid is taken to be electrically conducting, and this property couples its motion to the magnetic field. This model, in principle, allows calculations of the stability of the plasma to gross motions, and stability to such motions is, of course, a crucial issue.

Recognising that the theories then available were hardly relevant to real tokamak plasmas, study contracts were placed to try to improve the situation. This produced a breakthrough when it led to the development of the first numerical code capable of calculating stability in full toroidal geometry. In particular, the stability of any proposed JET plasma could then be explored. It was

to turn out that the question of the stability of JET plasmas would drive many of the major advances in the understanding of tokamak stability.

An important discovery arising from the stability code was that an instability of the plasma core which was predicted to occur in cylindrical geometry can be stable in toroidal geometry. Another development arose from the choice of a vertically elongated plasma for JET. It was already known that this configuration is subject to an instability force in the vertical direction. Without stabilisation this force would lead to an extremely fast instability. However, analysis showed that the vacuum vessel would slow the instability to a growth-rate which could be controlled by a feedback system, and such a system became part of the JET design.

The Design Proposal

The design team had started their work in September 1973. By September 1975 they had prepared their design proposal. This document, called R5, had more than 600 pages. It listed the scant information about tokamak physics then available, made its arguments for the specific JET design, and presented an impressively detailed design of the many components. Figure 4.3. shows a simplified illustration of the design, giving the basic dimensions. Its structure is almost identical to the device which would ultimately be built.

This design, together with the plasma heating systems represents a courageous step from the then existing tokamaks. The great uncertainties, which prevented precise predictions, had presented a considerable challenge to the scientists and engineers involved. Time would judge their decisions.

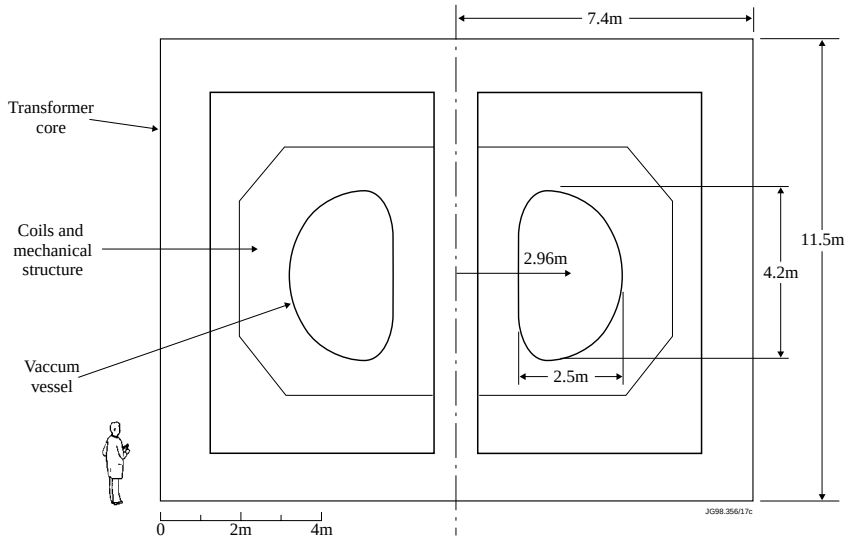

Figure 4.3. Cross-section showing the basic elements and dimensions of the JET design.

The Stated Aims

As we have seen the design was based on assessments as to what were reasonable aims, and what could be achieved. Along with the design, the aims were spelt out clearly in the design document and we must record these stated aims.

"The essential objective of JET is to obtain and study a plasma in conditions and dimensions approaching those needed in a thermonuclear reactor. These studies will be aimed at defining the parameters, the size and the working conditions of a Tokamak reactor. The realisation of this objective involves four main areas of work:

(i) the *scaling of plasma behaviour* as parameters approach the reactor range,
(ii) the *plasma-wall interaction* in these conditions,
(iii) the study of *plasma heating* and
(iv) the study of α*-particle production, confinement* and consequent *plasma heating.*"

We shall recall these goals when we come to summarise JET's achievements.

Bibliography

The best reference is the report R5, or more fully EUR-JET-R5, entitled "JET Project - Design Proposal". This is a splendid account of the work of the design team led by Paul-Henri Rebut. Its contents and approach are best represented by giving the report's abstract is full.

> This proposal describes a large Tokamak experiment, which aims to study plasma behaviour in conditions and dimensions approaching those required in a fusion reactor. The maximum plasma minor radius (a) is 1.25 m and the major radius (R_o) is 2.96m. An important feature is the flexibility to study, for plasma currents in the $1 \rightarrow 3$ MA range, a wide range of aspect ratios ($R_o/a = 2.37 \rightarrow 5$), toroidal magnetic fields (up to 3.6T), minor radii ($0.6 \rightarrow 1.25$m) and elongation ratios ($b/a = 1 \rightarrow 3.5$).
>
> The cost of the apparatus, power supplies, plasma heating equipment and specific diagnostics is estimated as 70.1 Muc [1975 prices, in year 2000 prices 200 Meuros]. The total construction phase cost including commissioning, buildings and staff is 135 Muc. These figures include an average overall contingency of 30%. The construction time for the project is estimated at 5years and requires 370 professional man years of effort in the construction organisation with additional effort deployed by the Associated Laboratories in such areas as diagnostics and plasma heating.
>
> This design proposal is arranged as follows:
>
> The Preface gives an introduction to the field of fusion research and relates JET to

> the European and International programmes. Chapter I is a concise summary of the design proposal, it describes the objectives of research with JET, and gives a brief description of: the apparatus; the cost and construction schedules; the proposed experimental programme and the possible modes of operation of the device. A detailed account of the project is given in the rest of the report of which Chapters IV and VII comprise the engineering design and the staff and cost estimates respectively.

The design team was comprised of 7 groups totalling 56 members. The “Scientific” group, responsible for “Physics, Additional Heating, Diagnostics, Divertor and Cost Scaling”, was led by Alan Gibson.

5. THE CONSTRUCTION

The major components of the JET device each demanded that a range of design criteria be satisfied, and in addition had to be designed so that they could be assembled in a way which allowed the necessary access. A further requirement was the need to maintain and modify components by remote handling when they had been made radioactive by neutron bombardment. Figure 5.1 gives a drawing of the JET design showing the general layout. We can best appreciate what was involved in the construction by considering the components in turn, starting with the innermost element - the vacuum vessel.

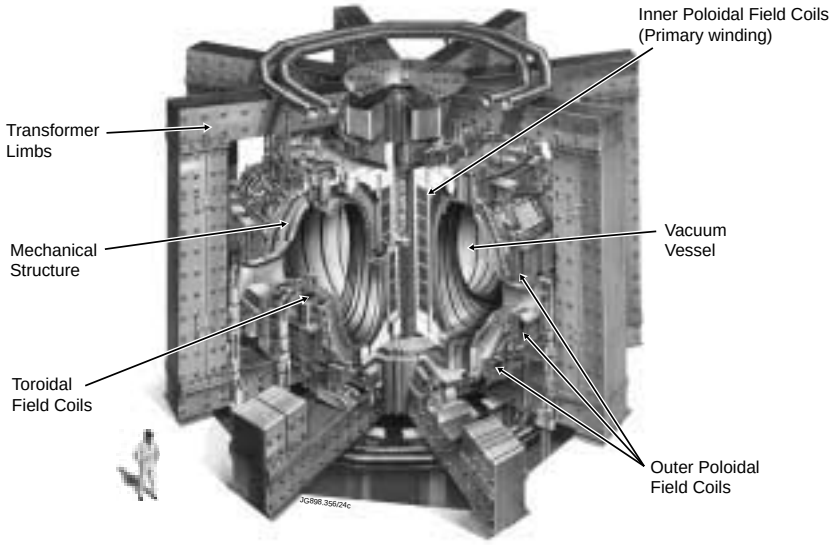

Figure 5.1. Drawing of the JET design.

The Vacuum Vessel

The basic purpose of the vacuum vessel was to hold a vacuum in which the pressure was less than one millionth of atmospheric pressure. This meant of course that it would have to carry the force of atmospheric pressure over the whole of its surface, 10 tonnes per square metre over an area of 200 square metres.

In order to cleanse the plasma-facing surface of the vessel of impurities it was designed to be baked at 500^{o}C, and this implied the additional requirement that the heating and cooling had to be carried out without unacceptable stresses from expansion and contraction. The vessel was designed with a double skin to allow heating by hot gas which is passed through the interspace.

Mechanically the simplest structure would be toroidally symmetric. However, the thickness of metal required to support the pressure forces would be such that the electrical resistance

would be very low. The consequence would be that the toroidal electric field applied to drive the plasma current would also drive an unacceptably large current through the vacuum vessel. The solution was to alternate sections with enough metal to provide the required strength with sections having a high resistance. The high resistance sections were bellows whose convolutions substantially increase their resistance. This structure is illustrated in Figure 5.2.

As if these complications were not enough the nickel alloy construction called for eight kilometres of vacuum tight welds.

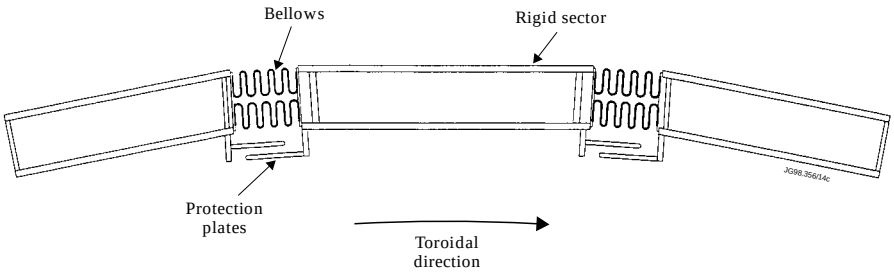

Figure 5.2. Part-section of the vacuum vessel wall, showing the alternating rigid and bellows sectors.

Magnetic Field Coils

The toroidal magnetic field was to be produced by 32 D-shaped coils enclosing the vacuum vessel, and the layout of these coils is illustrated in Figure 5.3. Each coil was wound with 24 turns of copper bar and weighed 12 tonnes. The combined current carrying capacity of all the coils was 51MA. The coils were to carry currents for several tens of seconds, and consequently they had to be provided with a cooling system, using water as the coolant.

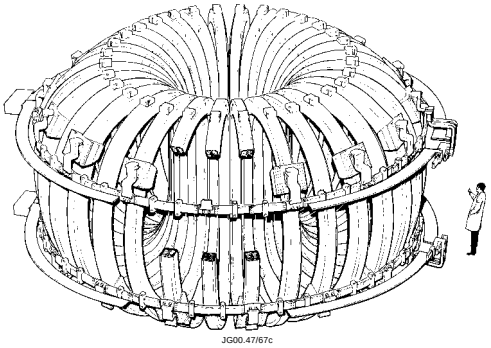

Figure 5.3. The toroidal field coil system.

The magnetic field exerts an expansive force on the coils and the tensile force on each coil would be up to 600 tonnes, this force being carried by the tensile strength of the copper. The total

force on each coil would be almost 2000 tonnes, directed toward the major axis of the torus. A further force arises from the interaction of the currents in the coils with the poloidal magnetic field. The current in the toroidal field coils crosses the vertical component of the poloidal field in opposite directions in the upper and lower halves. This produces a twisting force which, in the JET design, is carried by an outer mechanical structure, illustrated in Figure 5.4.

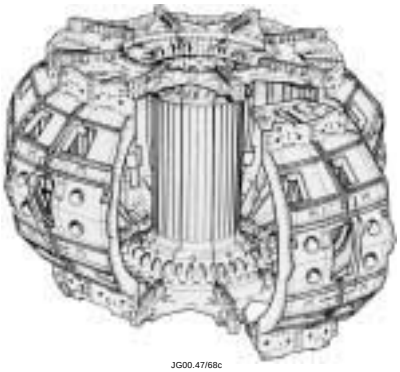

Figure 5.4. The mechanical structure which supports the toroidal field coils against the magnetic twisting force.

The poloidal field coils are horizontal circular coils. If these coils were placed inside the toroidal field coils the two sets of coils would be linked, with the associated problems of assembly. The poloidal field coils are therefore placed outside the toroidal field coils, and their layout is shown in Figure 5.5.

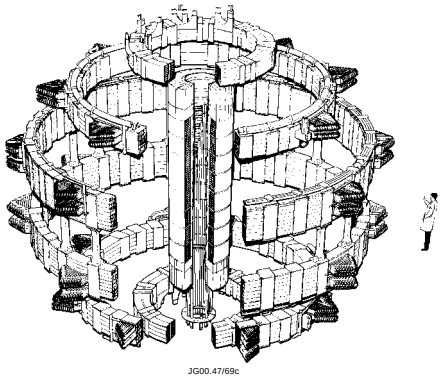

Figure 5.5. The poloidal field coil system.

The main poloidal field coil is the inner coil wound round the central column of an iron transformer core, to act as the primary of the transformer. The other six coils are optimally placed to provide control of the plasma shape and position. The largest of the coils is 11 metres in diameter.

The laminated iron transformer core would dominate the appearance of JET having 8 limbs enveloping the other components. This massive structure, which would weigh 2,600 tonnes, is illustrated in Figure 5.6.

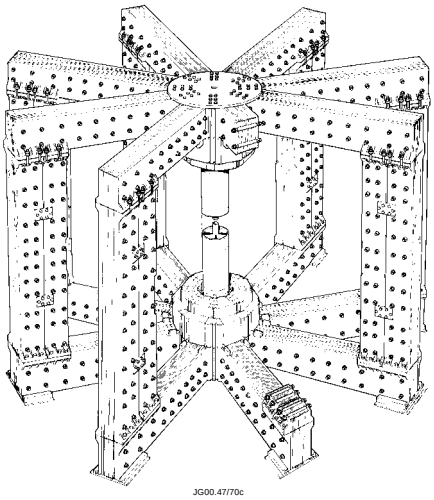

Figure 5.6. Layout of the iron transformer core.

Power Supplies

Electrical power was needed to supply the currents in both the toroidal and poloidal field coils, a similar power being required for each.

JET was designed to allow a pulse repetition rate of one every 15 minutes. Each pulse would call for a total power of up to 800MW - the output of a medium sized power station. In previous machines this pulsed load had been dealt with using heavy flywheels driven up to speed by motor generators, the energy in the flywheel then being extracted during the plasma pulse. The system used for JET combined this procedure with several hundred megawatts taken directly from the electricity grid.

Plasma Heating Systems

It was decided that the main heating would be provided by two heating systems - neutral beam injection and ion cyclotron resonance heating. Each of these systems consisted of a number of separate units, so the power could be increased over time by increasing the number of injectors and antennae. The plan was for an initial installation of a few megawatts in each system, to be increased later to 25MW of neutral beams and an ion cyclotron power of around 15MW.

The choice of energy for the netural beam particles involved a compromise. At too low an energy the beam would not penetrate to the centre of the plasma. At too high an energy the

neutralisation process becomes inefficient. The chosen energy for hydrogen beams was 80k eV, to be increased to 160 keV with the introduction of deuterium operation. Figure 5.7 shows a drawing of the injection system.

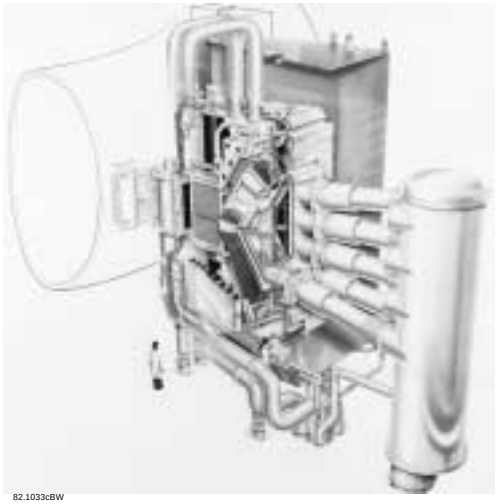

Figure 5.7. Drawing of the neutral beam injection system.

The frequency of the ion cyclotron waves is determined by the ion cyclotron rotation of the plasma ions, and this in turn is decided by the magnetic field. However, since the magnitude of the magnetic field changes by a factor 2 across the plasma, the region of power deposition can be controlled by a choice of frequency. The range of frequencies chosen for JET was 25-55 MHz. The RF waves are emitted into the plasma by antennae placed inside the vacuum vessel. The antenna structure is illustrated in Figure 5.8.

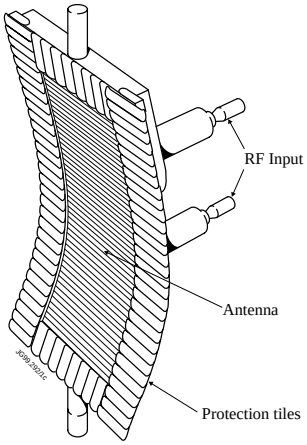

Figure 5.8. Drawing of one of the ion cyclotron heating antennas.

Data Acquisition and Control

Each JET pulse would make available an enormous amount of data. Some of this would be required to control the plasma and the auxiliary systems. Even more would be essential to diagnose the plasma behaviour, with as high a spatial and time resolution as the measurement systems would allow. It was originally envisaged that a hundred thousand readings per pulse would have to be recorded. It ultimately turned out to be more than a hundred million readings per pulse.

The basic information acquired for each pulse had to be supplied immediately to the control rooms with their arrays of monitors, shown in Figure 5.9. A broader range of data had to be made available to all of the scientists involved, and the information from all pulses had to be stored.

Figure 5.9. Overview of control rooms.

Diagnostic Systems

Once JET started producing plasmas it would be crucial to know the basic quantities characterising the plasma. The diagnostic systems designed to provide this information called for a higher degree of sophistication than had been necessary for smaller tokamaks. They had to be integrated into the complex JET structure, and provide a consistent reliability even when subject to high levels of radiation.

Small coils placed around the plasma would detect changes in the magnetic field and determine the plasma current. Larger loops encircling the plasma toroidally would give the voltage around the plasma. The plasma itself would partly be diagnosed by measuring the emission of varies forms of radiation. The rapid cyclotron motion of the electrons in the magnetic field causes them to emit radiation, and measurement of this electron cyclotron emission allows the electron temperature to be determined. The full power radiated from the plasma in chosen directions was to be detected by the temperature rise produced in a set of bolometers. Neutron detectors were installed to measure the thermonuclear reaction rate when deuterium, and later deuterium-tritium, plasmas were produced.

The ion temperature would be measured utilising the small number of neutral particles in the plasma, and analysing those which escape. These neutral particles have been formed by the

neutralisation of plasma ions, and their energy, which is characteristic of the ion temperature, can be measured by external detectors.

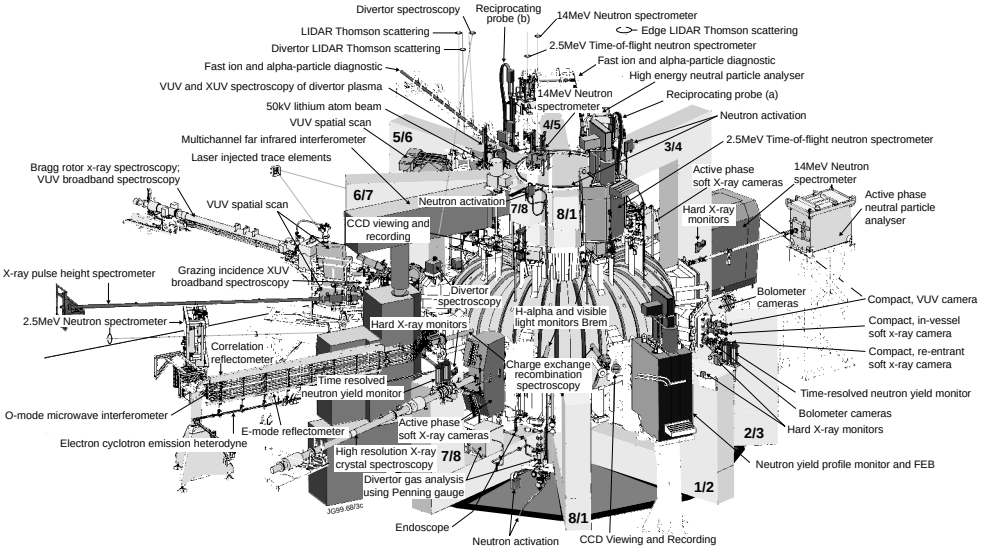

Figure 5.10. Layout of the diagnostic systems.

The plasma also emits soft X-rays and this emission can be followed with very high time resolution. Thus the soft X-ray detectors installed could be expected to see phenomena occurring within the plasma which most other detectors could not resolve. The ultra-violet radiation from the plasma would be analysed using spectrometers to give information on the impurity content of the plasma.

The average density of the plasma was to be measured robustly by interferometry. The wavelength of electromagnetic radiation is modified in the plasma according to its density. An interferometer would count the change in the number of wavelengths along a microwave beam passing across the plasma, and so determine an average plasma density. A more complete technique for measuring the local density and the electron temperature would use the scattering of a laser beam by the plasma electrons, so-called Thomson scattering. The layout of the diagnostic systems is illustrated in Figure 5.10.

Completion

The construction of JET was completed on time, and Rebut and his colleagues from the design team had the first reward for their efforts which had begun ten years earlier. Figure 5.11 is a photograph of the completed device. The detail in the photograph gives some indication of the complexity of the construction - in contrast to the simplified drawing of Figure 5.1.

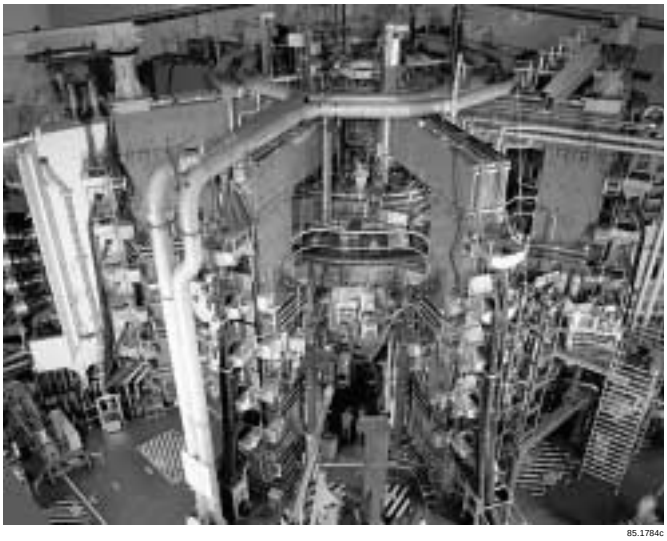

Figure 5.11. Photograph of JET on completion.

Bibliography

Following the death of JETÕs first director Dr. Hans-Otto WŸster a complete issue of the journal Fusion Technology was dedicated to his memory. This issue, Volume 11 (1987) was entitled ÒDesign, construction and first operational experience on the Joint European Torus (JET)Ó, and gives an excellent summary of the engineering aspects of JET.

The articles are:

Rebut, P.H. and Keen B.E. The JET experiment, evolution, present status and prospects.

Bertolini, E., Mondino, P.L. and Noll, P. The JET machine design, construction and operation of the major systems.

Van der Beken, H., Best, C.H., Fullard, K., Herzog, R.R., Jones, E.M., and Steed, C.A. CODAS: The JET control and data acquisition system.

Claesen, R., and Mondino, P.L. Neutral beam injection and radio-frequency power supplies.

Duesing, G., Altmann, M., Falter, H., Goede, A., Haange, R., Hemsworth, R.S., Kupschus,P ., Stork, D., and Thompson, E. Neutral beam injection system.

Kaye, A., Jacquinot, J., Lallia, P., and Wade T. Radio-frequency heating system.

Millward, P., Ainsworth, A., Caldwell-Nichols, C.J., Lobel, R., and Hancock, C.J. Engineering aspects of JET diagnostic systems.

Dean., J.R. and Raimondi, T. JET remote maintenance during active operation.

6. AND NOW EXPERIMENTS

JET started operation in 1983, four years after site work began.

As the starting date approached, excitement was mixed with an appreciation that with such a complex system there would be unexpected problems. However, the start of machine operation went smoothly and the first plasma was produced on 25th June. The operator's note reads "first light, a bit of current". The plasma current was a tiny 17kA, but in subsequent plasmas the current was increased in stages and by October had reached 1 MA.

Operation of JET involved a large team of engineers and scientists, each of these groups being based in a control room equipped with an array of monitors. The control rooms were over a hundred metres from the tokamak itself. The conditions for forming the plasma were worked out by the engineers and scientists in collaboration, the setting up procedure requiring the programming the huge power supplies to provide the toroidal magnetic field and plasma current necessary to generate and maintain the required plasma. The experimentalists had the diagnostic systems ready for the moment the plasma current started and a plasma was formed.

An unusual experience for those operating JET was to be able to watch the traces of the measured plasma characteristics on the computer screens in real time. At the start of fusion research, plasmas typically lasted for a thousandth of a second. By the time the construction of JET was started, times had increased to a fraction of a second. Now, with pulse lengths of ten seconds it was possible to take an interest in the plasma evolution as it occurred.

In the early experiments the plasma was formed from hydrogen, and the only heating was the ohmic heating of the plasma current. Despite this the early experimental results were eagerly awaited. The result of most interest was the energy confinement time. It turned out to be in the middle of the anticipated range, the best confinement times being about half a second. It would have been encouraging to have found a much longer time, but at least the most pessimistic forecasts could be discounted.

The temperatures were something of a surprise. Using empirical formulas for confinement, temperatures of 1 keV or less had been predicted but temperatures of up to 4 keV were obtained. This was partly due to the high level of impurity in the plasma, which substantially increased its resistance and hence the ohmic heating. In retrospect it is now clear that another effect was playing a role. It was explained earlier how particles can be trapped in the weaker, outboard magnetic field. Electrons so trapped cannot carry their share of the current, and consequently the resistance of the plasma is increased. In the experiments this increased the heating and raised the temperature still further. At the time, any increased resistivity due to trapped particles was conjectural and, as we shall see, it was only later that the phenomenon was directly demonstrated.

Although the high level of impurity produced a higher plasma temperature, it was completely unacceptable. Many of the impurity atoms were not fully ionised and the residual atomic electrons allow radiation and energy loss from the partially ionised ions. In the early experiments radiation

from impurities constituted 70% or more of the power lost from the plasma. A concern for the longer term was that the presence of a high level of impurities would dilute the plasma and reduce the thermonuclear power.

There were also indications that the presence of impurities played a direct role in the abrupt disruptive terminations of the plasma which, as with other tokamaks, soon became a regular feature of the experimental programme. It was conjectured that radiation from impurities could lead to a contraction of the plasma leading to a violently unstable configuration. Disruptions were to remain a serious problem and considerable effort was to be expended in clarifying their causes.

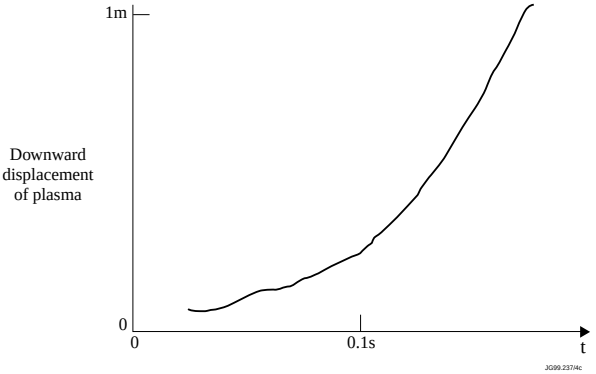

Figure 6.1. Showing the growth of the plasma displacement resulting from the uncontrolled vertical instability.

Much of the behaviour on JET was familiar from experiments on smaller tokamaks. However, in the early JET experiments the first of many unexpected phenomena appeared.

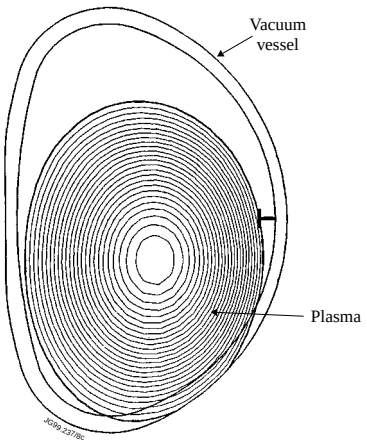

Figure 6.2. As the plasma moves downward during the instability it interacts with the vacuum vessel. The induced currents produce very large forces.

Vertically elongated plasmas were produced by an appropriate distribution of the toroidal currents in the external coils. The required current distribution of these currents is such that a small vertical displacement of the plasma leads to a force on the plasma which enhances the displacement. That is, the plasma is unstable to a vertical movement. All of this was known and understood and, as mentioned earlier, the plasma would be held in position by a feedback system. With the first few, low current, plasmas the feedback was not operational and Figure6.1 sho ws a graph of the growth of the resulting instability. The feedback system was soon available and the plasma could then be held central to within less than a centimetre of the desired position. However, one day, a plasma with two great an elongation was produced and the feedback system lost control. The plasma, carrying a current of 2.7MA, underwent a large vertical displacement leading to a force on the vacuum vessel. The attraction between the external coils currents and the plasma current pulled the plasma against the vacuum vessel, as shown in Figure6.2, inducing currents in the vessel. The repulsive force between the vacuum vessel and the plasma then held the plasma in place. Unfortunately the force on the vacuum vessel was several hundred tonnes! This experience led to an improved feedback system and a strengthening of the vacuum vessel mounting, with the introduction of hydraulic shock absorbers to prevent possible damage.

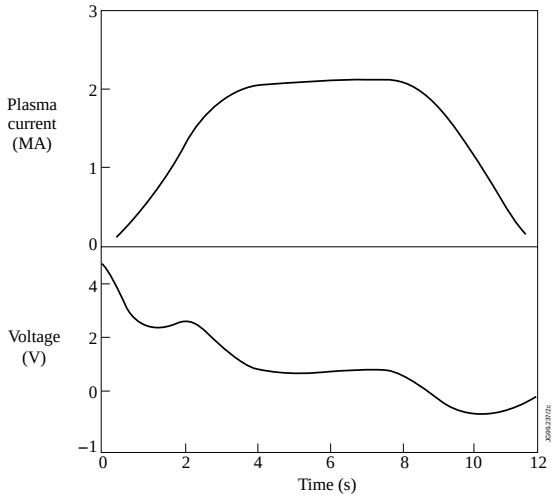

Figure 6.3. Time traces of the plasma current and the toroidal loop voltage.

Traces of the plasma current and the voltage around the torus are shown in Figure 6.3. The current is seen to rise to 2MA and to be maintained at a steady “flat top” for around 4 seconds. The voltage measured by the toroidal voltage loops does not follow the current for several reasons. Firstly, a high voltage is necessary to breakdown the resistance of the initial plasma. The application of the toroidal voltage drives the free electrons round the torus producing further electrons in an ionisation cascade until the plasma is fully ionised. From that point the toroidal

electric field in the plasma simply drives a current against the plasma resistance. This resistance falls as the plasma temperature increases causing a drop in the voltage measured by the voltage loop. The voltage loop also measures inductive voltages produced by the changes in the plasma current, leading to an increase in the loop voltage during the current rise and a reduction during the current decay.

The basic plasma parameters are the density and temperature. The requirement of charge neutrality relates the electron and ion densities, and in a pure hydrogen plasma they are equal. Figure 6.4 shows the time variation of the line integrated electron density as measured by the microwave interferometer. The build up of density over several seconds is due to the release of neutral hydrogen from the walls and its ionisation at the surface of the plasma.

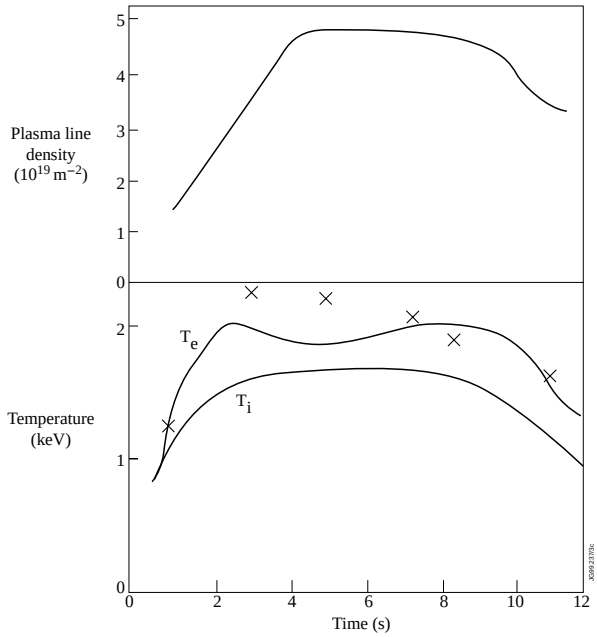

Figure 6.4. The density, and electron and ion temperatures in an early plasma. The electron temperature measured by ECE is given by the full curve, and that measured by Thomson scattering is marked by crosses.

The electron and ion temperatures are also shown in Figure 6.4. The electron temperature graph shows the satisfactory agreement of two methods of measurement, one using electron cyclotron emission (ECE) and the other using Thomson scattering. The ion temperature was measured by the technique of neutral particle analysis. The plasma heating is ohmic, and this predominantly heats the electrons. The underlying mechanism is that the electrons are dragged past the much heavier ions by the electric field to produce the plasma current, and in the process they are scattered by the ions. This produces a randomisation of the electron motion and the

resulting thermal energy of the electrons determines their temperature. The ions are passive in this process and the ohmic heating of the ions is negligible.

Nevertheless, it is seen from the two temperature traces that the ion temperature almost reaches the 2 keV attained by the electrons. The reason for this is that, through collisions, the heated electrons share their energy with the ions. Under the conditions of this experiment the timescale for this exchange of energy is about a tenth of a second.

The flat top temperatures are determined by the balance between ohmic heating and energy losses. The two main components of the losses are transport of energy across the plasma and radiation. Together these losses balance the ohmic heating which is given by the product of the voltage and the current. Taking values from the graphs of Figure 6.3 we find that the ohmic heating is between 1 and 2 MW.

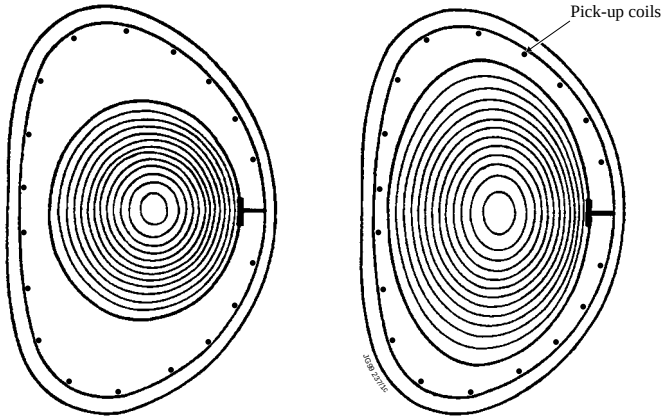

Figure6.5. The plasma shape could be varied from circular to elliptical, the shape being calculated from the magnetic field measured by the pick-up coils around the plasma, placed as shown in the figure.

The control of the plasma shape is illustrated by Figure 6.5 which shows magnetic flux surfaces of two plasmas bounded by surfaces touching the limiter. These show the ability to produce both circular and elongated plasmas. The flux surfaces themselves were calculated using the magnetic signals picked up by the set of magnetic coils whose positions are also shown in the figure.

Bibliography

The first major conference after the start of JET operation was the Tenth IAEA Conference on Plasma Physics and Controlled Nuclear Fusion Research, held in London in 1984. The early results were presented there in the papers:

Rebut, P.H., et al. First experiments in JET. Vol. I p11.

Cordey, J.G. et al. Particle and energy confinement in ohmically heated JET plasmas. Vol. I p167.

Behringer, K.H. et al. Impurity studies and transport code modelling of JET plasmas. Vol. I p291.

Thomas, P.R., Wesson, J.A., et al. MHD behaviour and discharge optimisation in JET. Vol.I. p353.

This last paper reports the first observations of the vertical instability, and a more complete account is given in

Noll, P. et al. Stabilisation of vertical position and control of plasma shape in JET. Proc. 11th Symposium on Fusion Engineering , Texes 1985. Vol. I p33.

7. THE SCIENTIFIC SPRING

JET was a new and substantially different tokamak. With the impressive array of first class diagnostics and an enthusiastic team of scientists and engineers, it was not surprising that the first two years of operation saw the first shoots of what were to become major scientific research projects.

Plasma Confinement

The subject destined to have the most prolonged attention was the confinement of the plasma energy. With the introduction of additional heating, using up to 4.5MW of ion cyclotron resonance heating (ICRH), the first indication of so-called confinement degradation, already seen on smaller tokamaks, was observed.

The confinement is conveniently measured by the confinement time. If a steady state is reached with an applied power P, this power is related to the total energy, W, in the plasma by the balance between the input power and the power loss. The power loss can be written W/τ_E where τ_E is the time which characterises the confinement of the plasma energy W. The power balance equation is then $P = W/\tau_E$.

This can be regarded as the definition of the energy confinement time, τ_E, in terms of the two known quantities P and W, and we then re-write the power balance equation

$$\tau_E = \frac{W}{P}$$

When the first ion cyclotron heating became available on JET, and this was added to the ohmic heating, it doubled the total input power. If the confinement time were unchanged the energy in

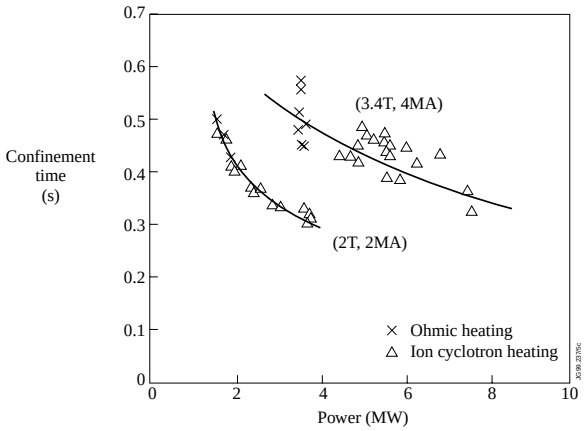

Figure 7.1. Increasing the heating power reduced the energy confinement time. The results shown are for two sets of plasma conditions with plasma currents of 4MA and 2MA and toroidal magnetic fields of 3.4T and 2T.

the plasma would also have doubled. In fact the increase in plasma energy was only 50%, implying a reduction of the confinement time by 25%. The deterioration of confinement time with increased power is shown in Figure 7.1.

This early result only raises further questions. What happens at higher powers? How does neutral beam heating behave? How does the confinement depend on each of the variable parameters - plasma current, magnetic field, temperature, density and so on. And very importantly - could the confinement be improved? We shall return to these questions later.

Disruptions

The JET design team had given much attention to the causes of the disruptions which occur at high density. They recognised that at higher electron densities the radiation from impurities would be increased, and their idea was that at a critical density this radiation caused a disruption. In its simplest form the suggestion was that a disruption would occur when the power lost through impurity radiation became equal to the power input.

If the total radiation power from the plasma is equal to or greater than the power input, there is no power left to reach the plasma boundary by transport processes. In this situation the plasma loses effective contact with the material limiters, and it can be imagined that it would be unstable to a contraction. This contraction would then make the plasma current profile subject to instability.

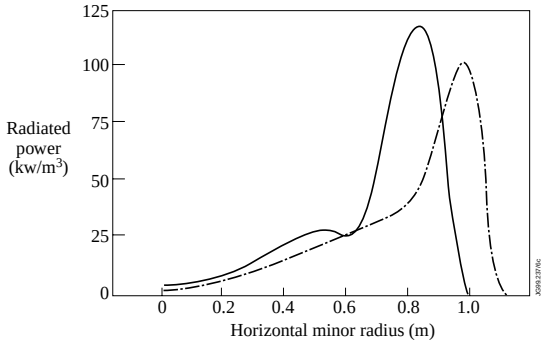

Figure 7.2. Two radiation profiles, separated by one second, measured just prior to a disruption. The later profile, drawn with a full line, shows the contraction of the radiating layer towards the centre of the plasma.

In practice it is found that the radiation comes predominantly from the cool layer at the edge of the plasma where the atoms of oxygen and carbon are not fully ionised and are therefore able to radiate. If the proposed disruption mechanism was valid we would expect to see the plasma contract as a disruption was approached, and the radiation layer at the edge of the plasma would move inwards.

When the experimental results were examined both of these processes were found. Figure7.2 shows the inward movement of the radiation layer and Figure 7.3 gives a sequence of temperature profiles consistent with the contraction of the plasma and the movement of the radiating layer. A first step had been made toward understanding disruptions. The years that followed would see a research programme aimed at clarifying the conditions for disruptions, and at understanding the physical mechanisms involved.

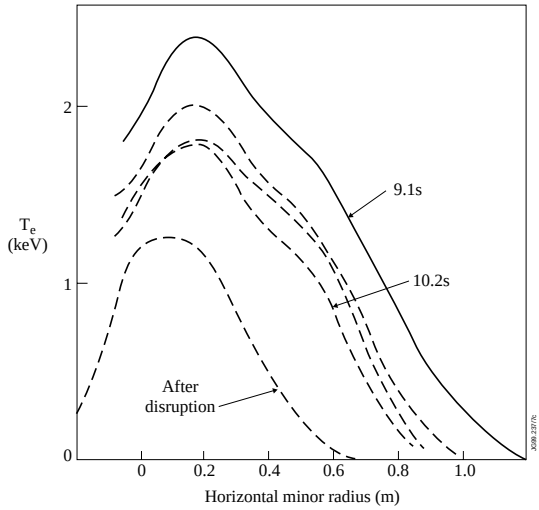

Figure 7.3. The impurity radiation induces a contraction of the plasma as shown by the sequence of electron temperature profiles. This finally leads to the violent mhd instability of the disruption.

Sawtooth Oscillations

Sawtooth oscillations were first observed on the ST tokamak in Princeton, the soft X-ray emission showing a relaxation instability in the core of the plasma. The emission rose slowly, and then collapsed rapidly as the instability occurred. The repetition of this behaviour produced the sawtooth-like traces shown in Figure 3.9.

The rapid collapse required an explanation, and an elegant model which seemed to account for the whole process was provided by Kadomtsev. The model involved a fast reconnection of the magnetic surfaces during the instability. Theoretical support for KadomtsevÕs model came from numerical simulations of sawtooth oscillations, these simulations showing clearly the role of the reconnection in the collapse process.

KadomtsevÕs model predicted that, because JET was much larger than previous tokamaks, the sawtooth collapse would be much slower. When JETÕs sawtooth oscillations were examined it was found that the collapse time was two orders of magnitude shorter than expected - in fact the collapse time was similar to that on smaller tokamaks.

In those early days there was optimism that this discrepancy could soon be resolved. However it was to turn out that this disagreement between theory and experiment over sawtooth oscillations was only the first. Subsequent analysis of the sawtooth instability on JET, mainly using the soft X-ray emission from the plasma, was to lead to several other difficulties, and to a world-wide effort by theoreticians to understand what is really going on.

Magnetic Geometry

Enhancements of the plasma control system were soon introduced. In particular feedback control of the plasma current and plasma shape became available. Control of the plasma shape allowed very elongated plasmas to be produced with height/width ratios up to 1.8. This was to be the starting point of a central part of the JET programme. With elongated plasmas there is a special magnetic surface called a separatrix, which separates two different types of magnetic topology as illustrated in Figure 7.4. Surfaces inside the separatrix form closed, nested magnetic surfaces, as needed for good confinement. Outside the separatrix the surfaces are open, with the field lines finding their way to material surfaces. At moderate elongations the separatrix lies outside the vacuum vessel, but with the new high elongations the separatrix entered the vessel with ÒX-pointsÓ just inside the vacuum vessel.

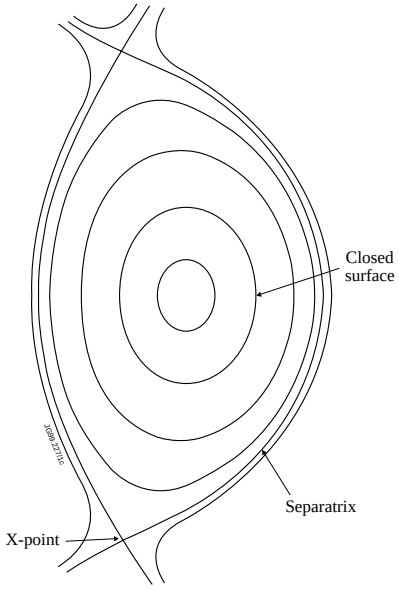

Figure 7.4. With plasma elongation a separatrix is introduced into the magnetic geometry. This separates the internal closed flux surfaces from external open surfaces. This change of geometry implies that there are "X-points" on the separatrix flux surface.

At first sight the introduction of open magnetic surfaces might not seem a good idea. However, the use of these open surfaces to lead the escaping plasma to a receiving material surface remote from the plasma had already been exploited on other tokamaks. The system is called a divertor. Furthermore such a divertor on the ASDEX tokamak had produced a different type of plasma with improved confinement at the edge of the plasma, giving a substantial improvement in overall confinement. This type of operation with higher confinement was called H-mode, in contrast to the normal lower confinement, now called L-mode.

The question, of course, was whether the separatrix created inside, but close to, the JET vacuum vessel would allow H-mode operation. The answer was yes. H-mode operation was found, and its merits and limitations were to become crucial areas of research, particularly concerning its compatibility with the divertor.

Impurities

The magnetic field provides insulation for the plasma and allows the achievement of high temperatures. Nevertheless it is inevitable that the energy leaving the plasma will be deposited on some kind of material surface. This leads to the release of impurities, and the problem of impurities entering the plasma from the surrounding surfaces soon became apparent. The radiation from these impurities was the principal energy loss mechanism, and impurities were also implicated in the disruptions suffered by the plasma. Finding the best way to overcome this problem soon became a major issue.

Metal surfaces with a high atomic mass, such as nickel and tungsten, have the advantage of high melting points. Their disadvantage is that, at the plasma temperatures of interest, their ions are not fully stripped of their electrons and are therefore able to radiate away the plasma energy. In the longer term there is also the disadvantage of diluting a thermonuclear plasma with the large number of electrons released from the metal ions.

The preference, therefore, was for materials with a low atomic mass and consequently few electrons per atom. These would be fully stripped in the bulk of the plasma, and would cause little radiation. This argument gained acceptance and graphite limiters were used rather than the nickel limiters which had been manufactured and were already available. In addition it was decided to install carbon tiles on the inboard wall of the vacuum vessel. Carbon was also evaporated on to all the plasma facing surfaces, this process being called carbonisation. While each carbonisation achieved its immediate aim of providing a fully carbon surrounding surface, the deposited carbon was soon eroded.

Is carbon the best material? A carbon atom has only 6 electrons, but there is a metal with only 4 atomic electrons, namely beryllium. On the other hand beryllium has a low melting point and its dust is toxic. Could a trial of beryllium be carried out in JET? These issues were regularly discussed as the JET programme got under way.

The early developments described above held the promise of a rich harvest of scientific results. They were, of course, all dependent on the wide range of quality diagnostics becoming available and on the advance of reliable machine operation. To illustrate the steady improvement in operational capability, Figure 7.5 shows the plasma current traces for a sequence of discharges. The first trace is from the first JET plasma, and the rest are for discharges in which the current first reached 1MA, 2MA and so on, up to the case which first exceeded the extended performance design current of 4.8MA in June 1985. Whether this current would be the limit was a question for the future years.

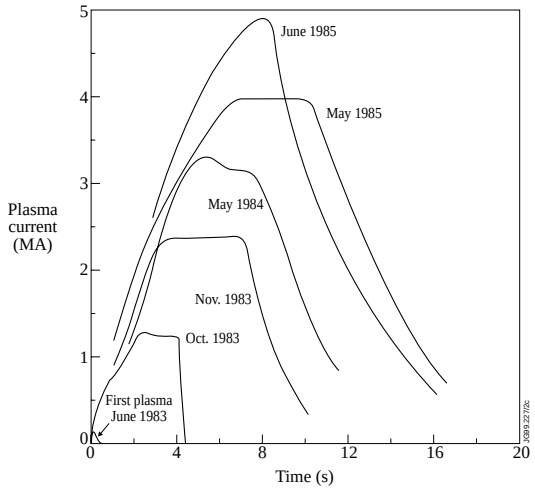

Figure 7.5. The JET plasma current was progressively increased as shown by the sequence of current traces.

Bibliography

The experimental results referred to in this chapter were reported in the first European Plasma Physics conference to be held after JET operation began. This meeting was in Budapest in September 1985 and the relevant contributions are:

Jacquinot, J., et al. ICRF studies on JET. Plasma Physics and Controlled Fusion, Vol. 28, p1(1986).

Bickerton, R.J., et al. Latest results from JET. Plasma Physics and Controlled Fusion, Vol.28, p55(1986).

Wesson, J.A. Sawtooth Oscillations. Plasma Physics and Controlled Fusion, Vol. 28, p243 (1986).

Campbell, D.J., et al. Analysis of sawtooth instabilities in JET. Proc. 12th Eur. Conf. on Controlled Fusion and Plasma Physics, 1985, Vol. I p130.

Wesson, J., Gowers, C., Han, W., Mast, F., Nave, F., Turner, M. and Watkins, M. Density limit disruptions in JET, Proc. 12th Eur. Conf. on Controlled Fusion and Plasma Physics, 1985, Vol. I, p147.

Tanga, A., et al. The formation of a magnetic separatrix in JET. Proc. 12th Eur. Conf. on Controlled Fusion and Plasma Physics, 1985, Vol. I, p70.

Denne, B., et al. Spectroscopic measurements of the impurity content of JET plasmas with ohmic and RF heating. Proc. 12th Eur. Conf. on Plasma Physics and Controlled Fusion, 1985, Vol. I, p379.

The suggestion that density limit disruptions occur at a critical level of radiation power loss was made by

Gibson, A. Radiation limits to tokamak operation. Nuclear Fusion 16, 546 (1976),

and the idea was further developed by

Rebut, P.H. and Green, B.J. Effect of impurity radiation on tokamak equilibrium. Plasma Physics and Controlled Fusion Research (Proc. 6th Int. Conf. Berchtesgaden 1976) Vol. 2, 3IAEA Vienna (1977).

8. JET PLASMAS

The Central Role of Heating

It is one thing to have the world's largest tokamak, it is another to heat its plasma. The large volume of the JET plasma meant that a substantial heating power would be required. In general terms the heating power needed to achieve given plasma conditions is expected to increase as the volume - which is proportional to the cube of the linear dimension, and to decrease with increased confinement time - which is roughly proportional to the square of the linear dimension. So the required power increases as the linear dimension of the tokamak, and JET would need a lot of power.

The key to producing plasmas with temperatures of thermonuclear interest was, therefore, to provide sufficient heating power. No one could know precisely how much heating would be required, but it would surely be tens of megawatts. The ion cyclotron heating system and the neutral beam injection were designed to achieve this, and by 1988 both were capable of providing about 20 megawatts of power.

Figure 8.1. Ion cyclotron antennas placed on the outer wall of the torus.

The ion cyclotron resonance heating (ICRH) was transmitted through eight antennas placed on the outer wall of the vacuum vessel as shown in Figure 8.1. The power is fed to the antennas through a network of coaxial transmission lines. The antennas emit high frequency electromagnetic waves which are then absorbed by the plasma through resonant coupling with the cyclotron motion. This coupling can be directly to the main ion component of the plasma or to a minority species, say hydrogen in deuterium.

Initially the ICRH had a problem - the antennas generated impurities. This was in large part due to bombardment of the nickel surfaces of the antennas by plasma particles accelerated along the magnetic field by the electric field of the waves emitted by the antenna itself. Once

this was realised the antennas were realigned to minimise the component of the electric field parallel to the magnetic field, and this brought a substantial improvement. The remaining effects were minimised by replacing the nickel by beryllium, which releases fewer atoms under bombardment and is a more acceptable impurity in the plasma.

The neutral beam system was designed to produced beam pulses of up to 10 seconds duration. The injection was made through two units each consisting of eight beam lines. In the early operation the deuterium ions were accelerated through a voltage of 80kV, and so their injection energy was 80keV. This was adequately above the desired plasma temperatures, 10-20 keV, but a higher energy would allow penetration to the centre of the plasma at higher plasma densities, and half the beam accelerators were modified to give 140keV.

When the beam particles are ionised and held in the plasma by the magnetic field they still have their initial beam energy, say 140keV. This energy is then transferred by collisions to the plasma particles. This heats the plasma, and slows the beam ions. The slowing continues until the beam ions have the same energy as the plasma ions. They then join the plasma ions as part of the basic plasma. The time for the slowing is typically a tenth of a second. These processes are found to be in agreement with theory and are, therefore, reliably predictable.

ICRH lifts a small number of resonant ions to a high energy. They are then slowed through collisions with the background plasma particles. The energy reached by ICRH driven particles is much larger than that of the neutral beam particles, a typical energy being 1MeV. At this high energy a large part of fast ion energy goes to electron heating, the electrons then sharing this heat with the plasma ions through collisions.

The Temperatures

The temperature envisaged for a fusion reactor is typically somewhat over 10keV, which is 100 million degrees. Temperatures well in excess of this were soon produced in JET. This is

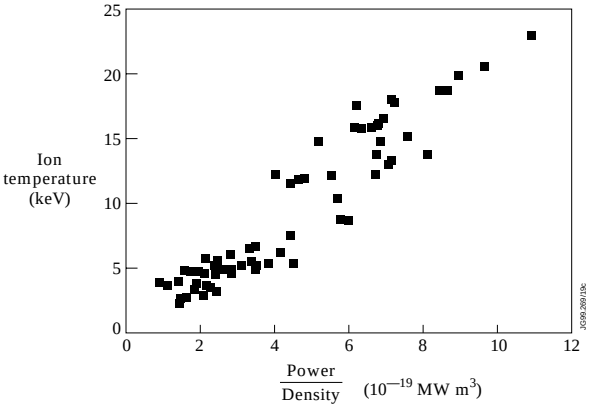

Figure8.2. Sho wingtheincr easeincentr aliontemper ature achieved with increasing power per particle, as measured by the central particle density.

illustrated in Figure 8.2 which plots values of ion temperature obtained for a range of power inputs measured in terms of the heating power per particle. It is seen that temperatures up to 23keV were reached. These results are from 1989 and subsequently ion temperatures over 40keV were achieved.

The results shown in Figure 8.2 were obtained with neutral beam heating. As the beam crosses the plasma the heat deposited at each magnetic surface is rapidly spread around that surface. Simply from the geometry, the volume over which this spreading occurs is smaller at smaller radii, and consequently the heating is most intense in the centre of the plasma, leading to very peaked ion temperature profiles such as that shown in Figure 8.3.

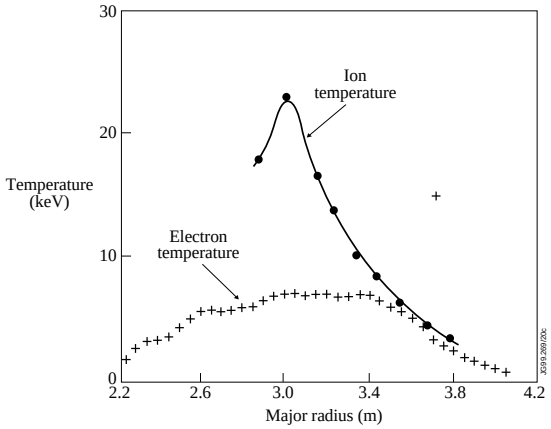

Figure 8.3. Ion and electron temperature profiles for a Òhot-ionÓ plasma, with a heating power of 20MW.

It is seen from the figure that the electron temperature is only 7keV, less than one third of the ion temperature. The reason is that for the neutral beam to reach the centre of the plasma the plasma density must not be too high, and operating at lower densities the transfer of heat from the ions to the electrons is quite small. Plasmas of this type are called “hot ion” plasmas. More equal ion and electron temperatures were obtained using combined neutral beam heating and ICRH, the electron heating by the ICRH tending to restore the balance.

Monster Sawteeth

Ion cyclotron heating came up with a complete surprise - monster sawteeth. The appearance of sawtooth oscillations on the traces of central temperature and density is so common as to generally pass unnoticed. With ICRH it was found that above a certain power level very large sawteeth would appear. Such a case is shown in Figure 8.4. The name monster sawtooth hides the reality, which is that the sawtooth instability has been stabilised - in some cases for up to 5 seconds.

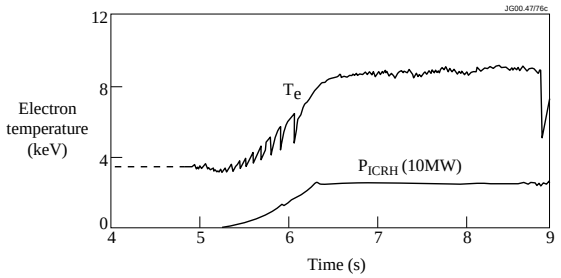

Figure 8.4. Monster sawtooth - actually the stabilisation of the sawtooth instability by the application of ion cyclotron heating. In this case the stabilisation lasts for about 3 seconds.

What is the cause of this stabilisation?

The theoretical story is quite interesting. It was shown that a sufficient number of sufficiently fast ions in the plasma core could stabilise the sawtooth instability and, of course, that is just what the ICRH can provide. It seems quite likely therefore that the fast ions are responsible for the stabilisation.

However, we shall find in Chapter 10 that the sawtooth instability is a mystery. While we apparently have a well developed stability theory, it does not explain what is seen experimentally. We might, therefore be in a situation where we have identified the stabilisation mechanism for an instability which is not itself understood.

Physics of the Temperature Measurements

The electron temperatures were first measured using the electron cyclotron emission, and the ion temperatures were determined from an analysis of the neutral particles escaping from the plasma.

The basis of the electron cyclotron method is that the emission from the plasma is characteristic of the electron temperature. With a simple black body the material is absorbent to its radiation except at its surface, and the radiation which escapes at the surface is therefore characterised by the surface temperature. The subtlety of the tokamak plasma is firstly that the surfaces from which the radiation escapes lie within the plasma, and secondly, for each emitting surface, the radiation has the cyclotron frequency associated with that surface. The cyclotron frequency is determined by the magnetic field and since the magnetic field varies across the plasma in a known way, essentially inversely proportional to the major radius, the location of the origin of radiation with a given frequency is known, and its intensity gives the temperature at that location.

Great care is needed to calibrate the detectors and there are many detailed complications to be allowed for, but this method provides a reliable electron temperature measurement.

The ion temperature measurement relies on the existence of the small number of neutral atoms in the plasma. It is somewhat surprising that there is a significant number of neutral particles deep inside the plasma. Neutral particles enter the plasma at its surface and, being slow, are typically ionised within a centimetre. However some of the incoming neutrals undergo charge exchange - transferring their electron to a plasma ion. The hot plasma ion, now neutralised, has a much longer mean free path than the original incoming neutrals and can reach the central plasma. If such neutral atoms now undergo charge exchange with the even hotter ions the resulting fast neutrals, with an energy distribution characteristic of the plasma temperature, can escape from the plasma and be measured. The measurement process involves stripping the neutral atom of its electron and passing the resulting ion through a combination of electric and magnetic fields. The amount of deflection in these fields gives the energy of the particle and the distribution of energies gives the temperature.

It is seen from this account that the measured ion temperature will be an average determined by the trajectory of the charge exchanged particles, usually involving several charge exchanges, and this method was later superseded by a more precise method - charge exchange recombination spectroscopy.

Measurement of the ion temperature by charge exchange spectroscopy requires the presence of a neutral beam, and in JET this is conveniently provided by the neutral beam used for plasma heating. A small fraction of the neutral beam particles undergo charge exchange with impurity ions, an electron being transferred to the impurity ion. Some of the impurity ions are left in an excited state, and when these ions relax to a lower energy state they emit their characteristic spectrum. Because the thermal velocity of the ions is virtually unaffected by the charge exchange, measurement of the Doppler width of their spectral lines gives the ion temperature. By viewing the neutral beam at different positions along its length the ion temperature profile is obtained.

LIDAR

LIDAR is an ingenious system designed for, and introduced on JET to measure the electron temperature and density. Its name is a variant on RADAR, with which radio pulses are sent out, and reflections from objects along the path of the pulse are used for detection and range finding. With the JET system light pulses replace the radio pulses.

The method is based on Thomson scattering. When light is passed through a plasma the electrons are accelerated by the oscillating electric field of the light wave and this acceleration causes them to emit radiation - so-called scattered radiation. However, because of their thermal motion the electrons pass through the wave and see a different frequency from that of the original wave. This causes a change in the frequency they emit, and because the change depends on the electron temperature analysis of the scattered radiation can give this temperature. The amount of scattering naturally depends on the number of scatterers, and so Thomson scattering can also be

used to measure the electron density. Thomson scattering measurements normally give results for a single point in the plasma. The clever idea with LIDAR is that the laser-produced light pulses are so short that they move across the plasma like bullets. This means that the measurements made at any instant correspond to the temperature and density of the electrons at the position of the pulse from which the detected scattered light was emitted. So, with a single pulse we obtain a space resolved measurement.

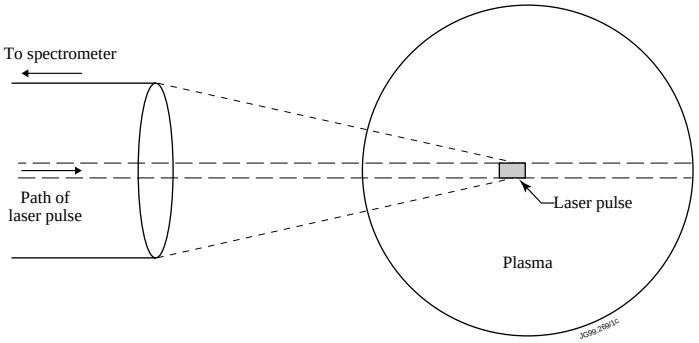

Figure 8.5. Illustrating the principle of LIDAR. The short laser pulse passes through the plasma, and the scattered light is transmitted to a spectrometer for analysis.

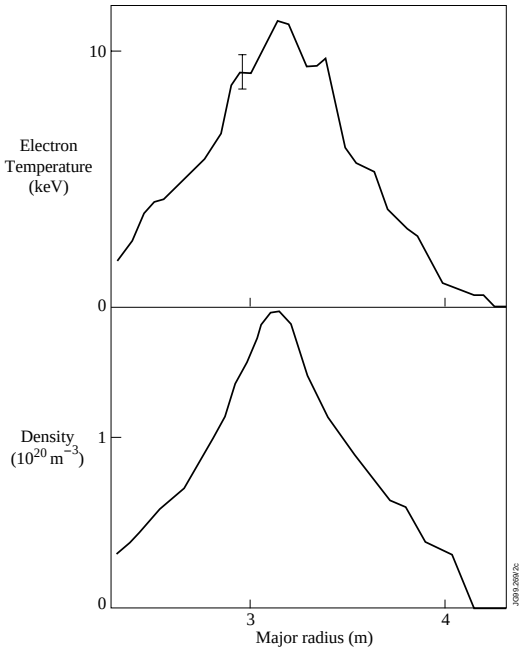

Figure8.6. Typicalmeasur ementsoftheelectr on temperature and electron density using LIDAR, giving the profiles across the major radius.

The principle of the measurement is illustrated in Figure 8.5, and typical measurements of temperature and density are shown in Figure 8.6. Initially the pulses were produced every few seconds, but the system was developed to produce regular pulses 4 times a second, giving both time and space resolved measurements.

Pellet Injection

Once a discharge has been formed the plasma density is controlled by the gas feed to the vacuum region around the plasma. Ionisation of the gas atoms as they enter the plasma provides a source of plasma particles, and the rate of gas supply is regulated to give the required plasma density.

Because the gas feed provides a source near the surface of the plasma, the resulting density profiles tend to be flat. There are obvious advantages from having a more peaked density profile. A higher density in the hotter central plasma would give a higher rate of fusion reactions and would not interact so directly with the surrounding material surfaces.

The required particle source can be achieved by firing high speed pellets of solid frozen hydrogen or deuterium into the plasma. When such pellets enter the plasma they are heated through the bombardment by plasma particles. The surface layer of the pellet evaporates, to become ionised and form part of the plasma. As the pellet moves across the plasma, successive layers are removed until the pellet is completely evaporated. With high speed pellets and the appropriate plasma conditions it can be arranged that the pellet provides a high central plasma density.

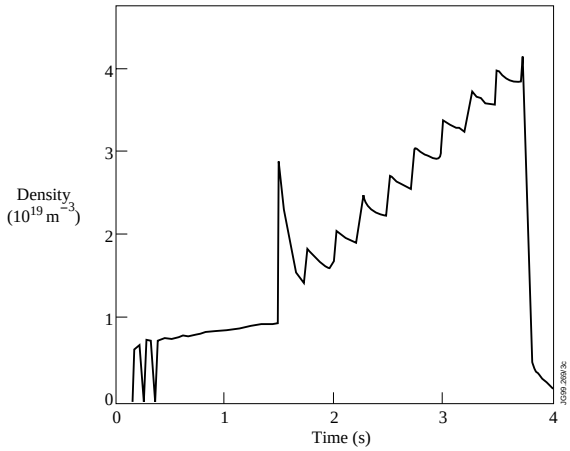

Figure 8.7. Density build-up resulting from the injection of a string of ten pellets into the plasma.

A multi-pellet injector was installed and operated on JET in collaboration with scientists from the United States. The pellets were 2.7mm and 4mm in diameter, and could be injected at

a rate of up to 5 per second with corresponding increases in plasma density as shown in Figure 8.7. The pellets were injected at a speed of 1km per second and at this speed they would reach the centre of the plasma in a millisecond. When injected into a high temperature plasma the pellets evaporated before reaching the centre, but when injected into an ohmically heated plasma they penetrated to the centre producing peaked density profile such as that shown in Figure 8.8. When such pellet injection was followed by plasma heating a remarkable improvement in central confinement was obtained, as will be described in Chapter11. The success in producing peaked density profiles is brought out in Figure 8.9 which shows how deeper pellet penetration gives improved density peaking as measured by the ratio of the central density to the average density.

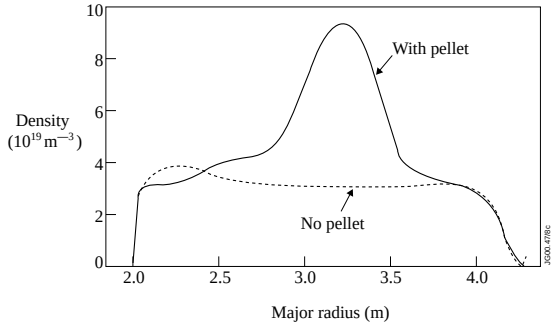

Figure8.8. Densitypr ofilef ollowingpelletinjection compar ed with a profile with no pellet.

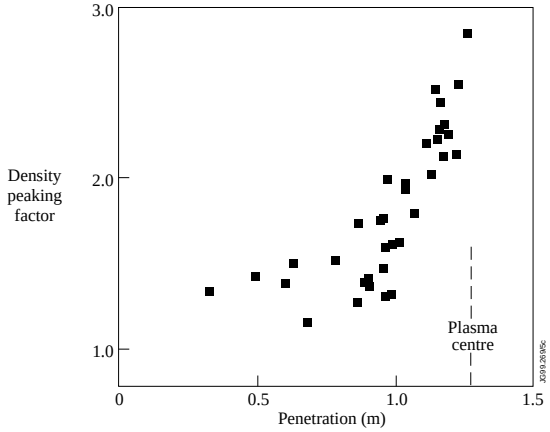

Figure8.9. Sho wing how the peaking of the plasma density achieved with pellet injection increases with pellet penetration into the plasma. The peaking is measured by the central density divided by the average density.

Plasma Density

Because the thermonuclear reaction rate is proportional to the square of the plasma density, it is important to obtain a high density. Two ways of fuelling the plasma have already been mentioned, gas feed and pellet injection. The density is also increased by the deposition of particles in the plasma during neutral beam injection as shown in Figure 8.10.

Unfortunately the density achieved is limited by a global disruptive instability which will be described in Chapter 10. The electron densities are usually a few times 10^{19} m^{-3}, with radial profiles which are generally flatter than the temperature profile. However, the peaked density profiles obtained with pellet injection have shown that it is the edge density which determines the disruption density limit. This implicates the plasma-surface interactions which introduce impurities into the plasma. It was of interest therefore to know the dependence of disruptions on the material of the surrounding surface.

Beryllium was seen as a possible alternative to carbon as a limiter and wall material, and a beryllium limiter was used in JET for a while. In addition, experiments were carried out with the vacuum vessel wall coated with an evaporated layer of beryllium. One result was that the disruption density limit was replaced by a different kind of density limit. As the density was increased a toroidally symmetric band of radiation appeared at the edge of the plasma on the inboard side. Such bands of radiation had previously been seen in the Alcator C tokamak, and the phenomenon was called by its discoverers a MARFE. The radiation is detected by an array of bolometers, and a tomographic reconstruction reveals the MARFE as shown in Figure 8.11. With beryllium coated walls attempts to increase the plasma density by gas feed would hit a limit, and further increase of the gas feed just led to a more intense MARFE.

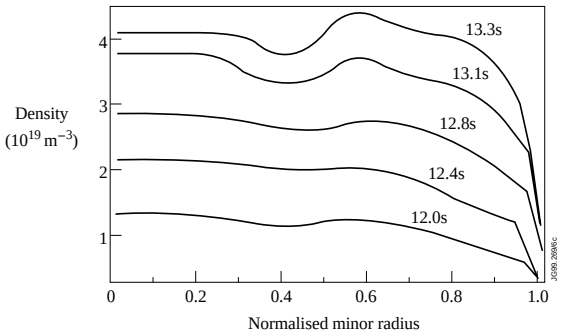

Figure 8.10. Electron density profiles over the normalised plasma radius showing how the plasma density is increased by neutral beam injection during a period of 1.3 seconds.

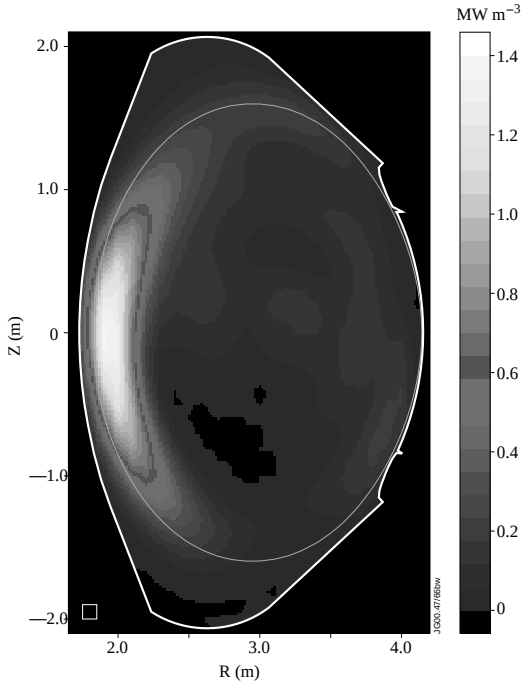

Figure 8.11. Tomographic reconstruction of the radiation from the plasma showing the formation of a MARFE on the inboard side of the torus.

Neoclassical Effects

The magnetic trapping of the particles toward the outboard side of tokamaks was described in Chapter 3. Theory predicts that important macroscopic effects can result from this trapping and these are termed neoclassical. Two important neoclassical effects have been observed experimentally. They were first reported by the Princeton Plasma Physics Laboratory and were also observed in JET.

The first effect is a modification of the resitivity. The reason in simple, trapped particles are unable to carry a current in response to an applied electric field. The effect is not just a small correction, it can result in a resistivity several times the classical value calculated without trapped particles, with a corresponding increase in the ohmic heating. Analysis of the JET results gives a neoclassical resistivity in agreement with theory.

The other effect, which is more subtle, was predicted by Bickerton, Connor and Taylor. It turns out that the radial pressure gradient causes a toroidal current to flow. Because the plasma "drives" this current for itself it is called the bootstrap current. The existence of this current is very fortunate because it partly relieves the problem of driving the toroidal current in a reactor. In present tokamaks the toroidal current is mainly produced by the electric field induced by a flux change linking the tokamak, as in a transformer. Clearly the amount of flux change is

limited, leaving the need for an alternative current drive, which the bootstrap effect can partly provide.

The bootstrap current is more difficult to observe experimentally than the neoclassical resistivity, but the results on JET are consistent with its existence and it plays an accepted part in the interpretation of results and in planning for a reactor.

MARFEs

By the time JET plasmas produced MARFEs, theoretical work at JET had already provided an explanation of the phenomenon. A key part of the physics involved is that, because the MARFE is toroidally symmetric whereas the field lines are helical, the MARFE is intersected by the field lines, as illustrated in Figure 8.12.

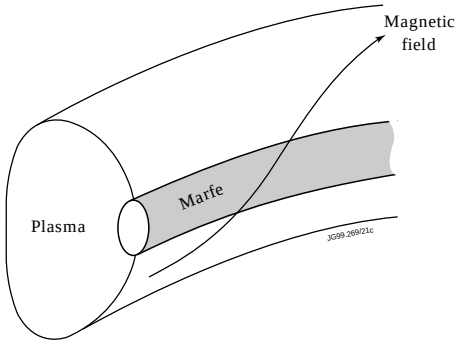

Figure 8.12. Showing how the magnetic field passes through the axisymmetric MARFE.

Because the thermal conductivity along the magnetic field is very high we would at first sight expect the plasma temperature and density to become constant along the field lines. In a MARFE they clearly do not, and we need a “drive” mechanism to maintain the MARFE.

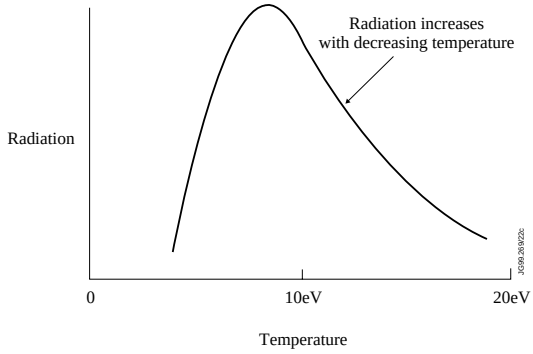

Figure 8.13. Over a range of temperatures the radiation increases with decreasing temperature. Radiation from the plasma lowers the temperature and increases the radiation still more, producing the MARFE instability.

The MARFE region is cooled by radiation from impurities, and it is the temperature dependence of this radiation which holds the key. In the temperature range of interest the impurity radiation increases with decreasing temperature as shown schematically in Figure8.13. As the radiation energy loss causes a fall in temperature, the radiation is further increased - and we have an instability. A further destabilising factor is that, because the pressure is constant along a field line, the lower temperature in the MARFE implies an increased density. The radiated power increases with density and this provides an additional drive.

What limits this process? The fall in temperature in the MARFE produces an increasing temperature difference between the MARFE and the surrounding plasma. This leads to conduction of heat into the MARFE, and a steady state is reached when the thermal conduction balances the radiated loss.

The Magnetic Field

Since the plasma is confined by the magnetic field we expect the plasma behaviour to depend on the magnitude of the magnetic field and, more subtley, on its structure.

The toroidal component of the magnetic field is basically straightforward. It is produced mainly by external coils, and a simple calculation shows that its strength will fall with major radius as 1/R.

The poloidal field is produced mainly by the toroidal plasma current. Although the total current is controlled, the distribution across the plasma is determined by the plasma itself. The ohmic current is driven by an applied toroidal electric field, but the local current density depends on the electron temperature, on the extent of electron trapping in the magnetic field, and on the impurity content. In addition, there is the bootstrap current, driven by the radial pressure gradient in the plasma.

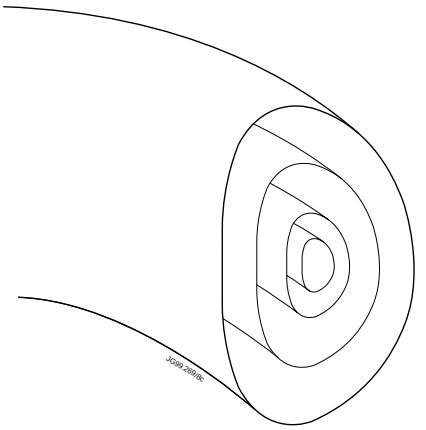

Figure 8.14. The magnetic flux surfaces form a set of nested toroids.

The distribution of the toroidal current and the associated poloidal magnetic field are difficult to measure, and we shall turn to this subject shortly. Firstly, however, we need to understand how the magnetic field structure in a tokamak is described. In its simplest form each magnetic field line lies in a toroidal surface. As it winds its helical path around the torus it stays within this magnetic surface. These surfaces do not intersect, and form a set of nested surfaces as shown in Figure 8.14. Each surface is characterised by a quantity, q, describing the rate of twist of the helical field lines. This q, called the safety factor, is a crucial quantity in understanding tokamaks and we shall now look at it more carefully.

The Safety Factor, q

The toroidal component of the magnetic field carries the field lines around the torus "the long way", and the poloidal component carries the field line round the magnetic surface "the short way", with the overall effect that the field lines wind a helical path around the torus.

The definition of the safety factor q, is that it is the number of toroidal turns a field line makes in completing one poloidal turn. Thus for field lines with little twist, q is high, and for field lines with a strong twist q is low.

The magnetic field lines lying in a given surface do not cross each other, so they all wind at the same rate and all have the same value of q. This means that each surface has its own q-value. Most surfaces do not have an integral value of q, and q varies continuously across the plasma. Tokamaks are characterised by having q greater than one everywhere except in a small region near the centre of the plasma, where q can be slightly below one.

For a special subset of surfaces the field lines join up on themselves after a number of turns. Such surfaces have rational values of q, its value being given by the ratio of two integers. If q= m/n, field lines join up after m toroidal turns, having made n poloidal turns. These surfaces, particularly for small m and n, are especially vulnerable to instability because a helical plasma deformation can match, or be "resonant" with, the field line. For example the sawtooth instability, having an m=1, n=1 structure, requires the presence of a q=1 surface.

The rate of change of q across the surfaces is called the shear. Generally shear is stabilising because an instability matching a resonant surface is forced to bend the field lines in neighbouring surfaces, and the larger the shear the more the bending required.

The safety factor q is a crucial quantity in understanding how tokamaks behave. In particular it is the key parameter in determining stability against the most dangerous types of instability. Since the toroidal field is known, measurement of q calls for a measurement of the poloidal magnetic field.

Preliminary measurements of q had been made by Peacock and Carolan using Thomson scattering in DITE in 1978, but the major step occurred when Soltwisch performed careful Faraday rotation measurements on TEXTOR in 1987, the same technique being adapted to JET shortly afterwards.

Measurement of q

In the Faraday rotation technique a polarised beam of light from a laser is passed through the plasma. In the absence of a magnetic field the direction of the polarisation would be unchanged by the plasma, but the effect of a magnetic field is to cause the direction of polarisation to rotate. Careful measurements of the small rotation allow the poloidal magnetic field to be measured and the q profile to be determined. However, the Faraday rotation measurement of magnetic field is indirect because it only gives a line average of the product of the magnetic field and the density.

We shall see later that the early measurements of q were full of surprises and uncertainties. This brought into focus the remarkable fact that, although magnetic fields are central to confinement in tokamaks, our ability to measure the magnetic field inside the plasma had for several decades remained very limited. This situation was radically changed by a chance observation on JET.

When neutral beams are injected to heat the plasma, some of the atoms are excited by plasma electrons and emit radiation in the form of spectral lines, these spectral lines being characteristic of the type of atom. The spectrum of the hydrogen atoms forming the beam is well known. It was surprising, therefore, that when the spectrum from the beam was examined it seemed to be full of strange lines.

It was soon realised that the magnetic field was the cause. It has been known for a century that an object moving across a magnetic field experiences an electric field, and it is also known that an electric field splits each spectral line of the atom into three lines. What had happened in the JET experiment was that this so called “motional Stark effect” had split the lines, and the superposition of lines from different beams had further complicated the spectrum.

Once the explanation was realised, the spectral pattern was understood. It was also clear that the motional Stark effect provided a way of measuring the magnetic field. In particular, the polarisation of the light emitted by the beams is related to pitch of the field lines and so to q. A flawed attempt at this measurement was made in JET but plasma physicists in the United States were quick to exploit the technique, and were able to obtain accurate measurements of the q-profile.

A Measurement of Shear

We shall see in the next chapter that understanding of the sawtooth instability depends upon knowledge of the q-profile, particularly inside and around the q=1 surface. In the early years of JET hard information about q was not available, but an ingenious piece of analysis provided an estimate of the rate of change of q, called the shear, at the q = 1 surface.

When hydrogen pellets are injected into the plasma, the hydrogen evaporating from their surface emits radiation. It was found that as the pellet passed through the q=1 surface the

radiation was much reduced, and a plot of the intensity of the measured radiation across the plasma radius showed a dip around this surface as shown in Figure 8.15.

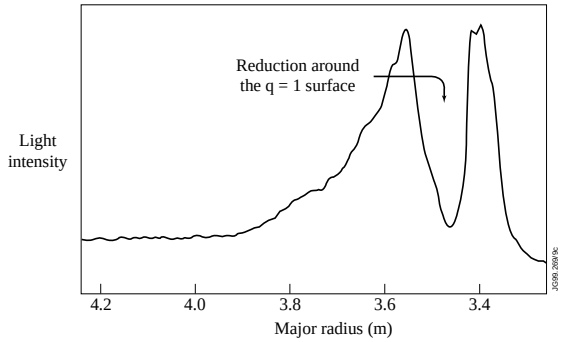

Figure8.15. As the injected pellet crosses the q=1 magnetic surface there is a dip in the radiated light.

The basic reason is that the field lines on the q=1 surface join up on themselves after one turn. So when the pellet passes through this surface, the cooling is localised to the field lines passing through the pellet. At other radii the field line will wind round the magnetic surface, and the cooling effect is more widely spread. The dip in radiation is therefore simply due to the reduced thermal capacity of the interacting plasma around the q=1 surface.

The key point is that the rate of transition from strong cooling on the q=1 surface to normal cooling away from it depends on the magnetic shear, and so measurement of the radial width of the dip in the radiation enables us to calculate the shear.

The calculated value of shear was very small, implying a very flat q profile in the region around q=1. This seemed to be in conflict with the q-profile obtained using the Faraday rotation measurement. Could there be a local flattening of q around q=1, not detected by Faraday rotation?

This measurement of magnetic shear became one of the pieces of the puzzle presented by the sawtooth instability and described in the next chapter - a puzzle not yet resolved.

Lower Hybrid Current Drive

So-called lower hybrid waves propagate in the plasma at frequencies between the electron and ion cyclotron frequencies. When these waves are launched in the plasma they can drive a current with good efficiency and this allows some control of the current profile. With this aim a lower hybrid current drive system was installed on JET using a grill structure of waveguides placed close to the plasma edge.

A prototype wave launcher was put in place in 1990 and, after an experimental programme, the full system was installed and ready for use in 1994. This system operated at 3.7 GHz and was capable of producing up to 7.3MW of power and sustaining current drive for more than ten

seconds. Driven currents drive of up to 3MA were achieved and the current profiles obtained were in general agreement with the theoretical simulations.

By driving currents in the outer plasma the current profile could be modified to raise the central value of the safety factor above 1 and so suppress the sawtooth instability. The lower hybrid system was also used to modify the current profile in the optimised shear discharges which will be described in Chapter 11.

Plasma Rotation

The neutral beams injected to heat the plasma have a component of their motion in the toroidal direction. As a result the beam deposits toroidal momentum in the plasma, and the plasma spins in the toroidal direction.

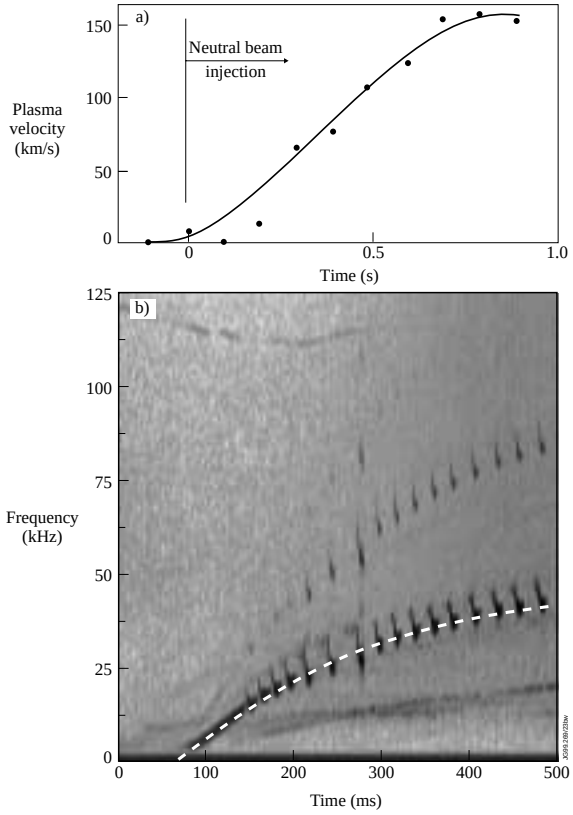

Figure8.16(a). When the neutral beam spins the plasma toroidally the resulting Doppler shift of the spectral lines emitted by the plasma allows a measurement of the plasma velocity. (b) The toroidal rotation is also detected by magnetic probes which measure the magnetic field perturbations of mhd instabilities, these instabilities being carried with the plasma.

This toroidal motion can be seen in the Doppler shift of spectral lines emitted from the plasma,

and an example is shown in Figure 8.16(a). It can also be observed in the externallymeasured magnetic perturbations. Mhd instabilities which arise in the plasma propagate with a small drift velocity even in a stationary plasma, but when the plasma is spun the magnetic perturbations are carried with the plasma, and can have much higher velocities than the natural drift velocity. Figure 8.16(b) shows the increasing frequency of a typical magnetic signal as the plasma is spun by beam injection.

Fluid driven through a pipe has its maximum flow velocity in the centre and a velocity profile which falls to zero at the wall. In the case of the plasma spinning round the torus it is not obvious what the corresponding boundary condition at the edge should be. If particles diffusing out of the plasma were simply lost we would expect the plasma to develop a uniform velocity over its minor cross-section. Figure 8.17 shows a typical experimental velocity profile. It is seen that there is a considerable fall-off in velocity toward the edge, indicating a drag force at the boundary. The radial gradient in velocity also implies a viscous drag in the plasma with an associated transport of momentum outward across the plasma radius.

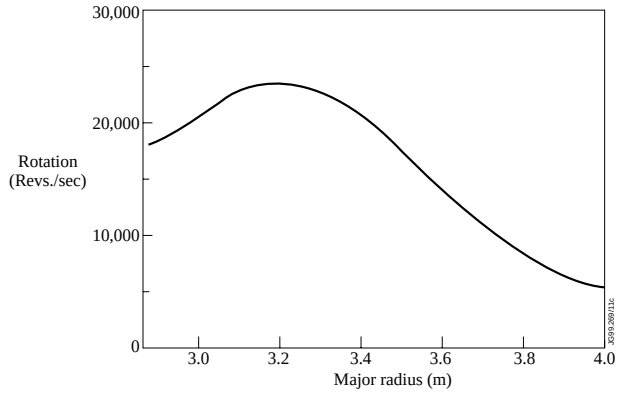

Figure 8.17. Typical radial profile of the toroidal rotation of a plasma spun by neutral beam injection.

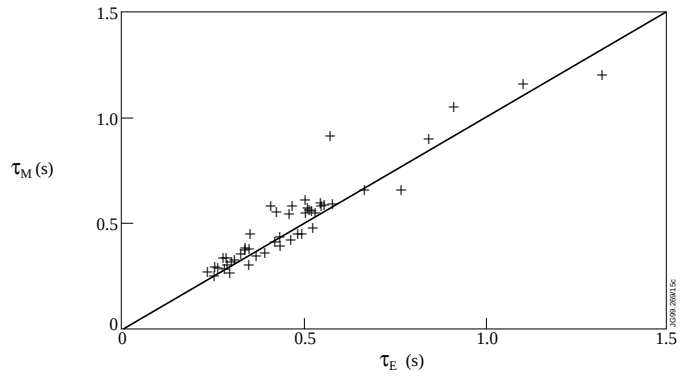

Figure8.18. The angular momentum confinement time plotted against the energy confinement time for a number of plasmas. The graph shows a clear correlation between the two.

It is found that there is a strong correlation between the ion temperature and the rotation velocity. Both, of course, are generated by the injected neutral beam, but the observed correlation, shown in Figure 8.18 also requires similar confinement times for the thermal and directed motion of the ions.

Centrifugal Effects

When the soft X-ray emission from spinning plasmas was examined it was found that there was a greater intensity from the outboard, larger major radius, side of the plasma than on the inboard side. A tomographic reconstruction of the radiation is shown in Figure 8.19. Because of the very fast connection along the magnetic field lines in a magnetic surface it is generally assumed that the temperature, density and impurity concentration are constant over a magnetic surface, and so the X-ray emission is also expected to be constant around the magnetic surface.

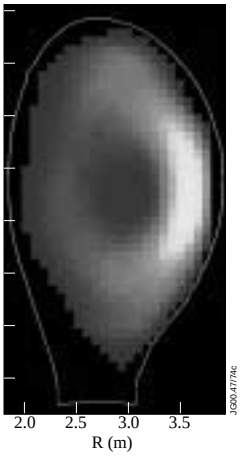

Figure8.19. Toroidal rotation of the plasma throws the impurity ions to the outboard side of the plasma. The tomographic reconstruction of the soft X-ray emission shows the resulting asymmetry.

However it was soon realised that the effect being observed was the same as had previously been found on ASDEX. The centrifugal force arising from the spinning was throwing the heavy impurities responsible for the X-ray emission to the outer part of the magnetic surfaces. Unlike most plasma phenomena, this centrifugal effect should be accurately predicted by theory, since it only involves an equilibrium force balance within the magnetic surfaces.

When the plasma spins round the torus it is subject to a centrifugal force. On each magnetic surface the rotation acts to throw the ions toward the outboard side. For the electrons, being much lighter, the centrifugal effect is negligible. Since the plasma must maintain quasi-neutrality an electric field is set up to pull the electrons outward with the displaced ions. In the resulting equilibrium the centrifugal force on the ions is balanced by a combination of two inward forces,

as illustrated in Figure 8.20. One is the pressure gradient force which arises from the outward displacement of the ions, and the other is the electric field force between the ions and electrons.

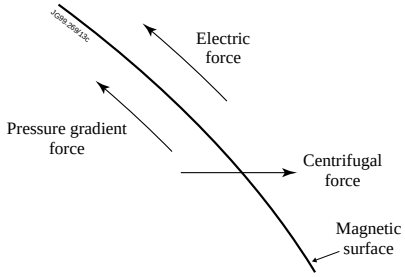

Figure 8.20. Force balance determines the distribution of the ions around the magnetic flux surface. The centrifugal force component along the surface is balanced by the sum of the pressure gradient force resulting from the redistribution of the plasma on the magnetic surface, and the electric field force necessary to maintain quasi-neutrality.

In fast spinning JET discharges the in-out imbalance in plasma density does not exceed 10%. However, the centrifugal force is proportional to the mass of the ion, and for heavy impurities the centrifugal force can be very large. The plasma from which Figure 8.19 was obtained had been seeded with a trace of nickel, and nickel ions have roughly 30 times the mass of deuterium ions. Typical cases had ratios of X-ray emission between outboard and inboard of around 5. When the interactions between the impurity ions, the deuterium ions and the electrons were fully taken into account, the theoretically predicted ratios were close to the experimental values.

Mode Locking

In JET the toroidal spinning of the plasma, as seen on the magnetic oscillations, sometimes comes to a rather abrupt halt. The magnetic perturbation is due to a mode of instability which has deformed the magnetic structure, producing a so-called magnetic island. These islands modify the magnetic structure in a similar way to that of knots in the otherwise regular grain of wood.

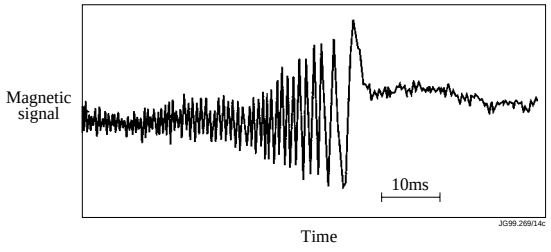

Figure8.21. The magnetic signal gives the frequency and growth of an mhd instability. The reduction in frequency shows the slowing of the plasma rotation. The signal measures the rate of change of the magnetic perturbation, and the removal of the gross oscillation indicates the final mode locking.

Figure 8.21 shows a time trace for a case where the plasma is slowed and halted. The measurement gives the time rate of change of the magnetic field as seen by a coil outside the plasma. As the plasma slows the observed frequency falls, and when the plasma comes to rest the signal disappears.

The reason the magnetic signal rotates with the plasma is that the magnetic perturbation is "frozen-in" to the plasma because of its high electrical conductivity. The explanation of the slowing involves a related phenomenon outside the plasma. The perturbed magnetic field extends to the conducting material surfaces surrounding the plasma, and the magnetic perturbations are partially frozen into these surfaces. However, the surrounding material is not as highly conducting as the plasma and the magnetic perturbations are able to slip through. Nevertheless some "friction" is involved and this imparts a drag on the plasma rotation. The theory of this process was developed and gave a good description of the experimental behaviour. Figure 8.22 shows the results of a numerical simulation of the mode locking process.

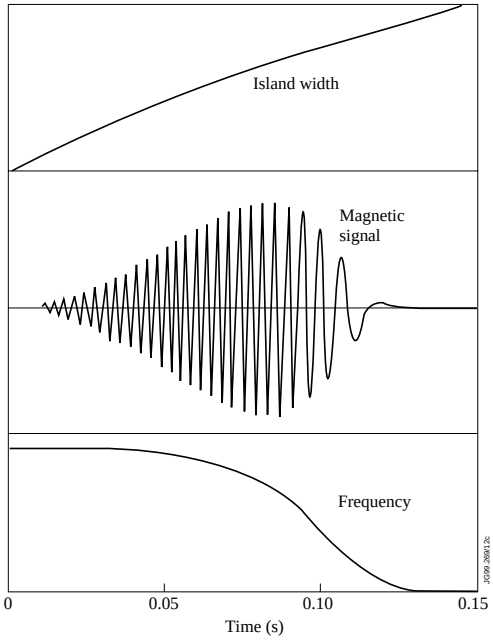

Figure8.22. A numerical simulation of the mode locking process shows the growth of the instability and the fall in frequency of the magnetic signal.

As the instability grows the drag increases and the plasma is brought almost to a stop. At very low velocities the magnetic perturbations "see" the non-uniformity in the structure of the surrounding surfaces, and ultimately lock into these non-uniformities bringing the rotation to a complete halt.

The experimental results on the basic features of JET plasma described in this chapter give some idea of the rich variety of the physics involved. In the next three chapters we turn to the main themes of the research involving these plasmas - the understanding and avoidance of instabilities, the study and improvement of plasma confinement and the control of the interaction between the plasma and the surrounding material surfaces.

Bibliography

An introduction to the JET ion cyclotron heating system together with some early results is given in

Jacquinot, J., Bhatnagar, V., Brinkschulle, H., Bures, M., Corti, S., Cottrell, G.A., Evrard, M., Gambier, D., Kaye, A., Lallia, P.P., Sand, F., Schueller, C., Tanga, A., Thomsen, K., and Wade, T. Additional heating experiments on JET with ion-cyclotron waves. Philosophical Transactions of the Royal Society A322, 95 (1987).

A companion paper for dealing with neutral beams is

Duesing, G., Lomas, P., Stäbler, A., Thomas, P., and Thomson, E. First neutral beam heating in JET, on p109 of the same journal.

A later account of neutral beam heating is given in

Thompson, E., Stork, D., de Esch, H.P.L., and the JET team. The use of neutral beam heating to produce high performance fusion plasmas, including the injection of tritium beams into JET. Physics of Fluids B5, 2468 (1993).

A further, more technical paper is

Jones, T.C.C., et al. Tritium operation of the JET neutral beam systems, Fusion Engineering and Design 47,205 (1999).

The technical aspects of the ICRH system are dealt with in

Kaye, A., Brown, T., Bhatnagar, V., Crawley, P., Jacquinot, J., Lobel, R., Plancoulaine, J., Rebut. P.H., Wade, T., and Walker, C. Present and Future JET ICRF antennas. Fusion Engineering and Design 24, 1 (1994).

Further papers relating to ion cyclotron heating are

Eriksson, L.-G., and Hellsten T. Electron heating during ion cyclotron resonance in JET. Nuclear Fusion 29, 875(1989).

Eriksson, L.-G., Hellsten, T., et al. Calculations of power deposition and velocity distributions during ICRH: Comparison with experimental results. Nuclear Fusion 29, 87 (1989).

Eriksson, L.-G., Gianella, R., Hellsten, T., Kallne, E., and Sundstrom, G. Observations of toroidal rotation induced by ICRH in JET Plasma. Physics and Controlled Fusion 34, 863 (1992).

Bhatnagar, V.P., Jacquinot, J., Start, D.F.H., and Tubbing, B.J.D. High concentration minority ion cyclotron resonace heating in JET. Plasma Nuclear Fusion 32, 83 (1993).

Eriksson, L.-G., Hellsten, T., and Willen, U. Comparsion of time dependent simulations with experiments in ion cyclotron heated plasmas. Nuclear Fusion 33, 1037 (1993).

Eriksson L.-G., Mantsinen, M.J., Rimini, F.G., Nguyen, F., Gormezano, C., Start, D.F.H., and Gondhalekar, A. ICRH heating of plasmas with third harmonic deuterium resonance. Nuclear Fusion 38, 265 (1998).

The discovery of the stabilisation implied by monster sawteeth was reported in

Campbell, D.J., Stork, D.M., and Wesson, J.A., et al. Stabilisation of sawteeth with additional heating in the JET tokamaks. Physical Review Letters 60, 2148 (1988).

Charge exchange spectroscopy has been highly developed at JET as described in the following papers.

Weisen, M., von Hellermann, M., Boileau, A., Horton, L.D., Mandl, W., and Summers, H.P. Charge exchange spectroscopy measurements of ion temperature and toroidal rotation in JET. Nuclear Fusion 29, 2187 (1989).

Mandl, W., Wolf, R., von Hellermann, M., and Summers, H.P. Beam emission spectroscopy as a comprehensive diagnostic tool. Plasma Physics and Controlled Fusion 35, 1373 (1993).

Zastrow, K-D, Core, W.G.F., Eriksson, L.-G., von Hellermann, M.G., Howman, A.C., and König, R.W.T. Transfer rates of toroidal angular momentum during neutral beam injection. Nuclear Fusion 38, 257 (1998).

Svensson, J., von Hellermann, M., and König, R. Analysis of charge exchange spectra using neutral networks at the JET tokamak. Plasma Physics and Controlled Fusion 4l, 315 (1999).

The Lidar system is described in

Saltzmann, H., Hirsch, K., Nielsen, P., Gowers, C., Gadd, A., Gadeberg, M. Murmann, H., and Schrodter, C. First results from the LIDAR scattering system on JET. Nuclear Fusion 27, 1925 (1987).

Studies of the behaviour of injected pellets are described in

Houlberg, W.A., Attenberger, S.E. Baylor, L.R., Gadeberg, M., Jernigan, T.C., Kupschus, P.,

Milora, S.L., Schmidt, G.L., Swain, D.W., and Watkins, M.L. Pellet penetration experiments on JET. Nuclear Fusion 32, 1951(1992),

and in

Baylor, L.R. Schmidth, G.L., et al. Pellet fuelling deposition measurements on JET and TFTR. Nuclear Fusion 32, 2177 (1992).

The interferometer system for measuing the density is described together with some typical results in

Fessey, J.A., Gowers C.W., Hugenhotz, C.A.J., and Slavin, K. Plasma electron density measurements from the JET 2mm wave interferometer. Journal of Physics E, Scientific Instruments 20, 619 (1987).

The detection of a bootstrap current was reported by

Cordey, J.G., Challis, C.D., and Stubberfield, P.M. Bootstrap current theory and experimental evidence. Plasma Physics and Controlled Fusion 30, 1625 (1988).

More detail and information on the beam driven current is given in

Challis, C.D., Cordey, J.G., HamnÇn, M., Stubberfield, P.M., Christiansen, J.P., Lazzaro, E., Muir, D.G., Stork, D., and Thomson, E. Non-inductively driven currents in JET. Nuclear Fusion 29, 563 (1989).

Bootstrap currents carrying 70% of the plasma current were described in

Challis, C.D., Hender, T.C., O'Rourke, J., et al. High bootstrap current in ICRH plasma in JET. Nuclear Fusion 33, 1097 (1993).

The applicability of neoclassical resistivity theory in JET is discussed in

Campbell, D.J., Lazzaro, E., Nave, M.F.F., Christiansen, J.P., Cordey, J.G., Schüller, F.C., and Thomas, P.R. Plasma resistivity and field penetration in JET. Nucelar Fusion 28, 981 (1988).

MARFEs were explained by Stringer, T.E. in A theory of MARFES, Proceedings of 12th European Conference on Controlled Fusion and Plasma Physics I, 86 (Budapest 1985).

The measurement of q using Faraday rotation is described in

O'Rourke, J. The change in the safety factor profile at a sawtooth collapse. Plasma Physics and Controlled Fusion 33, 289, (1991).

The recognition of the motional stark effect is described in

Boileau, A., von Hellerman, M.G. Mandl, W., Summers, H.P., Weisen, M., and Zinoviev, B., Observations of motional Stark features in the Balmer spectrum of deuterium in the JET plasma. Journal of Physics B, At. Mol. Opt. Phys. 22, L145 (1989),

and its use in measuring the magnetic field is illustrated by

Wolf, R.C., Eriksson, L.-G., von Hellermann, M., Konig, R., Mandl, W., and Porcelli, F. Motional Stark effect measurements of the local ICRH induced diamagnetism in JET plasmas. Nuclear Fusion 33, 1835 (1993).

The measurement of shear using soft x-ray emission is described in

Gill, R., Edwards, A.W., and Weller, A. Determination of shear on the q=1 surface of the JET tokamak. Nuclear Fusion 29, 821 (1989).

Control of the shear using ion cyclotron waves is described in

Bhatnagar V.P. et al. Local magnetic shear control in a tokamak via fast wave minority ion current drive: theory and experiments in JET. Nuclear Fusion 34, 1579 (1994).

Measurement of the neutral beam induced rotation is described in the paper by Zastrow, et al., listed above, and rotation due to ICRH is reported in

Eriksson, L.-G., Gianella, R., Hellsten, T., Kallne, E., and Sundstrom, G. Observations of toroidal plasma rotation in JET discharges. Plasma Physics and Controlled Fusion 34, 687 (1992).

Rotation with ICRH only is described in

Eriksson, L.-G., Righi, E., and Zastrow, K.-D. Toroidal rotation in ICRF-heated H-modes on JET. Plasma Physics and Controlled Fusion 39, 27 (1997).

The centrifugal effect on impurities is reported in

Alper, B., Edwards, A.W., Gianella, R., Gill, R.D., Ingeson, C., Romanelli, M., Wesson J., and Zastrow, K.-D., Strong asymmetries in impurity distribution of JET plasmas. Proc. 23rd Eur. Phys. Soc. Conf. on Controlled Fusion and Plasma Physics, Kiev, Part 1 p. a51 (1996),

and the theory was given in

Wesson J.A., Poloidal distribution of impurities in a rotating tokamak plasma. Nuclear Fusion 37, 577, (1997).

The basic physics of mode locking was explained by

Nave, M.F.F. and Wesson, J.A. Mode locking in tokamaks. Nuclear Fusion 30, 2575 (1990).

The neutrons resulting from D-D reactions in the plasma provided a further diagnostic as described in

Jarvis, O.N., Gorini, G., Hone, M., Kallne, J., Sadler, G., Merlo, V., and van Belle, P. Neutron spectrometry at JET. Review of Scientific Instruments 57, 1717 (1985).

Further investigations were reported in the papers

Boyd, D.A., Campbell, D.J., Cordey, J.G., Core, W.G.F., Christiansen, J.P., et al. ^{3}He-d Fusion reaction rate measurements during ICRH heating experiments in JET. Nuclear Fusion 30, 307 (1990).

Jarvis, O.N., Adams, J.M., Balet, B., Conroy, S., et al. Determination of deuterium concentrations in JET plasmas. Nuclear Fusion 30, 307 (1990).

Marcus, F.B., Adams, J.M., Bond, D.S., Hone, M.A., Howarth, P.J.A., Jarvis, O.N., Laughlin, M.J., Sadler, G., van Belle, P., and Watkins, N. Effects of sawtooth crashes on beam ions and fusion product tritons in JET. Nuclear Fusion 34, 687 (1994).

Jarvis, O.N, Adams, J.M., Marcus, F.B., and Sadler, G.J. Neutron profile measurements in JET. Fusion Engineering and Design 34-35, 59 (1997).

In certain discharges Helium 3 is accelerated to high energies (MeV) by the ICRH, and reactions with impurity ions produce gamma radiation. This is described in

Jarvis, O.N., Adams, J.M., Howarth, P.J.A., Marcus, F.B., Righi, E., Sadler, G., Start, D.F.H., van Belle, P., Warrick, C., and Watkins, N. Gamma-ray emission profile measurements from JET ICRF-heated discharges. Nuclear Fusion 36, 1513 (1996).

9. TOWARDS A REACTOR

The ultimate aim is a fusion reactor and with JET constructed and operating thoughts now turned to the reactor issues which could be addressed.

A basic requirement is that the plasma should not be subject to gross instability. From both theory and experimental experience it was established that stability boundaries impose operational limits on various parameters. For example it was well known that lowering the surface value of the safety factor q would at some point lead to a disruption of the plasma. It was therefore important for JET to investigate and determine this boundary. Disruptions also occur under other conditions, and there are further instabilities which, although not destroying the plasma, lead to a deterioration of confinement. The JET experiments were to bring to light unexpected behaviour, both good and bad. The next chapter will tell the story of these investigations.

Given overall stability, attention turns to the confinement requirements of a reactor. To heat the plasma to reactor conditions the heating systems must be able to overcome the energy losses from the plasma. However, if the energy confinement could be made good enough, the heating provided by the fusion α-particles alone would be able to balance the heat loss from the plasma. The plasma would then ignite and continue to burn without any applied heating.

It is possible to calculate an approximate condition for ignition which, through a coincidence of the algebra, gives a simple requirement on the plasma. The α-particle production rate is proportional to n^2, the square of the particle density. In the temperature range of interest the production rate happens also to be approximately proportional to the square of the temperature, T^2, and the α-particle heating per unit volume is therefore proportional to n^2T^2.

For ignition, this α-particle heating must be sufficient to balance the power loss from the plasma which, per unit volume, is given by the plasma energy density, 3nT, divided by the confinement time τ_E, giving a power loss proportional to nT/τ_E. Allowing for the geometry, with a 50:50 deuterium-tritium mixture, and taking the peak values of n and T, the α-particle heating will exceed the power loss for

$$\hat{n}^2\,\hat{T}^2 \;>\; 5\times10^{21}\;\frac{\hat{n}\hat{T}}{\tau_E}$$

where $\hat{T}$ is measured in keV. So we obtain the ignition requirement

$$\hat{n}\,\hat{T}\,\tau_E \;>\; 5\times10^{21}\ \mathrm{m^{-3}\,keVs}.$$

It is quite neat that the obviously important quantities n, T and τ_E should appear in such a simple way. It is also very convenient that although we have calculated the ignition condition for a deuterium-tritium plasma, the figure of merit $\hat{n}\hat{T}\tau_E$ can be calculated for, say, a pure deuterium plasma - the idea being that, in principle, the deuterium could be replaced by a deuterium-tritium mixture.

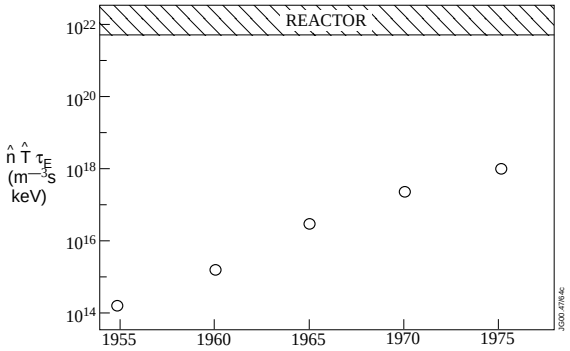

Figure 9.1. The product of the density, temperature and confinement time provides a measure of the progress towards reactor conditions. The graph shows the values achieved up to the design phase of JET.

Figure 9.1 shows the advance in achieved values of $\hat{n}\hat{T}\tau_E$ over the years up to the design phase of JET. We shall later add the values obtained on JET.

We saw in the previous chapter how the additional heating applied to JET produced the temperatures required for a reactor, and it will be seen in the next chapter how instability limits the density. What about the remaining factor, the confinement time τ_E?

It has already been made clear that plasma confinement is not understood. This means that we do not know the value of τ_E which would arise in a particular design of fusion reactor. We might have hoped that it would be possible to calculate τ_E, but the necessary theoretical understanding has not yet been achieved. This placed JET in a special position, for if we have to rely on empirical scaling to predict values of τ_E for a reactor, JET, being the largest tokamak, would have a crucial role. The results of the substantial research programme on this subject are described in Chapter 11.

The two chapters already mentioned, dealing with stability and confinement respectively, will be followed by one dealing with another crucial reactor relevant subject. The heat and particle loss from the plasma must be dealt with in a controlled way. The magnetic geometry is such that the “natural” heat loss results in a localised deposition on material surfaces at an unacceptably high level. Furthermore, impact of the plasma particles on the material surfaces releases atoms and molecules which can enter the plasma as impurities.

In the 1990s JET has concentrated on efforts aimed at solving these heat load and impurity problems by constructing divertors which carry the escaping plasma away from the main plasma and make its effects as harmless as possible.

When we have dealt with all of these reactor relevant issues we shall look at some basic plasma physics investigations, and then turn to the fusion power experiments using tritium. These historic fusion experiments were such an important step toward a reactor that almost all the areas of work on JET came to be seen as reactor oriented. This changed perception was

further strengthened by requests for reactor relevent information from the team designing a possible tokamak reactor to follow JET, namely ITER.

ITER stands for International Thermonuclear Reactor, and like JET its design team was based on an international collaboration. There were four partners - the European Community, Japan, the Russian Federation and the USA. The aim was to design a tokamak which would ignite and produce fusion power in the gigawatt range. The successful design of such a reactor calls for answers to many questions which only existing tokamaks can provide. In the crucial areas of stability, confinement, heat exhaust, and deuterium-tritium plasmas JET was very well placed to address the issues involved.

10. STABILITY AND INSTABILITY

In the early days of fusion research many approaches to magnetic confinement of plasmas were tried. Each had its particular magnetic configuration, and most were found to be grossly unstable. Tokamaks are basically stable. With the appropriate operating conditions they show none of the fluctuations of the magnetic field which are the signatures of unstable plasmas.

However in pushing the plasma parameters toward the desired high pressures, and in increasing the plasma current to achieve better confinement, a variety of instabilities appear. At a low level these instabilities do not significantly affect confinement, but there are circumstances where they completely disrupt the plasma and even bring a collapse of the plasma current.

Two other instabilities which are regularly seen are called the sawtooth instability and the ELM, standing for Edge Localised Mode. Both of these instabilities have the form of a relaxation oscillation - there is an abrupt instability, removing the destabilising conditions, and a slow recovery returning the plasma to an unstable condition once again. This leads to a repetitive instability. Both instabilities are localised, the sawtooth instability to the core of the plasma and the ELM typically to the outer 10% of the radius. In their milder forms the sawtooth instability and the ELM only have a weak effect on confinement, but in their grosser forms both present a serious problem.

We shall look at these instabilities in turn, but first it should be made clear that they are not the only instabilities. There are other small amplitude fluctuations and in particular, and crucially, it is generally believed that the observed "degradation of confinement" is due to the small fluctuations caused by an unidentified instability. The mysteries of plasma confinement are described in Chapter 11.

Disruptions

It is hard to imagine a more dramatic end to a tokamak plasma than that caused by a "disruption". In fast JET disruptions the plasma energy is wholly lost in a few milliseconds and the plasma current decays away in about ten milliseconds. Figure 10.1 shows the abruptness of the current decay for a typical fast disruption. The associated power loss from the plasma can be several gigawatts, a hundred times the applied heating power. These disruption events cause eddy currents to flow in the vacuum vessel with associated forces of hundreds of tonnes. Some JET disruptions end with part of the plasma current being transferred to a beam of relativistic electrons, constituting a further threat to the surrounding material surfaces. Clearly a fusion reactor must not be subject to such sudden destruction of the plasma, with the even larger forces involved.

There were two lines of investigation to follow. Firstly it was necessary to make an empirical exploration of the operational boundaries which disruptions impose on disruption-free operation. This was clearly an important question both for the operation of JET, and to provide design

constraints on a possible fusion reactor. Secondly it was important to understand what was happening in a disruption. In earlier days it had been common to ask as to "the cause of disruptions". When a careful examination of the problem was made it was found that there was a sequence of events, the importance and cause of each being dependent on the type of disruption.

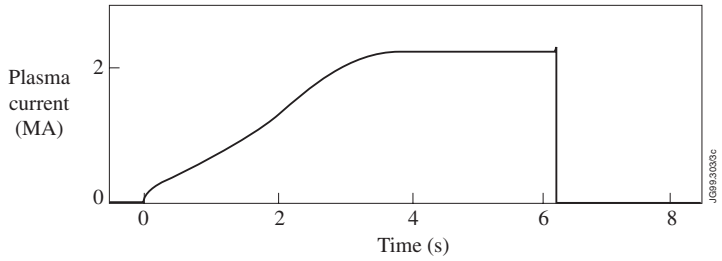

Figure 10.1. Time trace of the plasma current showing the abruptness of the current decay in a fast disruption.

Murakami Parameter and the Hugill Diagram

The empirical approach to disruptions had started at the Oak Ridge National Laboratory when Murakami noticed that disruptions in ohmically heated tokamaks limited the achievable value of the parameter nR/B_ϕ, where n is the plasma density, R the major radius of the tokamak, and B_ϕ the toroidal magnetic field.

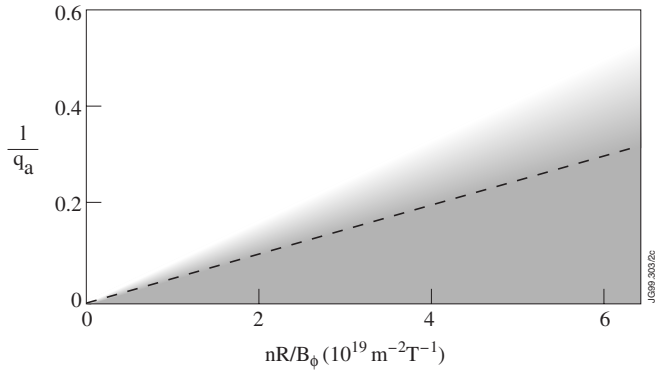

Figure 10.2. The Hugill diagram for JET. With ohmically heated plasma operation in the shaded region was precluded by disruptions. Some amelioration was achieved when additional heating was used, as indicated by the dashed line.

This idea was elaborated by Hugill who showed that the disruption limit also depended on the value of the safety factor at the edge of the plasma, q_a . He found that it was useful to plot disruptions in a diagram with $1/q_a$ as the vertical axis, and the Murakami parameter as the horizontal axis. The Hugill diagram for JET is shown in Figure 10.2.

With ohmic heating alone, attempts to enter the shaded region in the diagram resulted in disruptions, and the boundaries limited the achievable density and the minimum value of q_a. With additional heating there was some increase in the density limit as indicated by the dashed

line. This gave some support to the idea that disruptions were due to a loss of power balance, the additional heating being able to make up for the increased radiation losses occurring at higher density.

It must be made clear that the unshaded region is not free of disruptions. For various operational reasons, including too fast a current rise, disruptions can occur under almost all plasma conditions. The point of the disruption boundary is that, with careful operation, it is possible to be disruption-free away from it.

The Low-q Limit

The low-q limit in the Hugill diagram restricts the plasma current which can be used with a given toroidal magnetic field. The definition of q_a used in compiling the diagram is an operational one used for simplicity. It seems likely that the plasma is more aware of the q defined by the actual magnetic geometry - the true q. As described in Chapter 8 rational values of this q have special significance, in that the field lines "join up on themselves" and are associated with instability.

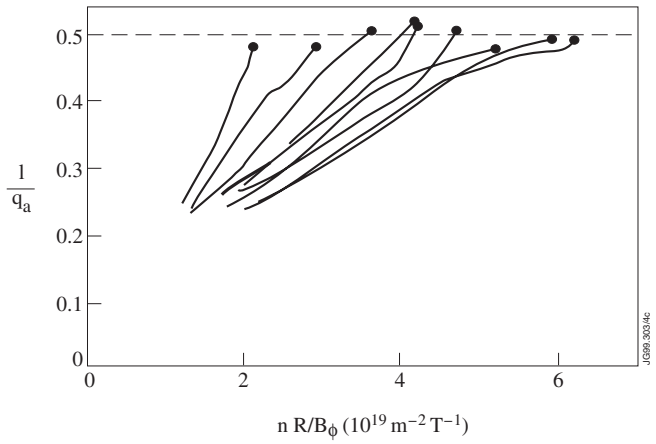

Figure 10.3. Trajectories of discharges in the Hugill diagram showing the disruption boundary to be close to $q_a = 2$.

To investigate this, experiments were carried out in which, by increasing the plasma current, the value of true q_a was gradually reduced until the plasma disrupted. Figure 10.3 shows the path of these discharges in the Hugill diagram for several starting densities, the dots indicating the disruption. It is seen that all of the disruptions occur close to $1/q_a = 0.5$, which means $q_a = 2$.

What happens in these experiments as the current is increased is that the q-profile falls, as illustrated in Figure 10.4. It is seen that in this process the position of the q = 2 surface moves outward and crosses the plasma edge when $q_a = 2$. Theory tells us that the plasma is prone to a strong instability driven by the current gradient when the q = 2 surface sits close to the edge of the plasma. We see, therefore, that the occurrence of the disruptions at $q_a = 2$ is in good agreement with theory.

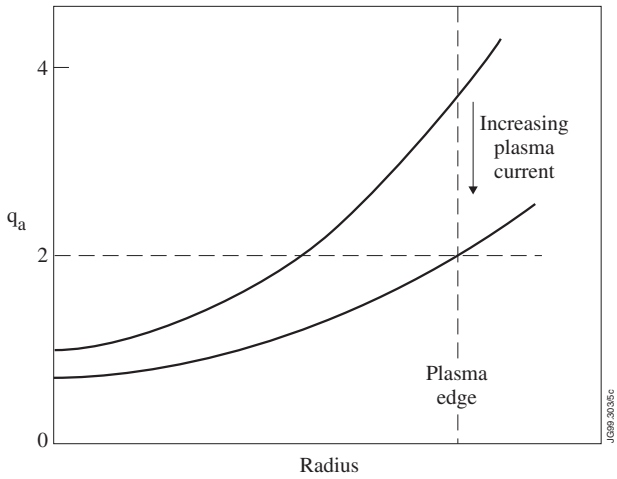

Figure 10.4. As the plasma current is increased the q-profile falls. Disruption occurs when the edge q-value reaches 2.

Density Limit Disruptions

The Hugill diagram implies that for given q_a and toroidal magnetic field the plasma density is limited by disruptions. The disruptions occur when the increased density leads to a critical form of current and q profile. The plasma is then subject to an mhd instability, usually a so-called tearing mode. Its name comes from the fact that the destabilising force tears the magnetic surfaces, which reconnect into a different geometry. The process is illustrated in Figure 10.5, which shows that the reconnected surfaces form a new localised set of magnetic surfaces called a magnetic island.

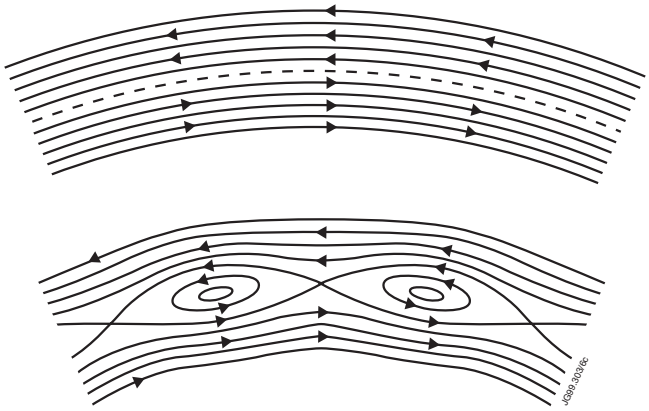

Figure 10.5. Illustrating how, in a tearing instability, the magnetic surfaces around a rational q surface reconnect to form a magnetic island.

The most easily detected feature of the instability is the perturbed magnetic field. Although the reconnection of the magnetic surfaces is localised, the magnetic perturbation extends outside the plasma surface and is easily detected using small magnetic coils as pick-up loops. The instability usually rotates toroidally passing repeatedly under the magnetic coils. The voltage

induced in the pick-up coils is proportional to the rate of change of the magnetic field, usually written as $\dot{B}$, and so the toroidal rotation produces a periodic signal.

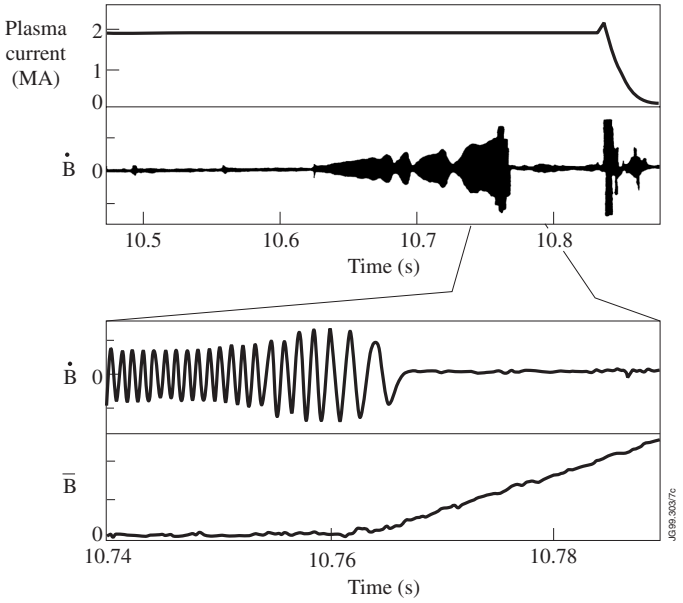

Figure 10.6. Showing the growth of an instability prior to a disruption, as detected by the magnetic coils measuring $\dot{B}$. The expanded trace shows the decreasing frequency of the signal as the toroidal rotation of the instability is slowed, and the continued growth in the directly measured amplitude of the instability, $\overline{B}$, after the $\dot{B}$ signal is lost by mode locking.

Figure 10.6 shows the growth of the $\dot{B}$ signal before a disruption. This growth implies the growth of the associated magnetic island in the plasma. In the expanded trace the separate oscillations are made clear. The trace also shows that the frequency drops and the signal almost disappears. This slowing of the rotation had previously been thought to be due to an internal effect within the plasma. Analysis of the JET results showed that the slowing is due to a coupling of the external magnetic perturbations to the vacuum vessel. As described in Chapter 8 the reaction on the plasma is a force which brings the rotation of the instability almost to a halt. In the experiment the rotation stops entirely, the perturbation becoming locked to some small toroidal non-uniformity in the tokamak structure.

However, the loss of rotation does not mean that the instability has stopped growing and Figure 10.6 also shows the continued growth using the magnetic perturbation directly rather than its rate of change. Theory indicated that the magnetic perturbation observed outside the plasma is associated with a tearing instability and the associated formation of a magnetic island inside the plasma. The magnetic field lines inside the island wind around the island's magnetic axis, and fast thermal conduction along the field lines leads to a flattening of the temperature profile over the island. When the electron temperature profile was measured just such an effect was found as shown in Figure 10.7. This provided direct evidence that a large magnetic reconnection was involved in the disruption.

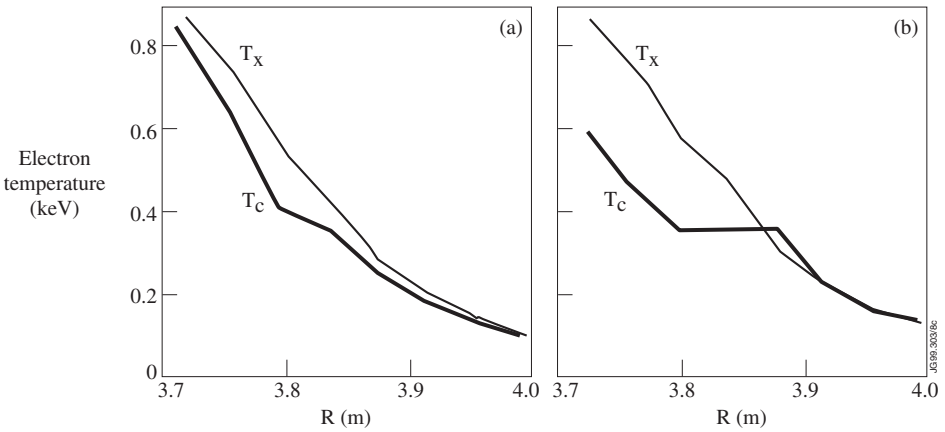

Figure 10.7. Graphs of the radial profile of the electron temperature. T_C is the profile through the centre of the magnetic island and T_X is that through the ends of the island (the X-point). Graph (a) is at an early stage in the island growth and graph (b), shows a more complete flattening of the temperature across the island a few milliseconds later.

Although the magnetic island might cover 10-20 cm of the plasma radius and effectively destroy the confinement of this region, it did not by itself explain the almost complete loss of confinement. The behaviour of the central electron temperature in a severe disruption is shown in Figure 10.8. It is seen that in the first stage the temperature falls by over 60%. While there is no direct evidence it seems likely that the initial growth of the tearing instability is followed by a more complete rearrangement of the magnetic field, producing a more general flattening of the temperature and loss of plasma energy. Numerical simulations of the JET disruption by Bondeson appear to bear this out.

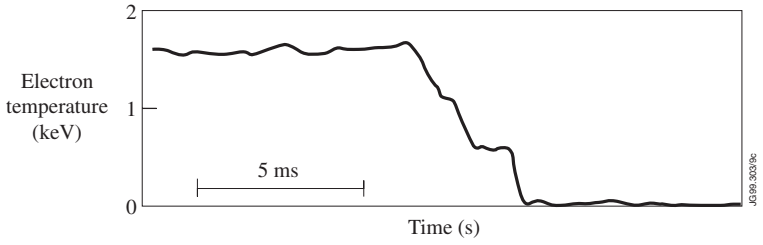

Figure 10.8. Collapse of the electron temperature during a severe disruption.

The Loss of Current

In severe disruptions not only is the plasma energy lost, the plasma current decays away also. It is generally accepted that the loss of energy is due to strong plasma turbulence induced by instability. It was also widely thought that this turbulence presented an increased resistance to the plasma current, making it decay. However, in that case it would be expected that as the current decayed, stability would be restored and the decay would slow or stop. In the current decay following JET disruptions this did not happen, and another explanation was clearly required.

Examination of the strongest disruptions provided a simple but puzzling explanation. The current decays because the plasma is cold, by the standards of tokamak plasmas - very cold. First, the electron cyclotron emission measurements showed that the temperature was less than 30eV, and then the spectroscopic measurements gave a few eV. Calculations showed that although magnetic turbulence could reduce the temperature to 100eV, it was impossible for it to produce temperatures as low as a few eV. How did the energy loss occur?

One possibility was impurity radiation. The total power emitted by the plasma was detected by bolometers, which measure the temperature increase brought about by the radiation on a surface of known thermal capacity. Examination of the results showed that enormous powers were radiated by the plasma at the time of severe disruptions - often several gigawatts. This was quite adequate to explain the fast energy loss from the plasma, and also explained the current decay. If the low measured temperatures were correct, the plasma would have a very high resistance, and the ohmic heating at these temperatures could be gigawatts, consistent with the measured radiated power. The energy for this heating and radiation comes from the magnetic field of the plasma current, and as the magnetic field is consumed, so the current decays.

The Impurity Influx

The above explanation of energy loss and power balance in disruptions leaves open an awkward question. How did the high level of impurities required for the large fall in temperature and jump in radiation suddenly arise? It seemed possible that the initial loss of confinement had poured heat onto surrounding surfaces, and that this had released impurity atoms allowing them to reach the plasma. But how did they penetrate into the plasma?

When an impurity atom enters the plasma it will be moving with a low velocity. As it moves into the plasma it will be bombarded by the fast plasma electrons and will quickly be ionised. Typically the impurity atom would penetrate only a centimetre into the plasma before being ionised and held by the magnetic field.

For some years this problem prevented acceptance of the impurity explanation of the rapid current decays in severe disruptions. A surprising resolution of the difficulty was then suggested. Perhaps the impurity influx occurred, not as a result of individual particles penetrating the plasma, but rather as a bulk inflow of gaseous impurity which displaced the plasma rather than penetrating it.

The obvious test of this idea was its prediction of an increase in the density. Examination of the interferometer measurements of the electron density after the disruption showed an increase by at least a factor 4, and spectroscopic analysis gave a 5-fold increase in the carbon density. These measurements therefore confirmed the model of severe disruptions in which an mhd instability allows energy to escape from the plasma to release impurities at such high intensity that they are able to force their way into the plasma.

The Negative Voltage Spike

An initially surprising feature of disruptions is the appearance of a negative voltage spike on the toroidal loop measuring the voltage, as shown in Figure 10.9. It would be expected that, since the predominant effect of the disruption is to produce a current decay, there would be an induced positive voltage, according to Lenz's law, to maintain the plasma current.

The explanation is that there is a brief *increase* in current before it decays. The magnetic energy associated with the plasma current, I, is $\frac{1}{2}LI^2$, where L is the inductance of the plasma current. The disruptive instability flattens the plasma current profile and this reduces the inductance. We see therefore that for a fixed magnetic energy the plasma current will increase - and this is what happens. So we have a *negative* voltage spike, which is then followed by a more prolonged, positive voltage as the current decays.

The JET experiments came up with a further surprise. In the disruption the negative voltage spike is associated with the instability-induced magnetic rearrangement which causes the initial energy loss. We would expect, therefore, that the negative voltage spike would occur at the same time as the main temperature drop. In fact it was found to be delayed as is apparent from Figure 10.9.

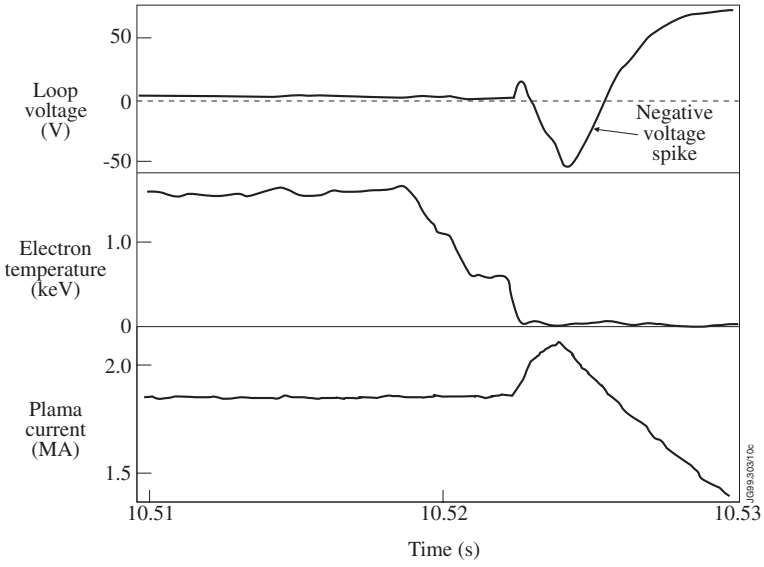

Figure 10.9. At the time of the disruption a negative voltage spike appears before the expected positive voltage which resists the current decay. The negative voltage results from the associated brief increase in the plasma current brought about by a fall in its inductance as the current profile is flattened by the instability.

The resolution of this problem appears to be that the rearrangement of the current does not reach the edge of the plasma. The induced negative voltage will then appear at the surface of the internal rearrangement, and will drive a negative current sheet inside the plasma at this surface. When, shortly afterwards, the plasma is cooled by the influx of impurities, the negative current rapidly decays. This produces a sudden increase in the total positive current with its associated negative voltage spike, now delayed, as seen in the experiment.

Sawtooth Oscillations

Sawtooth oscillations are a regular feature of JET discharges. They involve a repetitive collapse of the electron temperature in the plasma core and, as shown in Figure 10.10, are also seen on the measurement of the line integrated density.

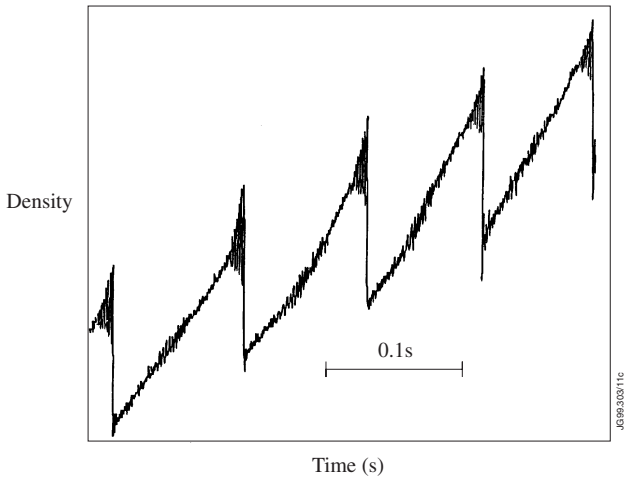

Figure 10.10. Sawtooth oscillations on the electron density.

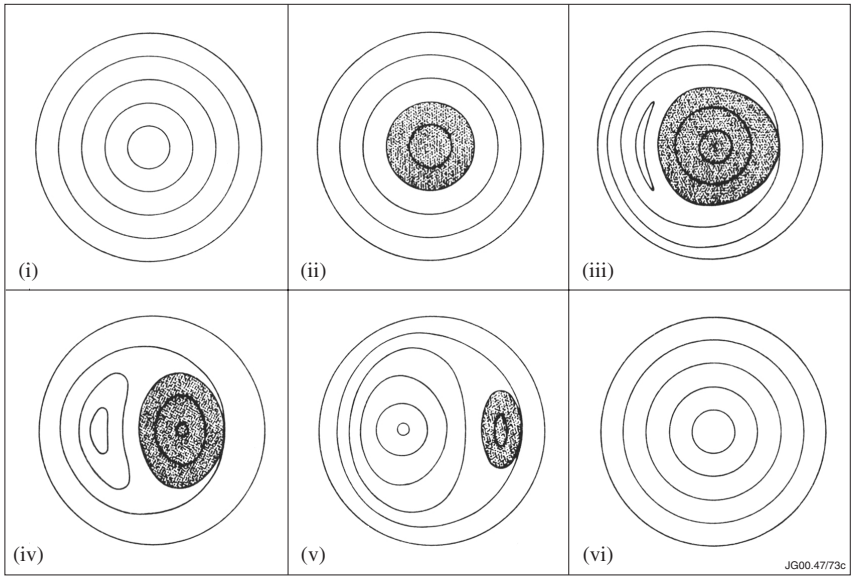

Figure 10.11. In Kadomtsev's model of the sawtooth instability magnetic reconnection in the centre of the plasma produces a magnetic island which grows to replace the original magnetic surfaces with $q < 1$ (shown shaded).

It was mentioned in Chapter 7 that Kadomtsev had proposed a model for the sawtooth instability, and that the collapse phase observed in JET was inconsistent with its predictions. Let us first look at Kadomtsev's model.

An instability starts when the central value of q falls below one. A magnetic reconnection then occurs through the growth of a magnetic island as illustrated in Figure 10.11. This is the fast phase of the sawtooth oscillation and results in a q profile with q approximately equal to one over the central part of the plasma as shown in Figure 10.12. During the ramp phase of the instability the q profile diffuses back toward its more natural state with q_o, the central value of q, falling below one. After a while this profile becomes unstable and the next collapse occurs - this cycle being followed repeatedly.

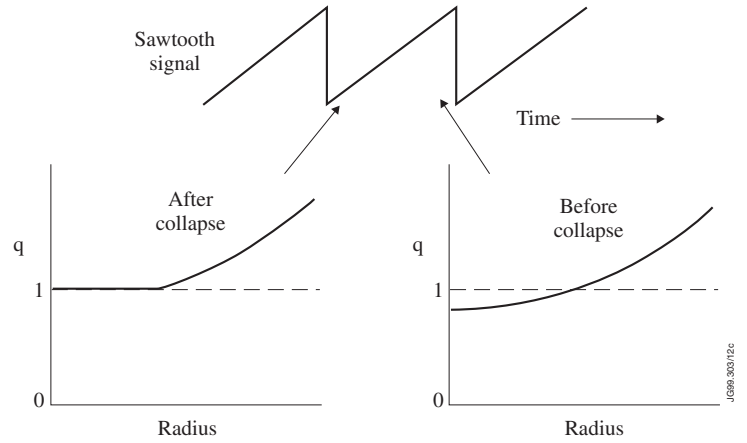

Figure 10.12. Kadomtsev's model predicts a flattening of the q-profile at the sawtooth collapse and the development of an unstable profile with q < 1 during the ramp phase.

Quasi-interchange

Examination of this cycle for sawtooth oscillations in JET revealed an inconsistency in the model. At the high temperature of JET, and with its large physical size, it was calculated that the diffusion of the q-profile during the ramp phase was so slow that q_o would hardly change from

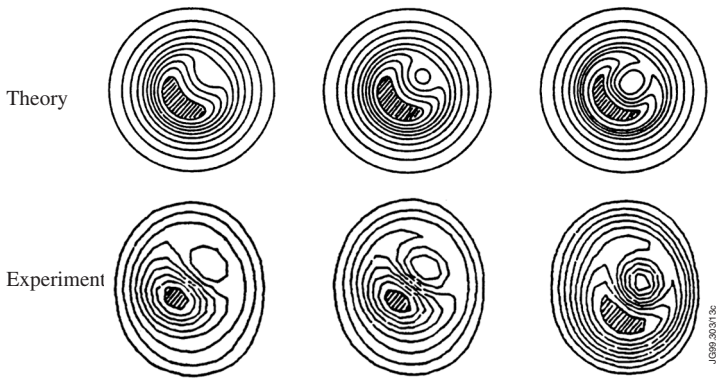

Figure 10.13. Comparison of the type of deformation predicted for the quasi-interchange instability, and the observed deformation as reconstructed from the soft X-ray emission.

one. If it started at 1.0 it would typically reach 0.97. With such a value of q_o, so close to one, the instability takes quite a different form from that envisaged by Kadomtsev. Instead of magnetic

reconnection through the growth of a magnetic island, there would be a convective motion involving the interchange of almost parallel magnetic field lines, resulting in the formation of a cold bubble surrounded by hotter plasma.

This so-called "quasi-interchange" model was promising in that it was predicted to be fast, overcoming the timescale problem. Even better, the soft X-ray images conformed to that predicted by the model, as shown in Figure 10.13.

However, this apparent success was short-lived, the quasi-interchange model immediately being put into question by measurements of the q-profile by Soltwisch on the TEXTOR tokamak in Germany. He used the Faraday rotation technique, in which the rotation of the plane of polarisation of a laser beam by the magnetic field is used to measure that field.

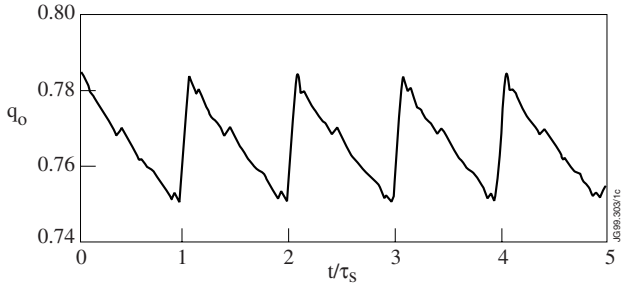

Figure 10.14. Soltwisch's measurement of the time variation of q_O on TEXTOR.

What Soltwisch found was remarkable. The value of q_o after the collapse was not close to one, it was typically between 0.7 and 0.8. As shown in the time trace of Figure 10.14 it did not fall much during the ramp phase, that at least being consistent with the JET calculations. However, that q_o, remained well below one was inconsistent with both the Kadomtsev and the quasi-interchange model.

Later it became possible to measure the q-profile on JET, again using the Faraday rotation technique. These measurements confirmed Soltwisch's result, q_o was generally well below one.

Fast Reconnection

The problem of the rapidity of the sawtooth reconnection was resolved by examining the Kadomtsev model more carefully. In this model the magnetic reconnection occurs in a narrow layer, and the rate of reconnection is determined by the resistivity of the plasma. However, at the high temperatures of the JET plasma the electrons are essentially collisionless and the development of the current in the reconnection layer is determined by the electron mass. Theoretical work in JET showed that allowing for the electron inertia the reconnection rate should be increased by an order of magnitude, bringing experiments and theory much closer together.

Subsequent work by the Chinese theoretician Qingquan Yu made clear that, although the reconnection would indeed be limited by electron inertia, it was more appropriate to regard the effect as a form of viscosity leading to an even faster reconnection rate.

More Sawtooth Problems

Despite the progress on the physics of reconnection, the problem of the discrepancy of the measured q-profile with theory persisted, and remains to this day. And more difficulties arose.

The first of these concerns the *onset* of the instability which causes the collapse. The evolution of the q-profile during the ramp phase takes it into an unstable regime. At the point where the configuration reaches this regime, so-called marginal stability, the growth rate is zero. As already explained the evolution of the plasma equilibrium is very slow. So slow, in fact, that during the very short time of the observed collapse the configuration would hardly have moved from marginal stability, and the instability should have a slow growth, inconsistent with the very fast growth observed in JET.

This has come to be called the trigger problem. It is unresolved for sawteeth, and is now seen as a more general problem applying to other instabilities such as ELMs, to which we shall return later.

The final sawtooth problem is that of the energy loss during the collapse. Since, apparently, the collapse leaves q_o well below one, any reconnection must be partial, and the central core, then retains its structure of nested magnetic surfaces. This deprives us of Kadomstev's mechanism for transporting energy out of the core. But the temperature and density in the core *do* drop. How can this be?

The explanation favoured by theoreticians was that the magnetic field lines are perturbed by the instability in a more subtle way. They are not reconnected in a gross restructuring, but the magnetic surfaces are broken by a smaller scale "wandering" of the magnetic field lines. As a field line winds around the torus it wanders away from its original surface. Mathematically the field line would eventually fill a whole region of space and is said to be ergodic.

It seems possible therefore that during the sawtooth collapse the magnetic field lines in the core become ergodic and the electrons, with their very high thermal velocity, are then able to carry their energy along the wandering field lines and out of the core. Theoretically this appears quite plausible. What is the problem?

There are occasions in JET where a small trace of nickel impurity has made its way to a region just outside the $q = 1$ surface which contains the potentially unstable core. The nickel is readily tracked through its soft X-ray emission. When the next sawtooth collapse occurs it is found that the nickel is transported into the core on the same short time scale as the electron temperature collapse. But the thermal velocity of the nickel ions is 330 times smaller than that of the electrons. If the electron temperature collapse is due to electrons moving along field lines from the centre to the $q = 1$ surface, the nickel in this time would only cover 1/330 of the journey. We see that the nickel could not reach the centre by moving along the supposedly ergodic field lines, and some other explanation is called for. Although it is not logically necessary, it seems likely that whatever explanation is found for the convection of the nickel would also explain the electron temperature collapse - without appeal to ergodicity.

These difficulties are compounded by the fact that the soft X-rays indicate that the nickel moves to the centre through a convective flow of the type predicted by the quasi-interchange instability - apparently ruled out by the measured q-profiles.

It is ironical that when JET started operation it was generally thought that sawtooth oscillations were understood, but that each new observation on JET undermined accepted theory, leading to the present set of theoretical problems. However, it is recognised that JET's experimental results have given us a better understanding of the facts, and a deeper insight into the theoretical issues.

ELMs

The Edge Localised Mode of instability appears when the plasma is in the high confinement H-mode configuration. The higher plasma energy in these configurations is partly due to a "pedestal" at the edge of the pressure profile. This pedestal results from pedestals on both the density and temperature profiles, and a comparison of L-mode and H-mode temperature profiles is shown in Figure 10.15. While it is obvious that the pedestal is advantageous to achieve a higher confined energy, the price to be paid is that the inevitable steep gradients at the plasma edge lead to instability - the ELMs.

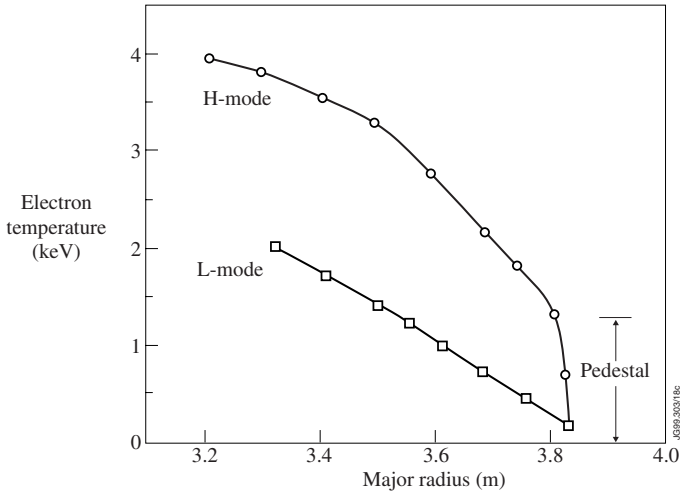

Figure 10.15. A comparison of L-mode and H-mode temperature profiles showing the effect of the temperature "pedestal" at the edge of the plasma.

A further complication is that the pressure gradient is predicted to drive a current and such a current at the edge of the plasma is also destabilising. It is difficult to measure the steep pressure gradient accurately and the current cannot be measured directly, so it is not possible to make precise comparisons with stability calculations.

The ELM has striking similarities to the sawtooth instability. The time traces even have a sawtooth form, as shown in Figure 10.16. Even more impressive, however, is the similarity of

the “collapse” phase. Both ELMs and sawteeth have an unexplained sudden onset - the trigger problem, both can have very short collapse times - tens of microseconds, and both involve a puzzling rapid radial transfer of energy over tens of centimetres.

ELMs appear in different forms. In their weakest form they occur as frequent small pulses, producing time traces that look like grass, giving them the name “grassy” ELMs. With higher power heating they become more separated in time and also larger in size. When they have become “giant” ELMs they present a serious problem, the associated sudden energy release producing a high heat loading on material surfaces - a subject we shall return to in Chapter 11.

Comparison with Theory

In general terms instabilities are driven by gradients in the pressure or the current. The main stabilising effect is the stiffness of the magnetic field lines. However, when a helical perturbation matches the helix of the magnetic field lines in a particular magnetic surface, this stabilising effect is small. Consequently we expect instability when there is a strong pressure or current gradient close to such a “resonant surface”.

With computer codes these concepts are made precise. Given an equilibrium, its stability can be calculated as accurately as required. There are two problems. Firstly we are not sure how much detail is necessary in the basic equations, and secondly the stability calculations are only as good as the experimental equilibrium profiles on which they are based.

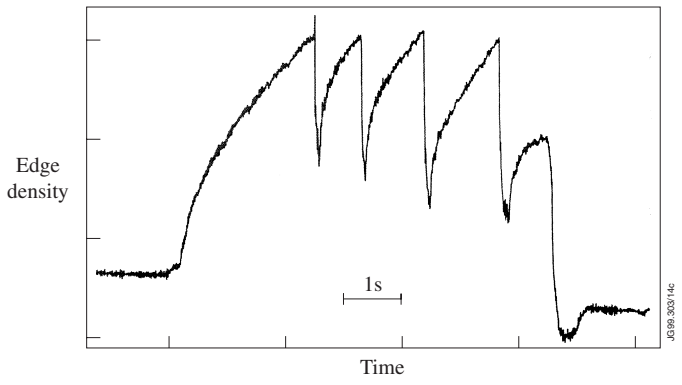

Figure 10.16. Time trace of the edge density showing the “sawtooth” nature of the ELM instability.

With the development of computer codes at JET and with careful diagnostic measurements it became possible to attempt a comparison of theory and experiment. An example is shown in the stability diagram in Figure 10.16. An instability which occurs in the outer part of the plasma was believed to be due to a so-called kink instability. This instability depends on the pressure gradient and the current density at the edge of the plasma, and these quantities give the axes of the diagram. Lines are drawn to separate the stable and unstable configurations. To the right of the diagram a kink instability occurs, and at the top a pressure driven instability called the

ballooning instability is predicted. At a given time the plasma configuration is at a point in this diagram, and as time progresses this point follows a path in the diagram. The right-hand line shows the path of a discharge in which an instability was observed at 12.9 seconds, and it is seen that this is compatible with the predicted kink instability.

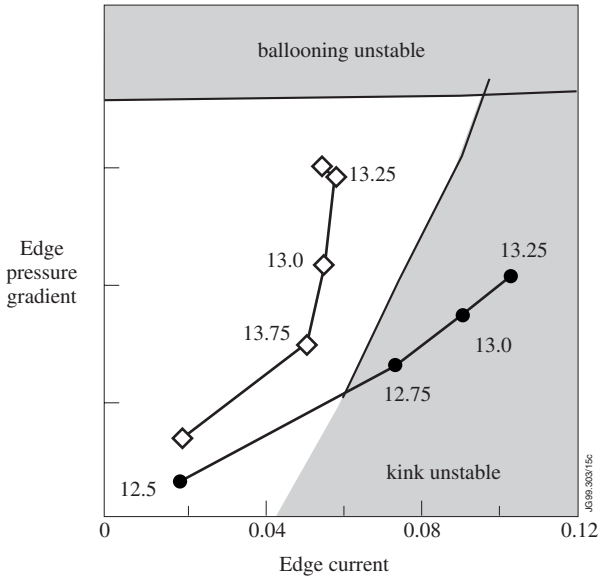

Figure 10.17. Comparison of theory and experiment. The axes of the stability diagram are the normalised pressure gradient and edge current density. The paths of the two discharges are plotted. One crosses the kink stability boundary and instability follows the crossing. The other avoids the boundary and no instability occurs.

As a further check on the theory a similar discharge was produced, but the edge current density was reduced by "ramping down" the total plasma current. The path of this discharge is also shown in Figure 10.17. It is seen that theoretically the discharge now avoids the kink unstable region and indeed the instability was not observed in the experiment. With the ramped current the path of the discharge approaches the ballooning stability boundary, and this happens in other discharges also, but the accuracy of the pressure profiles is not sufficient to say whether this boundary is actually crossed.

Another test of theory is to compare the predicted spatial structure of the instability with that observed. Figure 10.18 shows theoretically calculated soft X-ray emission contours with the corresponding experimental contours derived by tomographic reconstruction of line of sight soft X-ray measurements. The similarities indicate that the theoretically calculated instability is in fact that which occurs in the plasma.

Non-linear Instabilities

The instabilities described so far are said to be "linearly unstable". This means that no matter how small the perturbation of the plasma, instability will occur. A commonly quoted analogy

that of a ball sitting on top of a smooth hill - the smallest displacement will cause it to fall. However, there are instabilities which require a sufficiently large perturbation before they can grow.

Such an instability was conjectured in the early days at JET. The suggestion was that once a magnetic island was formed, its internal properties might cause it to grow. The idea was that if the magnetic island was cooled by radiation this would increase the electrical resistivity in the island. The current in the island would then fall and the associated change in the magnetic field is then such as to make the island grow - that is, to make it unstable. While the physics underlying this model is sound such an instability was not clearly identified experimentally.

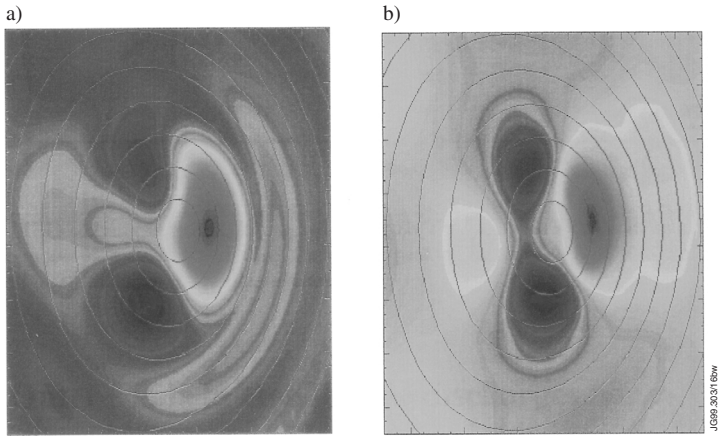

Figure 10.18. (a) The perturbation of the plasma determined from tomographic reconstruction of the soft X-ray emission from the precursor instability of a disruption, compared with (b) the theoretically calculated form of the instability.

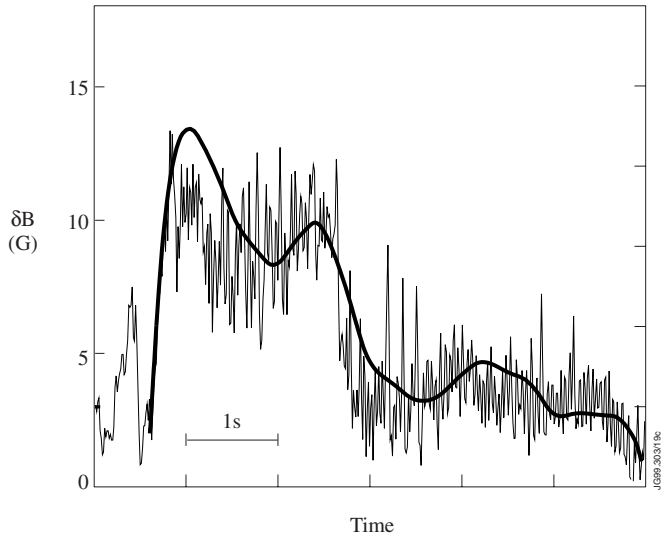

Figure 10.19. Comparison of the modelled evolution of a neoclassical tearing mode with experiment. The heavier line gives the theoretical prediction.

In 1996 Carrera, Hazeltine and Kotschenreuter discovered another type of non-linear tearing mode. The physics of these so-called neoclassical tearing modes is quite simple. The pressure

gradient in tokamaks drives a local current - the bootstrap current. If an island is formed the pressure is "short-circuited" and the pressure gradient is partially removed. This reduces the bootstrap current in the island and, as in the previous example, this enhances the island still further. This type of tearing mode has been seen in several tokamaks including JET. The simplest theory predicts the widespread appearance of this instability, but allowance for thermal conduction across the island's magnetic surfaces, introduces a threshold amplitude below which instability does not occur. Figure 10.19 shows the modelled evolution of the magnetic perturbation for a JET discharge together with the experimental value observed width, providing supporting evidence for this mode of instability.

Another variant of the non-linear tearing mode is that caused by errors in the magnetic field. In JET small errors were found to arise from the internal winding structure of the coils and from coil connections. Theory shows that these errors will lead to small magnetic islands. However, it was found that for field errors above a critical size the islands grew unstably and resulted in a disruption. This result places a severe constraint on the level of field error allowable in a tokamak reactor.

Overview

The observed instabilities can always be related to one or other of the theoretically expected modes. They are generally associated with the predicted driving mechanisms such as pressure and current gradients. In some cases a quantitative comparison with theory shows convincing agreement.

However, the experiments on JET have uncovered aspects of the behaviour of instabilities which were more difficult to understand. The rapid growth of the sawtooth instability was initially puzzling, but finally explained. On the other hand the suddenness of the onset of the sawtooth instability and of ELMs remains a mystery. Another difficulty is the extremely fast loss of energy, both from the plasma core in the sawtooth collapse and from the edge in the case of ELMS. The rapidity of the energy loss in these instabilities together with related behaviour in disruptions, presents a fundamental question for plasma theory.

Bibliography

The two most influential papers dealing with plasma stability are

Bernstein, I.B., Freeman, A.E., Kruskal, M.D., and Kulsrud, R.M. An energy principle for hydromagnetic stability problems. Proceedings of the Royal Society A223,17 (1958), and

Furth, H.P. Killeen, J., and Rosenbluth, M.N. Finite resistivity instabilities of a sheet pinch. Physics of Fluids 6, 459 (1963).

These papers provide the tools for calculating the stability of given equilibria to small perturbations, so-called linear stability. The energy principle paper takes the plasma to be perfectly

conducting and the "F.K.R." paper extends this to include the effect of finite resistivity allowing, for example, tearing modes.

When the merits of tokamaks became apparent their linear stability properties were rapidly investigated and a summary of the stability theory was given in

Wesson, J.A. Hydromagnetic stability of tokamaks. Nuclear Fusion 18, 87 (1978).

However, as the JET experiments progressed it became apparent that the instabilities observed displayed features which could not be explained by the available theory. The first reason for this is that in some cases more complete equations are needed in calculating the linear stability. The other reason is that the linear approximation is inappropriate and a more general description is required. A further difficulty is the uncertainty regarding the precise equilibrium configuration at the time the instability occurs, especially when it is changing in time.

The most destructive instability observed is the disruption and the role of impurity radiation in producing an unstable configuration was described in Chapter 7. A summary of the studies of JET disruptions was given in the review

Wesson, J.A., Gill, R.D. Hugon, M. Schüller, F.C., Snipes, J.A., Ward, D.J., Bartlett, D.V., Campbell, D.J., Duperrex, P.A., Lopes Cardozo, N., Mast, K.F., Nave, M.F.F., Salmon, N.A., Smedulders, P., Thomas, P.R., Tubbing, B.J.D., Turner, M.F., and Weller, A. Disruptions in JET. Nuclear Fusion 29, 641 (1989).

This article describes the sequence of events in JET and includes evidence for the $q_a = 2$, low q limit and for the growth of magnetic islands, together with accounts of the production of runaway electrons and the negative voltage spike.

Two subsequent papers dealing with JET disruptions are

Wesson, J.A., Ward, D.J. and Rosenbluth, M.N. Negative voltage spike in tokamaks. Nuclear Fusion 30, 1011 (1990).

Ward, D.J. and Wesson J.A. Impurity influx model of fast tokamak disruptions. Nuclear Fusion 32, 1117 (1992).

Evidence for impurity influx and plasma cooling to a few eV is given in

Sawtooth oscillations and disruptions in JET, by the JET team. Plasma Physics and Controlled Nuclear Fusion Research (Proc. 14th Int. Conf. on Plasma Physics and Controlled Fusion, Würzburg, 1992) Vol.1, 437, IAEA Vienna 1993.

The numerical simulation of a JET disruption is described in Bondeson, A., Parker, R.D., Hugon, M., and Smeulders, P. MHD modelling of density limit disruptions in tokamaks. Nuclear Fusion 31, 1695 (1995)

Kadomtsev's model of the sawtooth instability is described in

Kadomtsev, B.B. Disruptive instability in Tokamaks. Fizika Plasmy 1, 710 (1975) [Soviet Journal of Physics 1, 389 (1976)],

and the quasi-interchange model was introduced in

Wesson, J.A. Sawtooth Oscillations. Plasma Physics and Controlled Fusion 28 (1A), 243 (1986),

and further developed in

Wesson, J.A., Kirby, P., and Nave, M.F.F. Sawtooth Oscillations. Plasma Physics and Controlled Nuclear Fusion Research. (Proc. 11th Int. Conf. Kyoto, 1986) Vol. 2, 3, IAEA Vienna 1987.

Experimental evidence indicating this mode of behaviour was given in

Edwards, A.W., Campbell, D.J., Engelhardt, W.W., Fahrback, H.U., Gill, R.D., Granetz, R.S. Tsuji, S., Tubbing, B.J., Weller A., Wesson, J., and Zasche, D. Rapid collapse of plasma sawtooth oscillation in the JET tokamak. Physical Review Letters 57,210(1986).

The linear theory of quasi-interchange stability was given by

Nave, M.F.F. and Wesson, J.A. Stability of the ideal m=1 mode in a tokamak. Nuclear Fusion 28, 297 (1988).

The idea that the extreme rapidity of the sawtooth collapse was related to the role of electron inertia was proposed by

Wesson, J.A. Sawtooth Reconnection. Plasma Physics and Controlled Nuclear Fusion Research, (Proc. 13th Int. Conf. Washington, 1990) Vol. 2, 79, I.A.E.A. Vienna 1991, and Nuclear Fusion 30, 2545 (1990).

These papers gave a kinetic non-linear theory, the linear theory was subsequently provided by Porcelli, F. Collisionless m = 1 tearing mode, Physical Review Letters 66, 425 (1991).

Later non-linear simulations of magnetic reconnection with electron inertia showed a fast growth in the non-linear phase as seen in JET sawtooth collapses. They were published in

Ottaviani, M. and Porcelli, F. Non-linear collisionless magnetic reconnection. Physical Review Letters 71, 3802 (1993), and Fast non-linear magnetic reconnection. Physics of Plasmas 2, 4104 (1995).

The importance of electron viscosity was pointed out by

Yu, Q. A new theoretical model for fast sawtooth collapse and confirming its quasi-interchange structure. Nuclear Fusion 35, 1012 (1995).

The experimental evidence from JET casting doubt on the ergodic field line explanation of

energy transport in the sawtooth collapse and confirming the quasi-interchange structure is given in

Wesson, J.A., Alper, B., Edwards, A.W., and Gill, R.D. Transport in sawtooth collapse. Physical Review Letters 79, 5018 (1997).

A theory of feedback control of tearing modes was presented in

Lazzaro, E., and Nave, M.F.F. Feedback control of resistive modes. Physics of Fluids 31, 1623 (1988).

The observations on the various forms of mhd activity in JET were described in the following papers,

Nave, M.F.F., Cambell, D.J., Joffrin, E., Marcus, F.B., Sadler, G., Smeulders, P., and Thomsen, K. Fishbone-like events in JET. Nuclear Fusion 31, 687 (1991).

Nave, M.F.F., at al. MHD activity in JET hot ion H mode discharges. Nuclear Fusion 35, 409 (1995).

Nave, M.F.F., et al. An overview of MHD activity at the termination JET hot-ion H-modes. Nuclear Fusion 37, 809 (1997).

Nave, M.F.F. et al. Discharge optimisation and control of MHD modes. Nuclear Fusion 39, 1567 (1999).

The error field instability is described in

Fishpool, G.M. and Haynes, P.S. Field error instabilities in JET. Nuclear Fusion 34, 109 (1994).

11. CONFINING THE PLASMA

The requirement on plasma confinement can be readily appreciated by considering the distance a plasma particle would travel in a tokamak reactor. For example a typical deuteron ion in a plasma with a temperature of 10 keV has a velocity of 1,000 km per second. Since in a reactor it would be necessary to confine such particles for several seconds we see that the ion would travel a distance comparable to the size of Europe.

The effect of the magnetic field is to turn the motion perpendicular to the field into small circular orbits. Typically the orbit of the plasma ions has a radius of a few millimetres. This means that the particles perform very many orbits, a deuteron ion completing about 30 orbits per microsecond. The electrons, being faster and less massive, move in an orbit 60 times smaller at 3672 times the frequency. The particles move freely parallel to the magnetic field, but this takes them along surfaces which are closed within the tokamak. In JET the particles are confined for times of around a second, during which time the electrons travel a distance comparable with the circumference of the earth, demonstrating the basic effectiveness of the magnetic field.

The question naturally arises as to what limits confinement in the magnetic field of a tokamak. Why would the particles not gyrate about a field line forever? The first answer is that the particles collide with each other and the collisions cause a displacement of the orbit. These displacements are random and so the particles diffuse across the magnetic field until they reach the edge of the plasma. The collisions also lead to a diffusive transfer of heat, as in a gas, the hotter particles passing energy to their cooler neighbours.

Although calculation of the collisional diffusion is complicated, the simple account given above implies a straightforward process of particle and energy loss. However, it is not like that. From the earliest days of fusion research it was recognised that experimental plasmas were not governed by the rules of collisional transport. The loss rates are higher than calculated, and a large part of the experimental effort on JET has been devoted to trying to understand this behaviour. However, before describing these endeavours, we must examine in more detail the basic collisional transport of particles and energy.

Collisional Transport

In a gas the molecules spend most of their time free of collisions, the collisions being hard and brief. We recall from Chapter 2 that, unlike gas molecules, the particles of a plasma have long range interactions with each other. As a result each particle of a plasma is colliding simultaneously and continuously with many other particles. However, when the effects of all these collisions are summed it is found that it is possible to describe the behaviour in terms of a characteristic collision time, τ. The collisional diffusion coefficients can be expressed in terms of this time. For a particle with an orbit size ρ the diffusion coefficient has the form ρ^2/τ. We see that in the

limit of an infinite collision time there would be no diffusion.

There are several diffusion coefficients depending on the type of particle, and whether particle or energy transport is involved. It turns out that for all of these there is a rather surprising complication to the theory. The trapped particles described in Chapter3 e ven when in a minority, contribute more to the collisional transport than the untrapped particles. This is because the size of the trapped particle orbit, the banana orbit, is larger than the orbit of an untrapped particle. Thus the larger ρ^2 factor in the diffusion coefficient can outweigh the smaller number of trapped particles.

The collisional diffusion coefficients depend basically on three quantities - the plasma density, n, its temperature, T, and the magnetic field. The coefficients are proportional to density for the obvious reason that the number of collisions increases with the density of particles. The temperature dependence is weaker. The collision time is proportional to $T^{3/2}$ but this is largely cancelled by the temperature dependence of the factor ρ^2. Since the orbit size is proportional to $T^{1/2}$, the diffusion coefficient, ρ^2/τ, varies as $1/T^{1/2}$.

We see that in terms of the plasma properties the diffusion coefficients are proportional to $n/T^{1/2}$. It would be expected, therefore, that the confinement would worsen at higher densities, but would improve at higher temperatures. Since the early experiments were carried out at low temperatures, typically less than 1 keV, there was the potential for a significant improvement as the temperatures were raised to the required 10-20 keV. We shall see later that the opposite turned out to be the case, confinement deteriorated with increased temperature. First, however, let us complete the description of collisional transport by examining its dependence on the magnetic field.

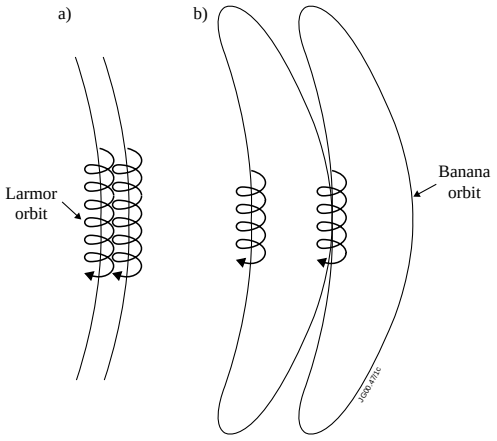

Fig. 11.1 (a) Classical transport: particle steps a Larmor orbit in a collision time. (b) Neoclassical transport: particle steps a banana width in a collision time.

In classical collisional transport the step-length is the Larmor radius, which is inversely

proportional to the magnitude, B, of the total magnetic field. So a larger magnetic field means a smaller orbit and consequently a smaller diffusion coefficient, varying as $1/B^2$. However as described above the trapped particle diffusion is dominant in tokamaks and the characteristic step-length for this process is the width of their banana orbit, as illustrated in Figure 11.1. The banana width is inversely proportional to the small poloidal component of the magnetic field, B_p, and the resulting, neoclassical, diffusion coefficients are therefore larger, being proportional to $1/B_p^2$.

Because of the need to heat the plasma to reactor temperatures, and for the α-particle heating in a reactor to sustain such temperatures, most interest attaches to the confinement of energy. In collisional transport the particles have a thermal diffusion coefficient proportional to ρ^2/τ. This means that the ion thermal diffusion at a given temperature would be much larger than the electron thermal diffusion. The ratio of ion and electron banana widths is the square root of their mass ratio, m_i/m_e, and so ρ^2 is proportional to m_i/m_e. Counteracting this, the ratio of the ion and electron collision times is $(m_i/m_e)^{1/2}$. The result is a collisional ion thermal diffusivity which is $(m_i/m_e)^{1/2}$ greater than that for electrons, giving a factor of 60 for deuterons.

Anomalous Transport

Having set the scene by describing the fundamental collisional diffusion process, we now face the reality that in tokamak experiments it is found that the transport is anomalous, the transport coefficients being much larger than predicted by collisional transport theory. The ion thermal transport is typically a few times the collisional value, the precise ratio depending on the conditions. The electron thermal transport is much more anomalous but, because the electron collisional transport is very small, the outcome is that experimentally the two types of thermal transport are comparable in magnitude. The obvious explanation of this anomalous behaviour, in general terms, is that the plasma is subject to instability. The fluctuations which arise from such instability would carry particles and energy across the magnetic surfaces and provide an additional contribution to the transport.

A large number of able theoreticians have, over many years, sought to determine the nature of the instability and to understand the resulting transport, but these efforts have not yielded a generally accepted explanation. This has led to the adoption of empirical approaches for the interpretation of the experimental results. The simplest formulation uses a measure of the quality of energy confinement in the form of the energy confinement time, τ_E , introduced in Chapter 7, which measures the time that the supplied energy resides in the plasma. In a steady state with a total heating power P, and a total plasma energy W, the confinement time is given by.

$$\tau_E = \frac{W}{P} \qquad 11.1$$

In the simplest model we can characterise the plasma by an average thermal diffusivity, χ. As with all diffusion processes, the thermal conduction losses are inversely proportional to the square of the length over which the conduction takes place, in this case the plasma radius,a. This allows us to relate the confinement time to the thermal diffusivity and we find that τ_E is proportional to a^2/χ.

Before turning to the experimental results let us ask what the scaling of the confinement time would be for the collisional, neoclassical transport. We recall that, because the ions have larger orbits than the electrons, the ion heat conduction is predicted to dominate, and that the ion thermal diffusivity is proportional to $n/(T^{1/2} B_p^2)$. Thus, using $\tau_E \propto a^2/\chi$, the neoclassical energy confinement time is given by

$$\tau_E^{neo} = c_1 \frac{T^{1/2} B_p^2 a^2}{n} \qquad 11.2$$

where c_1 depends upon certain geometric ratios, and n, T and B_p are representative values.

When JET was being designed it was already known that the relation 11.2 did not hold. In fact there was evidence from the Alcator tokamak at the Massachusetts Institute of Technology (M.I.T.) that the confinement time could increase rather than decrease with the particle densityn. The scaling relation obtained with this experiment, based on ohmically heated plasmas, was

$$\tau_E = 0.5\left(\frac{n}{10^{20}}\right)a^2 \qquad 11.3$$

Although this relation was only a tentative attempt to represent the plasma behaviour it did provide some estimate of what JET might achieve, at least with ohmic heating. It was not known then at what particle density JET would operate, but a typical tokamak value of $n = 3\times10^{19}\ m^{-3}$, with an average plasma radius of 1.4m, gave 0.3 seconds.

However tokamak experiments before the design of JET had low temperatures, typically less than 1k eV, and confinement times measured in milliseconds. Predictions based on such experiments were therefore clearly unreliable and, of course, one of the main purposes of JET was to study confinement and reduce the uncertainties of extrapolation.

Early Results

The early experiments on JET gave encouraging results. The confinement times in ohmically heated plasmas were up to two times greater than predicted by equation 11.3, a confinement time of 0.6 seconds being achieved.

After obtaining results with ohmic heating, attention turned to the effect of additional heating on confinement, and the scaling of confinement time with plasma current. Before

examining the outcome it is helpful to examine the procedures used to analyse the dependence of the confinement time on the experimental parameters. From the plasma physics point of view it is natural to think of the confinement as determined by the plasma properties including the temperature. However operationally the control parameters are the heating power, the plasma current and the magnetic field, and it is often more convenient to use these variables. Let us first examine the transformation to these variables for the case of neoclassical collisional transport. Equation 11.2 gives the neoclassical confinement time in terms of the poloidal magnetic field and the temperature. From Amp•res law the plasma current, I, is proportional to the product $B_p a$ where B_p is now the surface value of the poloidal magnetic field. This enables us to replace $B_p a$ with I in the scaling. Equation 11.1 allows us to eliminate the temperature if we write the total plasma energy as W = 3nTV, the energy per particle being $\frac{3}{2}$ T and a factor of two arising because there are both ions and electrons. V is the plasma volume which we take to be proportional to a^3. Equations 11.1 and 11.2 now combine to give

$$\tau_E^{neo} = c_2 \frac{PI^4}{n^3 a^3} \qquad 11.4$$

where c_2 is a new coefficient.

We see that the scaling given by equation 11.4 is very beneficial, the confinement time improving with increased heating power. But we also recall that the transport in tokamaks was known not to agree with this scaling, the energy confinement times with additional heating being substantially lower.

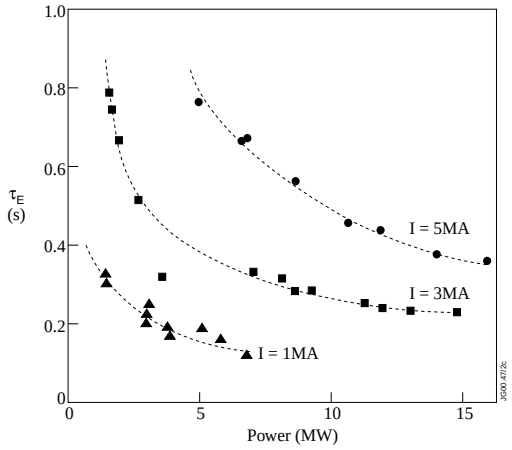

Fig. 11.2 The dependence of confinement time on heating power for three values of the plasma current.

The results with heated plasmas in JET confirmed the anomalous nature of the transport, and gave new information on the parametric dependencies of the confinement, in particular

extending the results to much higher currents than had been possible in smaller tokamaks. Figure 11.2 shows some experimental results, the measured confinement time being plotted against the heating power for a range of plasma currents. It is seen that the confinement degrades with increasing power at all values of the plasma current.

On the other hand, increased current does improve confinement, although not in the dramatic way of equation 11.4. In fact the confinement time increases roughly linearly with current. The dependence on the applied magnetic field and the plasma density was found to be weak.

These results also provided a remarkable confirmation of a scaling relation obtained by Goldston from an analysis of a number of smaller tokamaks. Apart from geometrical ratios GoldstonÕs scaling takes essentially the form

$$\tau_{EG} = c_3 \frac{Ia^{3/2}}{P^{1/2}} \qquad 11.5$$

and both the linear dependence on current and the $P^{1/2}$ degradation with power were consistent with the JET results.

When these results are used to extrapolate to the conditions needed for a reactor it is found that a tokamak reactor would require a current of around 30 MA. Such a current would be possible but clearly it would be better both for cost and for confidence if the confinement could be improved. As mentioned in Chapter 7, the possibility of such improvement had been unexpectedly discovered in the ASDEX tokamak in Germany. It was found that with sufficient heating the plasma spontaneously jumped from the lower confinement of the L-mode into the of improved confinement of the H-mode. Although not understood, the H-mode seemed to depend on a special feature of ASDEX, namely the existence of separatrix in the magnetic field geometry. The purpose of this geometry was to divert the plasma escaping from the main plasma into a separate chamber. The JET design did not have such a divertor, but the question arose as to whether, nevertheless, it might be possible to obtain H-mode confinement.

H-mode

It was found that by adjusting the currents in the external control coils it was possible to make the required change in the magnetic geometry - but only just. Figure 11.3 shows the initial geometry, with fully nested surfaces, and the modified geometry with a separatrix. It is seen that the X-point, which characterises the existence of a separatrix, is just inside the vacuum vessel. Since the reason for the H-mode was not understood, it was not possible to say whether this small change would affect the confinement.

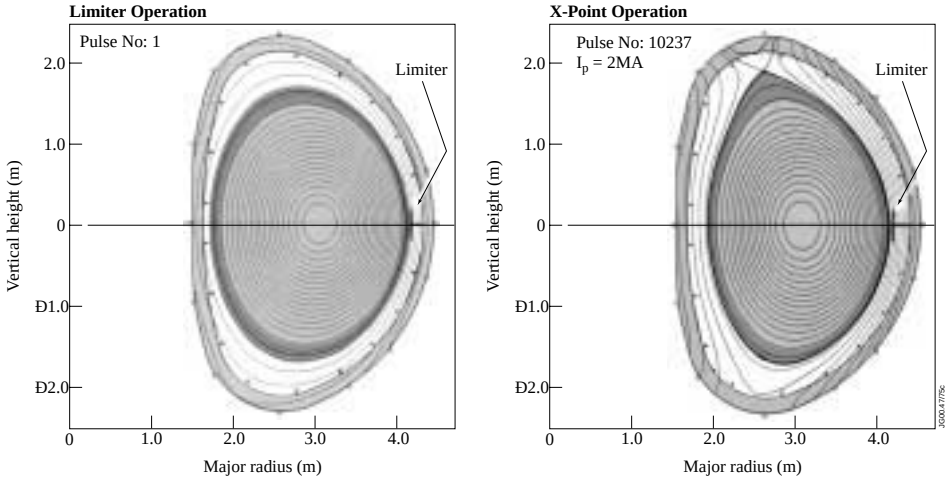

Fig. 11.3 Showing the modification of the magnetic geometry with the introduction of an X-point.

In fact an H-mode plasma was obtained. Figure 11.4 shows the temperature profile for two cases which are essentially the same except for the presence of a separatrix in the H-mode. It is seen that for the same power the plasma temperature is increased by 60% in the H-mode, corresponding to a similar improvement in the energy confinement time.

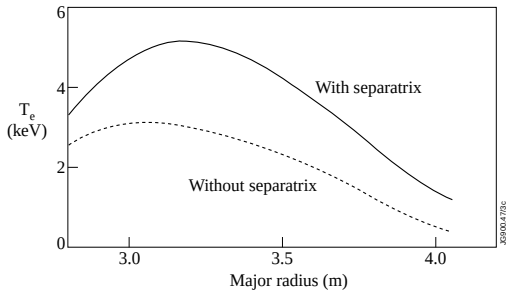

Fig. 11.4 Electron temperature profiles with and without a separatrix, illustrating the achievement of the H-mode.

Figure 11.5 gives a comparison of the H-mode confinement times with L-mode cases taken from Figure. 11.2. In addition to the improvement in confinement it is seen that the values of confinement time now exceed the ÒmilestoneÓ value of one second.

As found in ASDEX, the H-mode required a critical level of heating power. The transition to H-mode was marked by the formation of large gradients in temperature and density at the edge of the plasma. The fact that large differences in these quantities were sustained over a narrow region seemed to imply that the improved confinement could simply be attributed to a

transport barrier formed at the edge of plasma. The theoretical efforts to provide an explanation of H-modes concentrated on trying to find a bifurcation between states with and without this barrier.

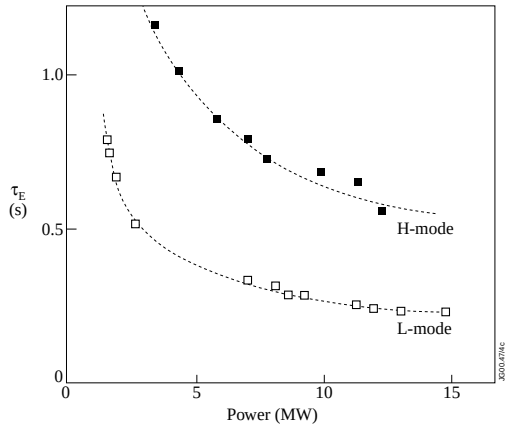

Fig. 11.5 Confinement time plotted against heating power for L-mode and H-mode discharges with a current of 3MA.

A study of the phenomenon in JET finally led to a contrary view. Cases were found in which at the onset of the H-mode an immediate change in the behaviour occurred, not just at the edge, but across the outer half of the plasma radius. Figure 11.6 shows the time dependence of the electron temperature at several positions across the plasma radius. It is clear that this behaviour is not just due to the formation of a barrier at the edge of the plasma. Had this been the case, the plasma away from the edge would have a delayed response over a longer timescale. The almost simultaneous change in the rate of temperature increase over the outer half of the plasma obviously calls for a different explanation. One possibility is that the conductivity is not determined locally. This might be the case, for example, if the anomalous transport is due to radially elongated convective cells.

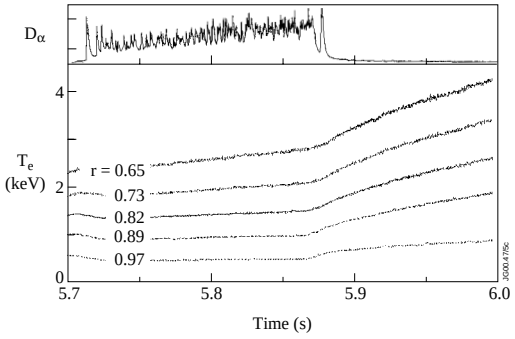

Fig. 11.6 The fall in the D_α signal marks the onset of the H-mode and it is seen that the electron temperature undergoes an increase in slope simultaneously over a large part of the radius. r is the radius normalised to the radius of the plasma.

Outstanding Plasmas

In exploring the various parameters determining the types of plasma obtained, it was found that certain regimes produced plasmas with particularly good confinement. We shall look at three of these types.

The first is the *hot ion* plasma, produced by injecting energetic neutral particle beams into a low plasma density. This mode of operation is possible because of a fortunate dependence of both the ion heating and the ion energy loss on the electron temperature. If the electron temperature is low, say a few keV, the neutral beam heating which goes to the electrons becomes comparable with that going to the ions. At very low electron temperatures the electron heating is the larger. Thus efficient ion heating requires a sufficiently high electron temperature. In the hot ion plasma the electron temperature is around 10 keV and almost all of the heating goes to the ions. As a result the ion temperature rises to a high value, typically 20k eV. The other factor contributing to this result is the low collisional transfer of energy from ions to electrons at low density and high electron temperature. This allows the ion-electron temperature difference to rise to around 10 keV.

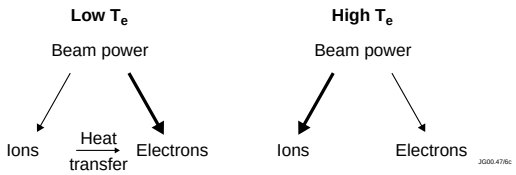

Fig. 11.7 With a low electron temperature the electrons are preferentially heated, as indicated by the heavier arrows, and also take heat from the ions. With a high electron temperature the ions are preferentially, and the energy exchange is small, allowing the achievement of a hot-ion H-mode.

The different flows of heat with low and high electron temperature are illustrated in Figure11.7. The experimental behaviour is shown in Figure 11.8 which gives the time dependence of the electron and ion temperatures in a hot-ion plasma. These plasmas can have very good confinement. They undergo a transition to the H-mode and have confinement times up to four times the value predicted by GoldstonÕs L-mode formula (11.5) for the same conditions. Since it is the *ion* temperature which determines the thermonuclear reaction rate these plasmas are particularly successful in achieving a high neutron production. As a consequence this type of plasma was used when JET carried out the worldÕs first deuterium-tritium tokamak experiments, as described in Chapter 14.

The second type of successful plasma is obtained with the injection of deuterium pellets into the plasma, as described in Chapter 8. This leads to a *Pellet Enhanced Performance* , or PEP, mode of operation. The solid deuterium pellets are produced by freezing deuterium to a temperature of 10K, and slicing off segments of a few millimetres. As the pellets cross the

plasma their surface is continually removed by the bombarding energetic plasma particles. For the pellets to reach the centre of the plasma before they are completely ablated they must be fired into the plasma with velocities of around 1 km per second. This is done by means of a gas expansion gun, the pellets being accelerated up to the required velocity by the expansion of a previously compressed gas.

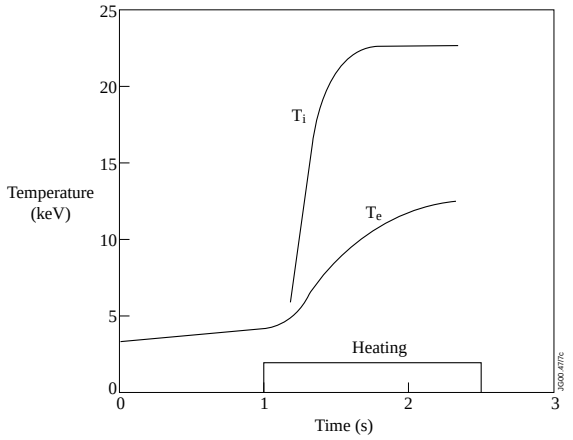

Fig. 11.8 The time development of the ion and electron temperatures in a hot ion H-mode plasma following the application of 18MW of heating power.

As the injected pellet penetrates the plasma, the gradually ablated material increases the density on each magnetic flux surface it crosses. However, because of the geometry, the volume between magnetic surfaces diminishes as the pellet moves inward along the plasma radius, and so the effect on the density increases towards the magnetic axis. A comparison of discharges with and without pellet injection was given in Figure 8.8 and a more impressive case is shown in Figure 11.9.

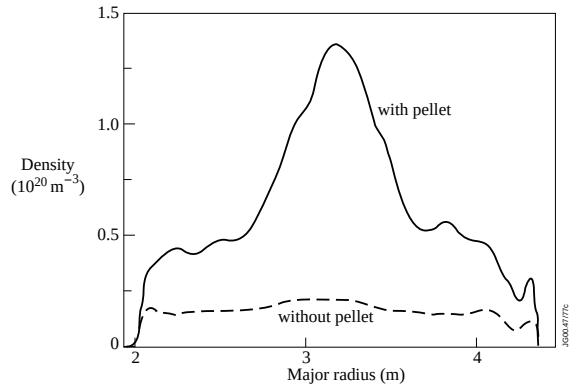

Fig. 11.9 Pellet injection produces an enhanced density in the region around the plasma axis.

The most interesting feature of PEP discharges is the improved confinement of the central part of the plasma. The effective thermal diffusivity is decreased in this region as seen from Figure 11.10. Because the outer part of the plasma normally has the least good confinement properties, and the central volume is small, the improvement in this case does not have a large overall effect. However, the core itself is strongly affected and the implications of the observed improved confinement could be of considerable significance.

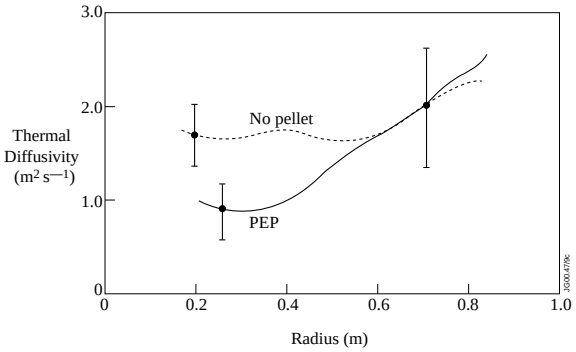

Fig. 11.10 Pellet injection led to an improvement of confinement in the central plasma as indicated by the reduced thermal diffusivity.

What could be the cause of the improved confinement in PEP discharges? As is usual in tokamak physics it is difficult to be sure. Nevertheless it is clear that the magnetic field will be modified by pellet injection and possibly in a significant way. The high pressure core which arises inevitably produces a high pressure gradient at the edge of the core. It will be recalled from Chapter 3 that pressure gradients drive bootstrap currents and the PEP core pressure gradient will be effective in this way. Since the total current is constant the bootstrap current actually produces a redistribution of current in which current is removed from the region close to the axis. The result is that the profile of the safety factor, q, is flattened around the axis, reducing the magnetic shear. In fact q may have a negative gradient, reversing the sign of the shear as illustrated in Fig. 11.11. Is this the reason for the improved confinement?

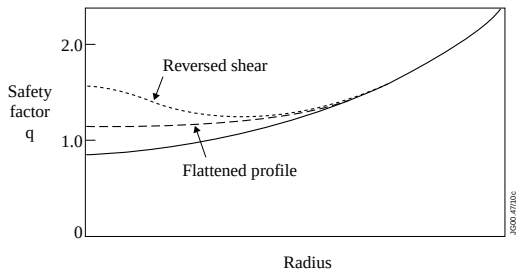

Fig.11.11 Modif ication of the q-profile following pellet injection indicating the flattening of the profile with a possibility of shear reversal.

It is significant that such a possibility had earlier been predicted theoretically within the JET team. The underlying idea related to the behaviour of the magnetic islands described in Chapter 10. A possible explanation of anomalous transport is that once formed, these islands are self-sustaining. This could occur, for example if the islands are driven by a reduction in the current along the flux tube formed by the island. However, the theory predicts this behaviour only for a positive shear. With reversed shear the self-sustained turbulence goes away. This then is a candidate for explaining the observed improvement in confinement in PEP discharges.

The third type of plasma we consider derives immediately from the account of the PEP mode given above. If negative shear is beneficial for confinement, why not impose it directly? This line of thinking was followed at the Princeton Plasma Physics Laboratory and the General Atomics Laboratory in San Diego, and improved confinement was achieved by modifying the magnetic shear. Similar experiments were carried out in JET.

The method of modifying the magnetic shear utilises the current skin effect. When the plasma current is switched on there is a tendency for the current to flow in the outer part of the plasma. Given sufficient time the current diffuses inwards at a rate determined by the resistivity of the plasma, and ultimately the current is peaked at the axis where the resistivity is lowest. The value of q on axis is inversely proportional to the axial current density and so during the early phase, when only partial current diffusion has occurred, the central region tends to have a higher value of q. The experiments to investigate the effect of shear were carried out at this early stage. Heating is applied at this time to raise the temperature. In addition to increasing the confined energy and nuclear reaction rate this has the effect of increasing the electrical conductivity and slowing the current diffusion, thus maintaining the desired q profile.

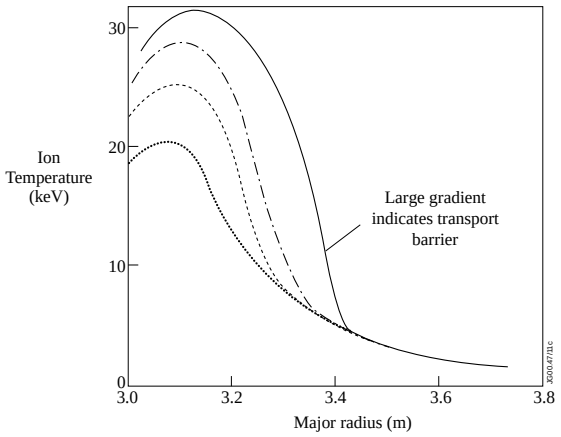

Fig.11.12 Sequence of temper ature profiles in a heated plasma with modified shear, showing the appearance of an internal transport barrier.

The plasmas produced in this way are among the best obtained in JET. The good behaviour is due to the formation of a transport barrier. Unlike the edge barrier associated with H-modes, this barrier forms internally. Such internal transport barriers had been found previously on the JT60 tokamak at the Japanese Atomic Energy Research Institute. Fig. 11.12 gives a time sequence of JET temperature profiles. The transport barrier is identified by the increased temperature difference which is sustained across it. Thus, in the figure the evolution of the strong localized temperature gradient demonstrates the barrier. It is further seen that the barrier moves outward in radius as it strengthens to its full effect. The magnitude of the improvement in the local confinement is shown in Fig. 11.13 which gives a graph of the time dependence of the ion thermal diffusivity. It is seen that the diffusivity falls by more than an order of magnitude and reaches a level comparable with the neoclassical diffusivity which would result from collisions alone. The reduction is also observed in the particle and electron thermal transport.

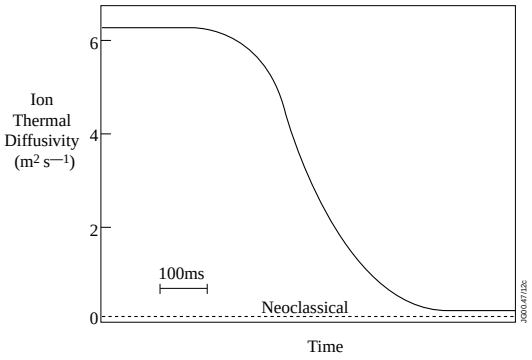

Fig.11.13 As the transport barrier forms the local thermal diffusivity falls to a low value, comparable with that expected from collisions alone.

Unfortunately a straightforward explanation of the improved confinement simply as the result of the modified magnetic shear does not seem possible. It was found that the transition to good confinement required a sufficient heating power in addition to the required magnetic shear, and it is clear that factors other than the shear must be involved. It was also found that the improved confinement could be achieved when the modification of the q-profile did not involve actual reversal of the shear.

The Confinement Time

In envisaging a tokamak reactor it is clearly important to know as accurately as possible its confinement capability. In particular we would like to know the dependence of the energy confinement time on the various parameters which must be extrapolated from present tokamaks. Let us first recall the requirement on confinement for a reactor.

In Chapter 9 we saw that for a self-sustaining reacting plasma the triple product of density, temperature and confinement time, $nT\tau_E$, must be approximately 5×10^{21} m^{-3} keV s. The density in a reactor must be around 10^{20} m^{-3} and the temperature around 15 keV. This means that the confinement time must be around 3 seconds. In JET, with a current of 5 MA the temperature has the required value but the density is about a factor 3 lower than required. The confinement time is a factor of 5 smaller, and so the triple product $nT\tau_E$ must be increased by a factor 15 for a reactor.

How large must a reactor be to achieve the required improvement? Because of JETÕs size it has played a crucial role in the research into this question. However, it turns out that it is very difficult to obtain a precise answer. Furthermore, because reactor cost increases rapidly with size we cannot take the easy option of a large safety margin. We shall look at the issues involved but first let us obtain a rough idea of the requirements by carrying out a simple, approximate calculation.

It is usual to assume that a reactor would operate in one of the regimes in which confinement is better than that of L-mode scaling. For example we can take the L-mode confinement time scaling of equation 11.5 and introduce an improvement factor H to write

$$\tau_E = c_3 \frac{HIa}{P^{1/2}}^{3/2} . \qquad 11.6$$

This equation appears to indicate that τ_E is proportional to the current, I. However, for given plasma conditions this is not the case. Using the definition $\tau_E = W/P$ to eliminate P in equation 11.6, together with the scaling relation for the total energy, $W \propto nTa^3$, we find

$$\tau_E = c_4 \frac{H^2 I^2}{nT} . \qquad 11.7$$

The confinement time is now seen to be proportional to the square of the plasma current and inversely proportional to the plasma pressure. We also note that it is proportional to the square of the improvement factor, H, as normally defined.

By a fortunate coincidence equation 11.7 gives a simple scaling for the triple product $nT\tau_E$

$$nT\tau_E = c_4 (HI)^2 .$$

It is now easy to see that, assuming the same value of H, the required improvement factor of 15 over the JET case cited above needs about a 4 times larger current, that is 20MA. The design current adopted for the International Thermonuclear Experimental Reactor, ITER, is 21MA.

The above calculation was only able to give a rough idea of reactor requirements. Faced with the crucial question of the conditions for a reactor to ignite and be self-sustaining it is necessary to use the best confinement data available and the best techniques for its analysis. This turns out to be a very complicated matter for reasons we shall now examine.

The first complication to recognise is that the conditions for a self-sustaining reactor are dependent on density and temperature through the reaction rate, and on the magnetic field and current through stability requirements. These are also, of course, the basic parameters determining confinement. We see, therefore, that a rather subtle optimisation is involved and we cannot simply specify a required confinement time of so many seconds.

Given that we do not understand the physical processes underlying the transport of energy in tokamaks the next best approach is to determine empirically the dependence of confinement on the plasma properties. Since it is rather difficult to make precise internal measurements, the energy confinement time is used as a measure of the overall confinement. The procedure adopted is to measure this time for a wide variety of parameters and to attempt to extract the form of the dependence on these parameters. A simple procedure which is widely adopted is to express the confinement time as a product of powers of the parameters.

Since the most important parameter to be investigated is the size of the plasma (and the associated magnitude of the plasma current) it is clearly necessary to use results from a range of tokamaks. An example of this type of result obtained is the scaling relation for H-mode confinement. The rather ungainly formula is

$$\tau_E^H = 0.029\, I^{0.90}\, B^{0.20}\, P^{-0.66}\, n^{0.40}\, M^{0.20}\, R^{1.84}\, a^{0.19}\, \kappa^{0.92} \quad \text{seconds} \qquad 11.8$$

where I is the current in MA, B is the toroidal magnetic field in teslas, P is the heating power in MW, n is the density in units of 10^{19} m^{-3}, M the atomic mass, R and a are the major and minor radii in metres, and κ is the elongation ratio of the plasma (height/width). In Fig. 11.14 experimental confinement times from several tokamaks are plotted against the values given by the formula11.8. This figure shows the role of the JET results in providing an anchor at the upper end of the confinement range.

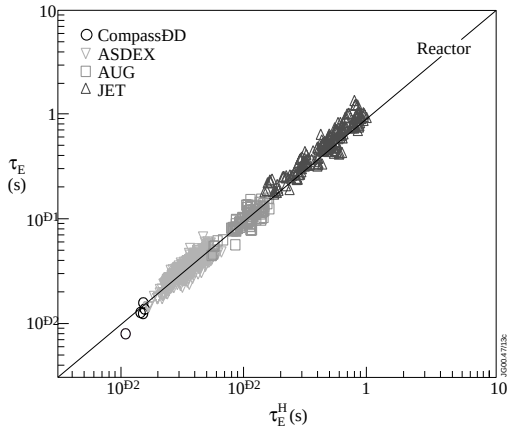

Fig.11.14 Values of confinement time obtained from several of tokamaks plotted against values calculated from Eqn. 11.8.

Equation 11.8 represents the data quite well but is completely barren of physics. It is widely felt that this is unsatisfactory and attempts have been made to rectify this apparent weakness. One way to do this is to turn to dimensional analysis. In fluid dynamics the flows in different sized but similar shaped systems can be described by a single formulation involving the ReynoldÕs number. The corresponding approach here allows us to write the confinement time as a product of a characteristic time and a function of a number of dimensionless variables. For example two of the dimensionless variables introduced earlier are β, which measures the ratio of plasma energy to magnetic energy, and the safety factor q.

Since the aim of the scaling formulas is to predict the behaviour in a tokamak reactor, it is possible to simplify the process by choosing experimental values of the dimensionless variables which will be the same in a reactor. For example if the effective value of q would be 3 in the reactor then the confinement in present experiments with q=3 can be examined. Using the proposed design of ITER, this allows simplified scalings. For example we have the H-mode scaling

$$\tau_E \propto \frac{1}{\omega_{ce}} \cdot \rho_*^{-2.9}\, \nu_*^{-0.1}\, \beta^{-0.7} \qquad 11.9$$

where the factor involving the inverse of the electron cyclotron frequency, $1/\omega_{ce}$, is chosen to give the dimension of time, ρ_* is the ratio of the Larmor radius to the plasma radius and ν_* is the ratio of the collision frequency to the bounce frequency of trapped particles.

The values of ν_* and β required for a reactor have already been obtained in tokamak plasmas. The quantity ρ_* on the other hand requires a significant extrapolation, basically because of the large increase in plasma size in moving to a reactor, without a corresponding increase in the Larmor radius.

The dependence of the confinement on ρ_* is believed to be related to the nature of the turbulence underlying the transport. If the scale-length of the turbulence is related to the plasma size the corresponding scaling is said to be Bohm-like, the name coming from an analysis of turbulent transport by Bohm. This turbulence could consist, for example, of radially extended convective cells. The scaling for smaller scale turbulence, such as that on the scale of the Larmor radius, is called Ògyro-BohmÓ.

Detailed analysis gives $B\,\tau_E \propto \rho_*^{-2}$ for Bohm-like scaling, and $B\,\tau_E \propto \rho_*^{-3}$ for gyro-Bohm scaling, B being the toroidal magnetic field. Noticing that ω_{ce} is proportional to B, we see from equation 11.9 that the experimentally determined dependence for H-modes is $B\,\tau_E \propto \rho_*^{-2.9}$, being close to the gyro-Bohm dependence.

It is difficult to determine the scaling from measurements on a single tokamak and the scaling of equation 11.8 was determined from measurements on several tokamaks. Nevertheless experiments were carried out on JET to check the scaling. Thus τ_E was measured for two pairs

of different values of ρ_* with plasma conditions arranged so that ν_* and β were constant for each pair. In addition τ_E was similarly determined for a triplet of ρ_* values with constant ν_* and β. The results are shown in Fig. 11.15 in which the measured values are plotted against the scaling predicted by relation 11.8. It is seen that there is quite good agreement.

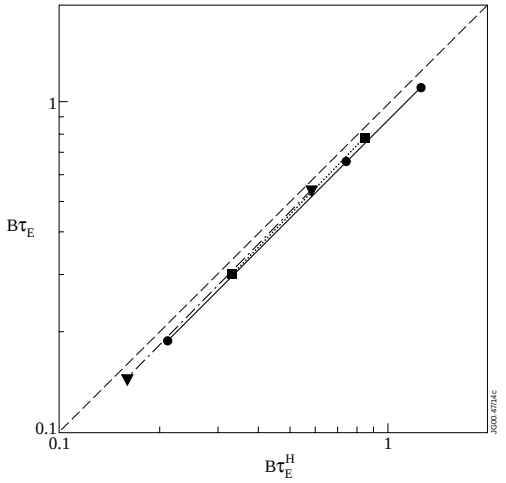

Fig.11.15 Compar ison of confinement times obtained in scaling experiments with those calculated using relation 11.8. For each symbol, ν_* and τ are the same and ρ_* is varied

Ripple Transport

A further transport issue investigated on JET is the effect of the periodic toroidal asymmetry introduced by the finite number of toroidal field coils. This asymmetry produces a short wavelength ripple in the magnetic field strength around the torus, leading to the local trapping of particles in the ÒwellsÓ produced by the ripple. The ripple introduces additional neoclassical transport depending on the well depth and the collisionality. The amplitude of the ripple is clearly less for a larger number of toroidal field coils and JET is well endowed, its 32 coils producing only a small ripple. This feature provided the opportunity of reducing the number of coils in use to investigate experimentally the effect of different levels of ripple in otherwise identical discharges.

The number of coils was reduced to 16, raising the field ripple form about 1% to 10%, and the changes in behaviour were studied. The effect of the ripple on thermal energy confinement and plasma rotation exceeded that predicted by theory. It was also found that the enhanced ripple had a severely deleterious effect on the H-mode of confinement. With 16 toroidal field coils in operation H-modes without ELMs could not be obtained with heating powers up to 12MW whereas with 32 coils ELM-free H-modes were readily obtained. These experiments demonstrated clearly the importance of having a low level of field ripple.

Anomalies

Under steady operating conditions we would expect the confinement time to depend on the gross operating parameters. The transport within the plasma would be determined by the internal conditions such as density and temperature profiles, and these would themselves be determined by the operating conditions. It is this belief which gives credence to the attempts to determine the confinement time scaling. There are however experimental results which give cause for uncertainty and which are certainly puzzling.

Figure 11.16 shows the change of plasma energy with time in a discharge with neutral beam heating. On a simple model the energy would be expected to rise to a ÒsaturationÓ value at which the energy loss rate from the plasma balances the power input. It is seen that there is little or no sign of approaching saturation. In fact, contrary to expectation, the confinement improves as the plasma energy increases. This behaviour is brought to an abrupt halt by instabilities. In this discharge the instabilities are a sawtooth collapse and an edge localised mode, both of which are discussed in Chapter 10. However these instabilities are short-lived transients and cannot explain the subsequent rapid fall in plasma energy. The lack of understanding of the sudden change in behaviour has led to its being called the X-event. The global plasma parameters immediately before and immediately after the X-event are the same and yet the confinement time is reduced by a factor 3.

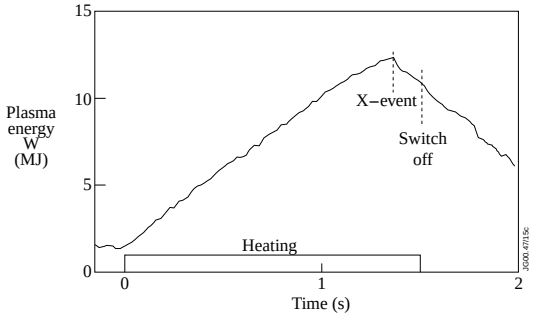

Fig.11.16 Time dependence of the plasma energy in a heated plasma showing abrupt changes in confinement.

Perhaps even more surprising is the behaviour at the later time when the heating is switched off. Without the heating to offset the heat losses the fall in plasma energy should be much more rapid. It is seen, however, that the rate of fall hardly changes. To explain this result in terms of the energy confinement time would require an abrupt improvement in the confinement time by a factor 3 at the time of switch-off without any change in the global plasma properties.

These results are bound to raise questions regarding the scaling of the confinement time. However the above anomalies occur in non-steady state conditions whereas confinement scaling is generally carried out using steady state results, and so should therefore be reliable.

Overview of Confinement

When JET was being designed in the early 1970s tokamak discharges typically lasted less than a second and good confinement times were measured in tens of milliseconds. With the operation of JET it became possible to follow the behaviour of the plasma in real time with discharges lasting up to a minute. The best confinement times in JET are greater than a second, approaching to within a factor of two the value required in a reactor.

In designing JET the question of confinement was clearly a key issue. Then, as now, there was no accepted theory of transport although it was, erroneously, thought that the confinement of the energy of the ions might be classical. There was so little experience of the confinement of plasmas with additional heating that the available empirical scaling was virtually useless as a predictive tool. One of the principal purposes of JET, of course, was to resolve these issues.

The best predictive procedure is still to use empirical scaling, and in this JET has played an important role, mainly because of its large size and high current. Even empirical scaling has become highly complex with different types of discharge and different modes of confinement. There are still unresolved issues but it is now possible to make scientific projections to a reactor and the research is now dedicated to reducing the band of uncertainty.

Bibliography

The achievement of H-mode confinement in JET was described in

Tanga, A., et al. Magnetic separatrix experiments in JET. Nuclear Fusion 27, 1877 (1987).

The pellet enhanced performance discharges, PEPs, are reported in

Tubbing, B.J.D., et al. H-mode confinement in JET with enhanced performance by pellet peaked density profiles. Nuclear Fusion 31, 839 (1991),

and further in

Hugon, M., van Milligan, B.Ph., Smeulders, P., et al. Shear reversal and MHD activity during pellet enhanced performance pulses in JET, Nuclear Fusion 32, 33 (1992).

RebutÕs model of self-sustained turbulence was described in

Rebut, P.-H. and Hugon, M. Magnetic turbulence self-sustainment by finite Larmor radius effect, Plasma Physics and Controlled Fusion 33, 1085 (1991).

JETÕs contribution to the confinement scaling is brought out in a paper written by the ITER Confinement and Database and Modelling Working Group, presented by

Cordey, J.G. Energy confinement scaling and the extrapolation to ITER. Plasma Physics and Controlled Fusion 39, B115 (1997).

Impurity transport in ohmic and L-mode plasmas was analysed in

Pasini, D., Mattioli, M., Edwards, A.W., Giannella, R., Gill, R.D., Hawkes, N.C., Magyar, G., Saoutic, B., Wang, Z., and Zasche, D. Impurity transport in JET using laser injected impurities in ohmic and radio-frequency heated plasmas. Nuclear Fusion 30, 2049 (1990), and extended to include H-mode in

Pasini, D., Giannella, R., Lauro Taroni, L., Mattioli, M., Denne-Hinnov, B., Hawkes, N., Magyar, G., and Weisen, H. Measurements of impurity transport in JET. Plasma Physics and Controlled Fusion 34, 677 (1992).

The behaviour of the JET temperature profiles with plasma heating, and the nature of the heat transport was investigated by

Callen, J.D., Christiansen, J.P., Cordey, J.G., Thomas, P.R., and Thomsen, K. Modelling of temperature profiles and transport scaling in auxiliary heated tokamaks. Nuclear Fusion 27, 1857 (1987), and

Balet, B., Cordey, J.G., Muir, D.G., and Schmidt, G.L. Heat transport with off-axis heating. Nuclear Fusion 32, 1261 (1992),

and the ion mass dependence of the transport was shown to be weak in

Tibone, et al. Dependence of L-mode confinement on plasma ion species in JET. Nuclear Fusion 33, 1319 (1993).

The surprising change in the electron thermal conductivity on a millisecond timescale over most of the plasma in L-H-L mode transitions was recognised by Neudatchin and reported in

Neudatchin, S.V., Cordey, J.G., and Muir, D.G., Sawteeth induced pulse propagation and the time behaviour of electron conductivity during L-H-L transitions in JET. Proc. 20th Eur. Conf. on Controlled Fusion and Plasma Physics, Lisbon ,1993, Vol. 1, p83,

and numerical simulations were presented by

Cordey, J.G., Muir, D.F., Neudatchin, S.V., Parail, V.V., Springmann, E., and Taroni, A. Anumerical simulation of the L-H transition in JET with local and global models. Nuclear Fusion 35, 1001 (1995).

The study was extended to include other transients in

Parail, V.V., et al. Transport analysis of transient plasmas in JET. Nuclear Fusion 37, 481 (1997).

The determination of the thermal diffusivity from sawtooth heat pulses in JET was first described by

Tubbing, B.J.D., Lopes Cardoso, N.J., and van der Wiel, M.J. Tokamak heat transport - a study of heat pulse propagation in JET. Nuclear Fusion 27, 1843 (1987),

and a more complete account is given in

Lopes Cordozo, J.J., de Hass, J.C.M., Hogeweij, G.M.D., OÕRourke, J., Sips, A.C.C., and Tubbing, B.J.D. Tokamak transport studies using perturbation analysis. Plasma Physics and Controlled Fusion 32, 983 (1990).

An analysis of the edge transport barrier is given in

Breger, P., Flewin, C., Zastrow, K.D., Davies, S.J., Hawkes, N.C., Kšnig, R.W.T., Pietrzyk, Z.A., Porte, L., Summers, D.D.R., and von Hellermann, M.G. Plasma-edge gradients in L-mode and ELM-free H-mode JET Plasmas. Plasma Physics and Controlled Fusion 40,347(1998).

An exploration of the application of theory to the transport in JET is made in

Strand, P., Nordman, H., Weiland, J., and Christiansen, J.P. Predictive transport simulations of JET L and H mode gyro-radius scaling experiments. Nuclear Fusion 38, 545 (1998).

The subjects of transport barriers and optimised shear are dealt with in the following papers

Parail, V.V., Guo, H.Y., and Lingertat, J. Fast particles and the edge transport barrier.Nuclear Fusion 39, 369 (1999).

Sips, A.C.C., et al. Operation in high performance in optimised shear plasmas. Plasma Physics and Controlled Fusion, 40, 1171 (1998).

Cottrell, G.A. et al. Transport in JET deuterium plasmas with optimised shear. Plasma Physics and Controlled Fusion 40, 1251 (1998).

The role of ELMs in energy confinement is discussed in

Fishpool, G.M. Loss of confinement due to reduction of the edge pedestal in JET. Nuclear Fusion 38, 1373 (1998), and

Zhang, W., Tubbing, B.J.D., and Ward, D.J. The effect of ELMs on energy confinement in JET. Plasma Physics and Controlled Fusion 40, 335 (1998).

The transport behaviour following the X-event is described in

Wesson, J.A. and Balet, B., Abrupt changes in confinement in the JET Tokamak. Physical Review Letters 77, 5214 (1996).

12. HANDLING THE POWER

The ultimate purpose of tokamaks is to produce power. Over several decades most of the research effort has been concentrated on achieving the plasma conditions necessary to yield this power. It is only in later years that the handling of the power has received its proper attention.

It has been recognised since the earliest days that, although the magnetic field prevents the hot plasma streaming directly to the surrounding material surfaces, the heat produced in the plasma will ultimately fall onto such surfaces. In JET this means tens of megawatts of power, and in a reactor hundreds of megawatts. The surfaces must retain their integrity and must absorb the heat load without undue damage or erosion, and without the release of impurities to contaminate the plasma.

In the case of a reactor the problem is ameliorated by the fact that four fifths of the thermonuclear power is produced in the form of energetic neutrons which pass through the vacuum vessel to be absorbed by the tokamak blanket. The remaining one fifth of the power comes from the α-particles produced in the nuclear reactions. These particles, being charged, are retained in the plasma by the magnetic field. They serve the purpose of heating the plasma and sustaining the burn conditions, but the heat they produce will leave the plasma and be loaded onto material surfaces.

It might be thought that the heat from the plasma could be distributed over the large surrounding material surface area by thermal conduction. Unfortunately this is much more difficult than might appear. The problem arises from a fundamental piece of plasma physics - the very large ratio of the thermal conductivities, parallel and perpendicular to the magnetic field. For a plasma edge temperature of 1k eV this ratio is around 10^{10}. The result is that as the heat is conducted out across the magnetic field, its first contact with a solid surface at some location allows a rapid conduction parallel to the magnetic field to that part of the surface, with the associated localised heating. The precision required to match the magnetic field surfaces to the material surfaces, and to maintain this relation, seems impossible.

The JET vacuum vessel has a surface area of $200m^2$ and a reactor would have an area around ten times larger. If the heat produced in the plasma were uniformly distributed over the surface the heat load would, in both cases, be less than a megawatt per square metre and would pose no problem. The heat could be distributed in a more or less uniform way if it could be released from the plasma in the form of electromagnetic radiation, and furthermore we can actually envisage such a scheme. If it were arranged that there were sufficient impurity atoms in the cool edge of the plasma, the plasma electrons could release their energy in exciting these atoms. This energy would then be emitted as radiation in the spectral lines of the atoms as they fell back into lower energy states. The problem is that the impurities are unwelcome. Firstly they contaminate the plasma and secondly, as described in Chapter 7, they are liable to cause the plasma to disrupt.

The outline given above only hints at the complexity of the problem. To see the full reality we shall follow the developments in JET. We shall start with the early system using so-called limiters which took the heat load in a localised, but controlled, way. This will bring out more clearly the role of the high parallel thermal conductivity. Then we shall consider the effect of introducing a separatrix into the magnetic geometry. This ultimately leads to a system in which the heat is diverted away from the main plasma region, being carried across the separatrix, and thence to a separate divertor region, to be deposited on material surfaces in a carefully designed geometry.

In the early tokamak experiments carried out in the Soviet Union it was discovered that a better plasma could be obtained if the plasma was limited locally by a solid surface whose cleanliness could be more easily controlled than that of the whole vacuum vessel. A simple form is illustrated in Figure 12.1. In this case the limiter is a poloidal ring which defines the plasma boundary.

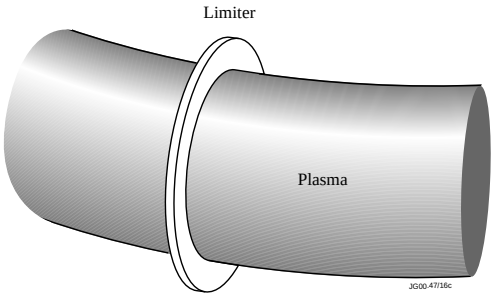

Fig. 12.1. Plasma bounded by a simple limiter.

Figure 12.2 shows in more detail the form of the limited plasma. Initially the plasma diffuses slowly out to the last closed magnetic flux surface. In JET the time for the plasma energy to flow across the plasma radius is around one second. Once across the bounding surface the particles and the energy are still restrained by the magnetic field, but flow rapidly parallel to the field lines. The energy is thus immediately lost to the limiter, typically in 100μs. In this short time the radial diffusion is around 1cm leading to a so-called Òscrape-off layerÓ with this thickness.

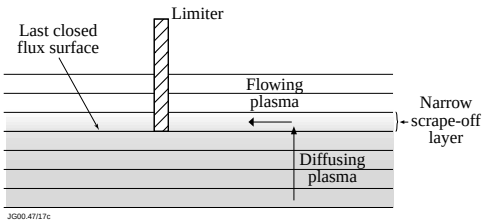

Fig. 12.2. Plasma flows to limiter in a narrow scrape-off layer.

The first limiters in JET did not have this simple form. There were four graphite limiters, each 40cm wide and 80cm high. They were fitted at the outer mid-plane and their surfaces had a slight curvature in the toroidal direction as shown in Figure 12.3. This curvature allowed a greater spread of the heat load than the simple geometry of Figure12.2. Dur ing discharges the surface temperatures of the limiters typically reached 800°C.

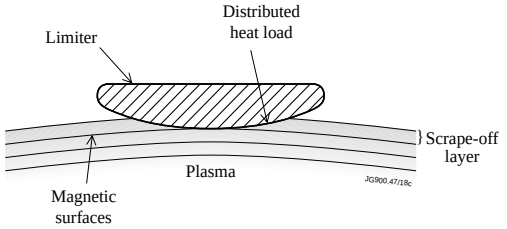

Fig. 12.3. Graphite limiter with curved surface to spread the heat load.

At this point it is necessary to recognise the dependence of the heat removal problem on that of impurity control. The heat deposited on the limiter surface is carried by energetic particles, and in particular by plasma ions. When these ions hit the surface they are capable of dislodging the atoms of the surface material through a process called sputtering. As these sputtered particles leave the limiter surface they ÒseeÓ the confined plasma. This is unfortunate since they enter the plasma, become ionised, and constitute a serious impurity source.

It is, therefore, necessary to have a way of driving the impurities away from the plasma. Indeed this is reinforced in a reactor by the need to remove the α-particles resulting from the fusion reactions. Once these α-particles have delivered their energy to the plasma they become simply a helium impurity which must be removed along with the other impurities.

The need to avoid a direct plasma-surface interaction with the main plasma, and to control the impurities, requires that the plasma be diverted to a region more remote from the plasma. This requirement led to the installation of a divertor in JET, and we shall consider the factors involved in the design of the divertor and the physical processes which determine the heat load and impurity removal. First, however, we shall look at a preliminary investigation which allowed examination of a simpler geometry without limiters.

Towards a Divertor

The original motivation to change the magnetic geometry in JET arose through interest in the higher confinement of the H-mode. The early evidence from other tokamaks was that this mode depended on having a plasma bounded by a magnetic separatrix. Although JET was not originally designed to operate with this geometry it was found that, by suitable choice of currents in the external coils, it was possible to produce such a configuration. The resulting magnetic geometry

was shown in Figure 11.3. As described in Chapter 11 the change successfully yielded H-mode confinement. However, there is a heat load problem associated with this geometry. In JET a typical plasma would be heated with, say, 20MW of applied heating. This power is lost across the separatrix to flow along a scrape-off layer of typically 1cm width. The heat flows to the foot of the separatrix where it intersects the vacuum vessel as shown in Figure 12.4. The circumference of JET is about 20m and so, allowing for the presence of two ÒfeetÓ, the basic scrape-off layer has an area of about $0.4m^2$. The heat flux density is therefore 50MW per m^2. This would be quite unacceptable as a steady heat load. However, the load can be reduced by arranging an expansion of the flux tube at its foot, and the transient heat load in JET can then be reduced to a tolerable level. In a reactor the higher power level and the requirement of steady state operation make the problem more severe.

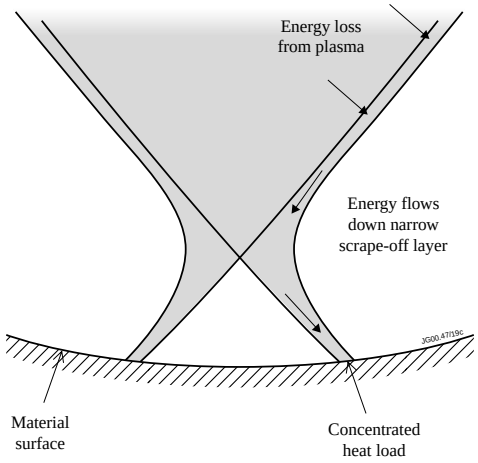

Fig. 12.4. Geometry of the energy flow in the scrape-off layer, showing the concentrated heat load at the foot of the layer.

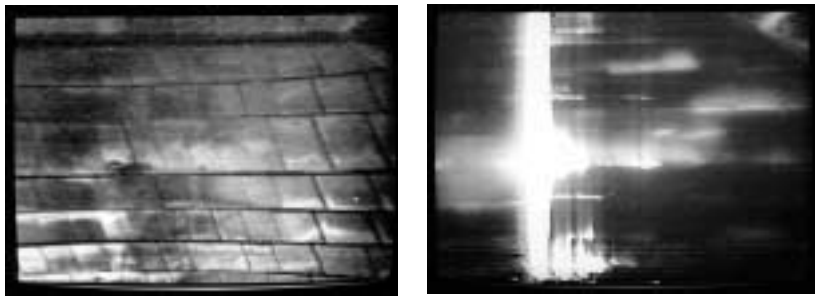

Fig. 12.5. Photograph of the tiles together with a later photograph showing the "carbon bloom" which occurs when the surface of the tiles is evaporated by an intense heat load.

The problem was made dramatically apparent in highly heated plasmas in which the termination of good performance was associated with a sudden evaporation of the carbon surface receiving the heat load. This produced a localised bright flash of visible radiation as the evaporated material was excited by the plasma, the flash being poetically called the Òcarbon bloomÓ. A photograph of the bloom is shown in Figure12.5.

Part of the reason for the sudden evaporation was the design of the tiles which receive the heat flux. The magnetic field is mainly toroidal and the field lines enter the tiles at a small angle. If the tiles formed a continuous surface there would be no problem. However, because of manufacturing limitations, there are necessarily gaps between the tiles and, as seen from Figure 12.6, this leads to a concentrated heating on the tile edges. Over a small area the magnetic field is almost perpendicular to the vertical surface, enhancing the heat flux per unit area by an order of magnitude.

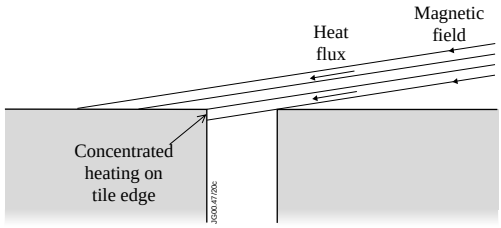

Fig. 12.6. Illustrating the concentrated heating on tile edges with the angled magnetic field.

It was decided to design and build a divertor at the bottom of the vacuum vessel which would not only overcome the tile edge problem, but would also be used to investigate possible ways of reducing the heat flux to the material surface.

The re-design of the tile arrangement was straightforward. It is only necessary to angle the surface of the tiles slightly and to use an accurately levelled base plate for the tiles. The edge problem is then resolved as illustrated in Figure 12.7. This procedure was adopted and found to be completely successful.

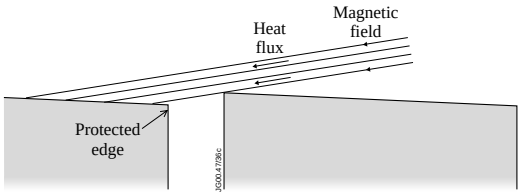

Fig. 12.7. Showing the protection of the tile edges obtained with sloped surfaces.

The design of the divertor is illustrated in Figure 12.8, which shows the layout in the poloidal cross-section. Now, although the problem of tile edges was removed, the more fundamental

matter of heat loading remained to be solved. To understand this problem, and the possible means of its resolution, we must examine the physical processes involved more closely.

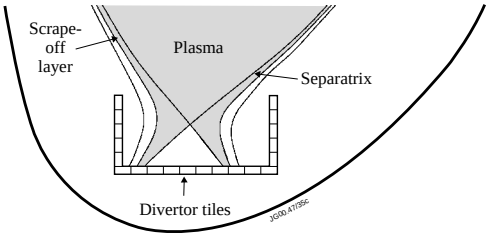

Fig. 12.8. Outline of the divertor design

Basic Divertor Physics

The particles and heat which leave the plasma flow along the narrow scrape-off layer to the divertor tiles. The basic, simple case is illustrated schematically in Figure12.9.

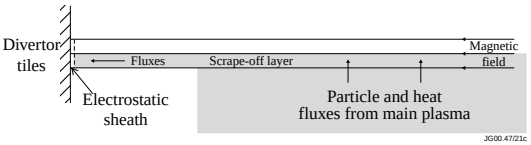

Fig. 12.9. Schematic diagram of fluxes from the plasma, through the scrape-off layer, to the divertor tiles.

The greater mobility of the electrons compared to the more massive ions gives rise to a thin electrostatic sheath adjacent to the solid surface of the divertor. This sheath determines the boundary condition for the fluxes along the scrape-off layer. Essentially, the plasma flows out at the sound speed, and this also determines the heat flux. Thus, if the ion flux is nc_s, where n is the particle density and c_s is the sound speed, the heat flux is αnc_sT where T is the temperature and α is a number typically around 8.

This loss of energy at the surface cools the electrons, and the result is a conduction of heat from the up-stream, higher temperature part of the scrape-off layer in contact with the main plasma. The heat carried by this thermal conduction, together with some convection, is just the heat coming from the plasma, and defines the heat load problem to be solved. How then can the heat be prevented from reaching the divertor surface?

It was necessary to look for means of transporting heat which ignore the constricting effect of the magnetic field. There were two possibilities - neutral particles and electromagnetic radiation. Both of these suggest the use of a gas to absorb the heat flow. Neutral hydrogenic gas

interposed between the high temperature plasma and the divertor surface would be able to radiate energy onto a large surface area. Furthermore, collisions of ions with the gas would allow an exchange of charge, neutralising the energetic ions. The resulting neutral particles, being unaffected by the magnetic field, could further spread the heat load.

Gas Cooling

The possibility of a plasma-gas transition in the divertor had been proposed by Tenney and Lewin in 1974, and experiments to investigate the physics were carried out by Hsu at Princeton. A simplified diagram of their apparatus is shown in Figure12.10. The plasma flows along the magnetic field produced by coils, being cooled and neutralised until it forms part of the background gas. With these experiments in mind it seemed possible that the divertor target could be protected by a neutral gas which removed the direct heat flux through a combination of radiation losses from electrons and charge exchange losses from ions. The conjectured arrangement is illustrated in Figure12.11.

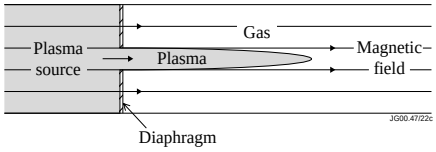

Fig.12.10. Schematic diagram illustrating the experiments of Hsu.

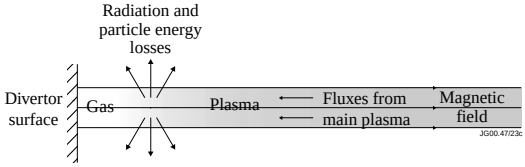

Fig.12.11. Illustr ating the principle of gas separation of the plasma from the divertor tiles, the energy being removed by atomic processes.

For the atomic processes leading to radiation cooling to be effective the electron temperature must fall to a few electron volts. If the plasma is to be transformed to a neutral gas the temperature must fall to a level where recombination of electrons and ions to form neutral atoms occurs more readily than re-ionisation of the resulting neutral atoms by electrons. This requires a temperature of one electron volt or less.

Preliminary attempts to detach the scrape-off layer plasma from the target plates were carried out before the installation of the divertor. The procedure was to increase the gas feed in order to increase the neutral gas pressure in front of the target. The only direct measure of the

resulting behaviour came from the solid-state video cameras which detect the radiated light. These indicated that, initially, increasing the gas feed led to the formation of radiation zones just above the target. However, with further increase in the gas feed these zones first moved upward to the X-point of the separatrix and then progressed further upward along the edge of the main plasma forming a radiating layer. This type of radiating layer, usually called a MARFE, is described in Chapter 8. Regarding the question of plasma detachment from the target plates, the experiments were promising but inconclusive and a fuller understanding awaited construction of the divertor.

The Mark I Divertor

The design of the first divertor was surrounded by many uncertainties as to how a divertor should work and how best to remove the heat arriving at the target plates. However, one clear necessity was to design the target tiles to avoid exposed edges, and this was done using the technique described earlier. In order to have sufficient control over the local magnetic field, and in particular the height of the X-point above the tiles, it was found necessary to place the divertor coils inside the vacuum vessel. The target plates and the divertor coils formed an integrated system as shown in Figure12.12. The opportunity was also taken to arrange for a sweeping of the feet of the scrape-off layer across the target tiles to reduce the heat load on each point. This was done by adding an alternating component to the coil currents, with a frequency of 4Hz.

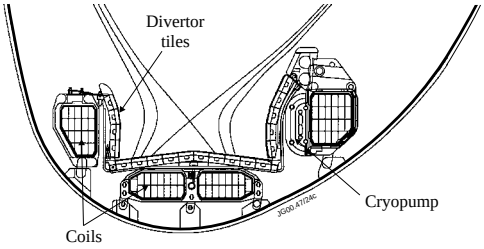

Fig. 12.12. The mark I divertor

An important element in the design was the concept of entrapment of impurities produced at the target tiles. The idea was that this would be achieved by the frictional drag on the impurities due to the plasma flow down the scrape-off layer. This drag force has to overcome the so-called thermal force which operates to drive the impurities toward the main plasma.

The thermal force derives from the higher collisionality of colder particles. Because of this the plasma particles striking impurity ions from the colder side impose a greater force than those from the hotter side. This produces a resultant force on the impurity ions in the direction of increasing temperature, that is toward the main plasma.

The impurities can be removed by having a pump at the bottom of the vacuum vessel. This

produces an additional pressure gradient which draws the flow toward the target tiles. Such a pump was installed behind the tiles of the divertor. The pump was a cryopump, which operates by condensing those particles striking its liquid helium cooled surface.

The successful use of sweeping is illustrated in Figure 12.13 which shows the evolution of the target temperature during a period of plasma heating. Following the application of the heating the target temperature rises from 500°C to 900°C. The sweeping is then switched on and the temperature falls back to a steady 700°C. Even without sweeping the improved design of the tiles produced a fundamental improvement. Whereas loss of good performance had been previously associated with gross evaporation and the Òcarbon bloomÓ, full power could now be applied without this limitation. This success also clarified a basic issue regarding confinement. In the earlier experiments the sudden loss of performance at the X-event could be attributed to the influx of impurities associated with the carbon bloom. Now the bloom was removed but the loss of performance persisted. It was clear, therefore, that another explanation was required.

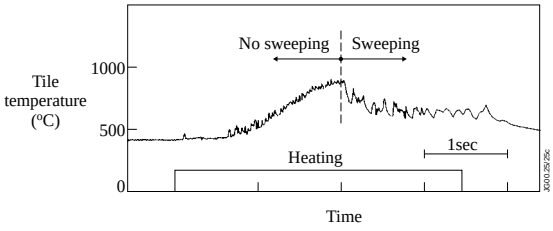

Fig. 12.13. Showing the fall in temperature resulting from sweeping the scrape-off layer over the divertor tiles with 12MW of heating.

Detachment

A crucial experiment with the mark I divertor was the test of the concept of gas cooling. The aim was to increase the gas pressure in the divertor to a level at which the plasma was detached from the target plates by an insulating layer of neutral gas.

Along with the design and construction of the divertor, new diagnostic systems were introduced to monitor its behaviour. The principal diagnostic consisted of Langmuir probes at the target plates. When a large negative potential is applied to a Langmuir probe, all the electrons are repelled and the probe collects a saturation ion current which is proportional to the ion density and to the square root of the temperature. Clearly detachment implies a fall in the ion density at the target plate and we would expect the saturation ion current would then be much diminished.

Figure 12.14 shows the result of an experiment in which the plasma was heated with 4MW of neutral beam heating. The gas input was increased as shown. Initially the ion saturation current to the probe increased as the neutral gas atoms were ionised and contributed to the ion density. Then, with further increase in the gas input, the saturation current fell to a very low value indicating

a successful detachment of the plasma from the probe.

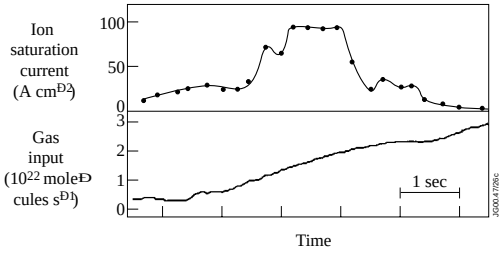

Fig.12.14. The introduction of gas leads to detachment of the plasma from the divertor tiles as seen from the virtual removal of the ion saturation current to the Langmuir probe.

The condition for the plasma to be neutralised to a gas is that the rate of recombination of electrons and ions into gas atoms be much larger than the rate of re-ionisation of the gas atoms so formed. Theory predicts that this occurs for an electron temperature of 1eV or less. Another test of detachment would therefore be a fall in the electron temperature to this low value. In principle the Langmuir probes are also able to determine the temperature by measuring the dependence of the probe current on the applied voltage. It turns out that a simple interpretation of the probe results indicates a temperature of a few eV, much to high for neutralisation to occur. However, this discrepancy has led to a careful re-examination of the theory of Langmuir probes, presenting an intriguing challenge to our understanding of plasma physics and leading to several possible explanations of the unexpected results.

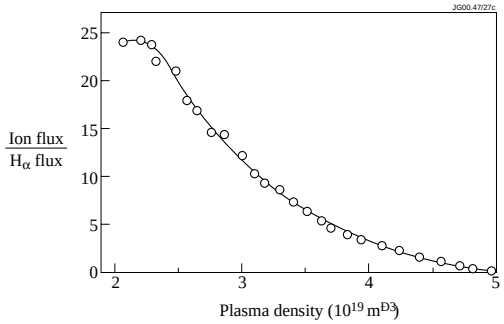

Fig. 12.15. The fall in the Johnson-Hinnov ratio as the plasma density is increased provides evidence of an insulating neutral gas.

Support for the belief that the electron temperature was reduced to a low value by the influx of neutral gas comes from measurements of the Johnson-Hinnov ratio. The rate of ionisation and the rate of emission of D_α line radiation have different temperature dependences. Ionisation

requires higher energy and is therefore less likely at temperatures below 10eV. Figure12.15 shows the fall in the ratio of ion flux to D_α flux in the divertor as gas is introduced and the line average density rises. The fall of the ratio by two orders of magnitude indicates a reduction in electron temperature to a very low value.

A direct view of detachment can be obtained using a reconstruction of the radiation profiles from bolometer measurements. Figure 12.16 shows three such profiles during detachment. The peak of the radiation moves to progressively higher positions as the density is increased. In the final figure this peak has reached the X-point of the separatrix and the radiation near the target is diminished, consistent with a lowering of the electron temperature.

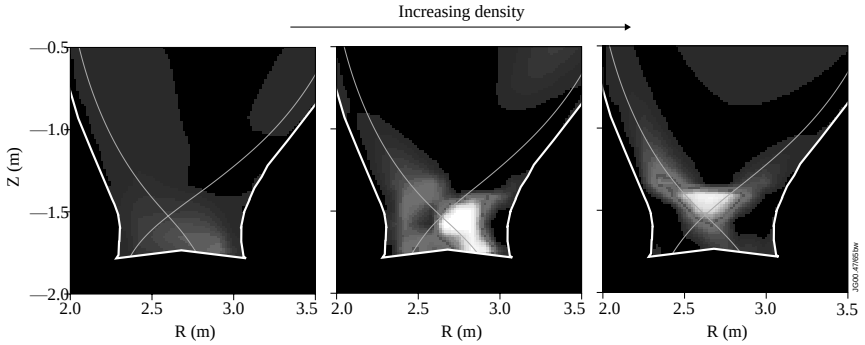

Fig. 12.16. Reconstruction of the radiation sources showing the movement of the radiation upwards as the plasma density is increased.

H-modes and ELMs

The successful achievement of detachment of the plasma from the divertor tiles described above was obtained with ohmically heated plasmas and plasmas with L-mode confinement. When this control of the heat flux is tried with the better confinement of the H-mode the behaviour is more complex. There are two basic reasons for this. Firstly, as the gas pressure is increased to achieve detachment the H-mode confinement deteriorates. The detachment obtained while maintaining good confinement is incomplete. The second reason is the effect of the Edge Localised Modes of instability described in Chapter 10. These ELMs release pulses of energy from the main plasma into the scrape-off layer. Consequently they impose a transient high heat load on the divertor tiles. This means that, although some detachment of the plasma from the tiles is obtained between ELMs, the gas shielding is punctured during the ELM. This is shown in Figure 12.7 where the large, pulsed increases in the ion saturation current to the Langmuir probe, caused by ELMs, indicate loss of detachment.

As the gas fuelling rate is increased the ELMs become smaller and more frequent. In the,

now shorter, periods between the ELMs there is a higher ion saturation current to the probe, indicating that a poorer level of detachment is achieved. If the gas fuelling is increased still further the confinement deteriorates to that of the L-mode.

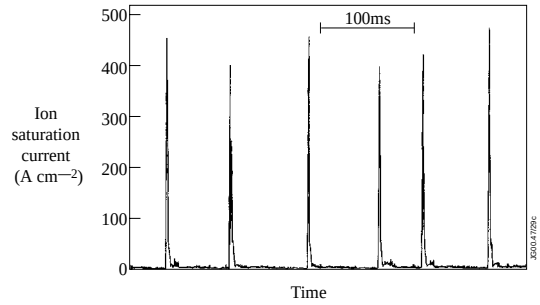

Fig. 12.17. Loss of detachment due to ELMs as indicated by the pulses in ion saturation current to a Langmuir probe.

It is clear that in these H-mode experiments the ÔnaturalÕ energy losses resulting from gas fuelling are inadequate to produce detachment during the pulse of heat flux associated with a large ELM. Furthermore there is a trade-off between achieving detachment and losing confinement. This leads us to ask whether the gas induced heat loss can be made more efficient. One obvious possibility is that of increasing the radiation from the plasma in the divertor by introducing a well-chosen impurity.

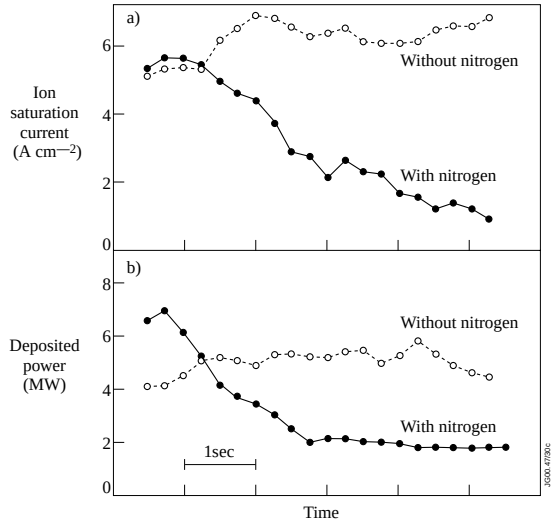

Fig. 12.18. a) Ion saturation current to Langmuir probe with and without nitrogen. b) Resulting reduction in power deposited on the divertor.

Experiments were carried out introducing nitrogen as the radiating impurity. Nitrogen is ionised at the low temperatures of interest but still retains most of its electrons. It is therefore able to radiate at temperatures of several electron-volts, whereas hydrogen is fully ionised and unable to radiate.

The addition of nitrogen changes the pattern of the ELMs. As the fuelling is increased the ELMs become smaller and more frequent. The increased radiation between ELMs leads to substantial detachment of the plasma from the target. Figure 12.18a shows a comparison of the ion saturation current to the Langmuir probe, with and without nitrogen. It is seen that the addition of nitrogen to the fuel leads to an order of magnitude fall in the ion flux. Figure12.18b shows the corresponding reduction in power deposited on the divertor.

Carbon and Beryllium

The choice of material for surfaces surrounding the plasma and for divertor surfaces involves a number of complex issues. One factor is the effect of atoms of the chosen material when they enter the plasma as impurities. Atoms with a high nuclear charge, Z, have the disadvantage of producing a high level of radiation loss and of releasing a large number of electrons. The problem with these impurity electrons is that they carry energy which could have been taken by a potentially reacting deuterium or tritium ion. Research in JET has therefore concentrated on the use of two low Z materials, carbon and beryllium.

Carbon, in the form of carbon fibre composite, is mechanically strong and has the advantage that it does not melt. As with all materials carbon releases atoms from its surface when bombarded with ions, and the released atoms can then enter the plasma. For most materials this process, which is called sputtering, can be prevented if the energy of the bombarding particles is kept sufficiently low. Carbon has a higher critical energy for this physical sputtering than beryllium but, unlike beryllium, carbon is subject to chemical sputtering. Chemical sputtering occurs through chemical reactions at the material surface, an example being the formation of methane, CH_4, when hydrogen impinges on a carbon surface. The threshold is very low, and chemical sputtering can be significant even at low plasma temperatures. Again, molecules so formed are free to enter the plasma, introducing carbon impurity.

Beryllium has the disadvantage of melting at a fairly low temperature (1270°C), and melting can destroy the carefully designed tile geometry, leading to high spots which are vulnerable to plasma bombardment. An advantage of beryllium is that it does not exhibit chemical sputtering. A further advantage is that a clean surface will collect and retain impurities such as oxygen and carbon in a process known as gettering. However, on a longer timescale this process reduces in effectiveness as the surface saturates.

Experiments in which the plasma was limited by beryllium surfaces produced plasmas with a lower impurity level than those limited by carbon. Figure 12.19 illustrates this result

using an effective value, Z_{eff}, of the ionic charge in the plasma as a measure of impurity level. However beryllium underwent melting and was particularly at risk with high performance discharges. An example of such melting is shown in the photograph of Figure 12.20. As a result carbon was generally preferred, and carbon surfaces were used during most periods of operation.

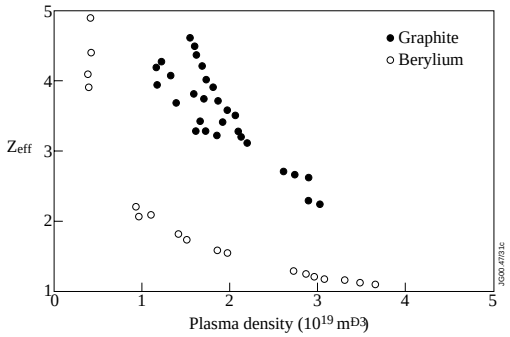

Fig. 12.19. Showing the reduced impurity level with beryllium as compared with carbon as measured by Z_{eff}, an average value of the ionic charge in the plasma.

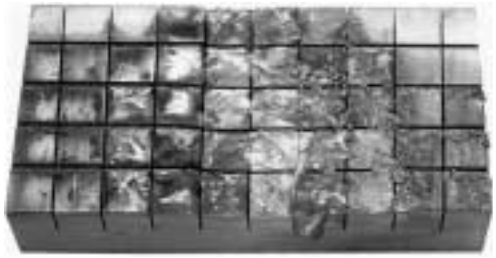

Fig. 12.20. Melting of the beryllium tiles.

The Mark II Divertor

As we have seen, the mark I divertor allowed a convincing demonstration of plasma detachment from the target tiles. However, it was thought that the design could be improved by a more closed divertor geometry. The first advantage would be that the higher neutral gas pressure in the divertor would facilitate detachment. The second advantage would result from the reduced neutral gas pressure in the main chamber. When neutral atoms collide with plasma ions they can undergo a charge exchange. The slow neutral atom becomes an ion, and the fast plasma ion is neutralised. The resulting fast neutral particles impinge on the walls of the vessel and release impurities. By reducing the neutral gas pressure in the main chamber the production of impurities is reduced.

With these considerations in mind a new divertor was designed with the aim of producing

a higher differential between the gas pressure in the divertor and that in the main chamber. This markII design with its mor e closed geometry is illustrated in Figure 12.21. A photograph of the layout is shown in Figure 12.22.

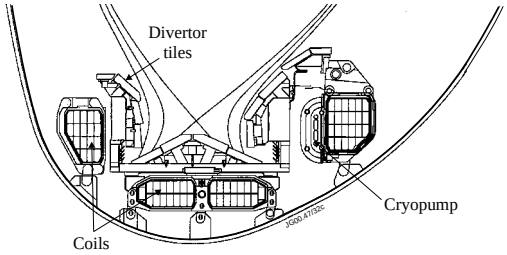

Fig. 12.21. The mark II divertor

Fig. 12.22. Photograph of the mark II divertor tiles.

The gas pressure in the main chamber provides fuelling for the plasma and so the plasma density is an indicator of the main chamber gas pressure. The success of the mark II design in increasing the gas density in the divertor region can therefore be judged by comparing the divertor gas pressure with that in the mark I divertor at given plasma densities. This comparison is made in Figure 12.23 where it is seen that the mark II divertor produced a large improvement, the divertor gas pressure being substantialy higher.

However, it still seemed that the gas pressure in the main chamber was too high and it was realised that there were leakage paths from the divertor to the main chamber which allowed an undesirable gas flow. These leaks were plugged and this produced a significant decrease in the gas pressure in the main chamber for a given fuelling rate as seen from Figure 12.24.

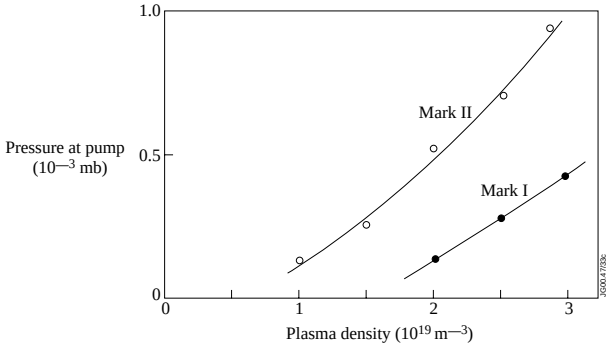

Fig. 12.23. The improved closure with the mark II divertor, as shown by the increased gas pressure for a given plasma density.

Since it was expected that the improved closure in changing from the mark I to the mark II divertor would reduce the sputtering from the main chamber carbon tiles, a reduction in the impurity level had been anticipated. However, this was not found. A possible reason for this behaviour is that the sputtering might be chemical rather than physical. Unlike physical sputtering the chemical interaction with particles arriving at the surface persists even at low energy of the impacting particles.

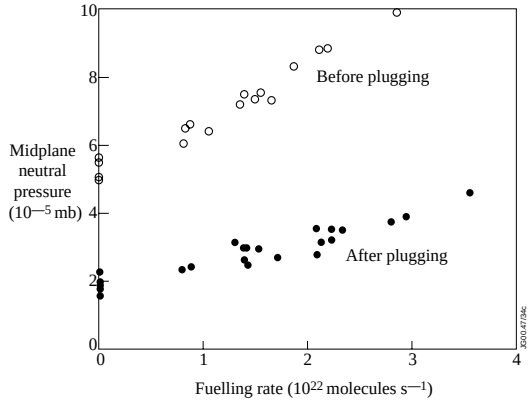

Fig. 12.24. Showing the reduction in the mid-plane neutral gas pressure resulting from reduction of the leakage.

A Complex Problem

Since the evolution of our understanding of divertors has been rather complicated it is perhaps worthwhile making a summary of the main points.

The carbon bloom which occurred in high performance plasmas forced a realisation that heat loading on the target tiles presented a serious problem. As a result the study of divertors

became the principal theme of the research in JET.

The problem was seen to have two aspects. Firstly the target tile geometry needed to be carefully designed to avoid high heat loading on tile edges. As we have seen, the improved designs provided a solution to this problem. The second aspect involved reducing the heat flowing to the divertor target by using neutral gas to cool the plasma before it reaches the tiles. Again it was found possible to achieve this type of cooling, but only satisfactorily at low powers. At higher powers the high gas pressure required led to a reduction in confinement. The cooling was successfully increased by adding radiating impurities. However the confinement was again deteriorated and the radiation moved further out of the divertor.

Another problem at high power and good confinement is that the energy escapes from the plasma in high energy busts through the ELM instability. The neutral gas insulation is unable to withstand these pulses and a solution has to be found without a significant loss of confinement.

We see therefore that much progress has been made, but that the understanding gained has exposed more clearly the complexity of the problem of handling the power leaving the plasma.

Bibliography

A discussion of wall materials is given in

Rebut, P.H., Dietz, K.J., and Lallia, P.P. Experience with wall materials in JET and implications for a future ignited Tokamak. Journal of Nuclear Materials 162-164, 172 (1988), and an ÒOverview of results from the JET tokamak using a beryllium first wallÓ was given by Keilhacker, M., and the JET team in Physics of Fluids B: Plasma Physics 2, 1291 (1989).

A later paper is

Campbell, D.T., and the JET team. Experimental comparison of carbon and beryllium as divertor target materials in JET. Journal of Nuclear Materials 241-243, 379 (1996).

An early model of impurity behaviour in the scrape-off layer is described in

Keilhacker, M., Deksnis, E., Harbour, P., Rebut, P.H., Simonini, R., Taroni, A., Vlases, G.C., and Watkins, M.L. Modelling impurity control by plasma flows in the JET pumped divertor. Plasma Physics and Controlled Fusion Research. (Proc. 13th Int. Conf. Washington, 1990) Vol. 1 p.345 (1991) IAEA Vinenna.

Measurements in the plasma boundary are described in

Erents, S.K., Tangle, J.A., McCracken, G.M., Stangeby, P.C., and de Kock, L. Probe measurements of density and temperature profiles in the JET boundary. Nuclear Fusion 26, 1591 (1986).

The relation of edge to plasma is dealt with in

Erents, S.K., Tagle, J.A., McCracken, G.M., Stangeby, P.C., and de Kock, L. Dependence of tokamak edge conditions on global plasma parameters in JET. Nuclear Fusion 28, 1209 (1988).

High temperatures measured at the plasma edge were reported by

Weisen, H., et al. Boundary ion temperatures and ion orbit losses in JET, Nuclear fusion 3l, 2247 (1991).

Investigations with the mark I divertor are described in

Campbell, D.J. and the JET Team. Confinement and fusion performance in JET. Plasma Physics and Controlled Fusion 39, A285 (1997),

and results from the change to mark II are analysed in

Vlases, G.C., Horton, L.D., Matthews, G.F., et al. The effect of divertor geometry on divertor and core plasma performance in JET. Journal of Nuclear Materials 266-269, 160 (1999).

A comprehensive summary of the work on detachment is provided by

Loarte, A., Monk, R.D., Martin-Solis, J.R., et al. Plasma detachment in the JET mark I divertor experiments. Nuclear Fusion 38, 331 (1998),

and recombination is discussed in

McCracken, G.M., Stamp, M.F., and Monk, R.D. Evidence for volume recombination in JET detached divertor plasmas. Nuclear Fusion 38, 619 (1998).

Summaries of the JET divertor research are given in the papers

Horton, L.D., Vlases, G.G., et al. Studies in JET divertors of varied geometry. I: Non-seeded plasma operation. Nuclear Fusion 39, 1 (1999).

Matthews, G.F., et al. Studies in JET divertors of varied geometry. II: Impurity seeded plasmas. Nuclear Fusion 39, 19 (1999).

McCracken, G.M. et al. Studies of JET divertors of varied geometry III: Intrinsic impurity behaviour. Nuclear Fusion 39, 41 (1999).

Vlases, G.C., Horton, L.D., Matthews, G.F., et al. The effect of divertor geometry on divertor and core plasma performance in JET, Journal of Nuclear Materials 266-269, 160 (1999).

13. BASIC PHYSICS

Tokamak plasmas are complex and, as we have seen in the preceding chapters, much of the behaviour is only understood in an empirical way. There are areas of the research however where the investigations on JET involve more physics and we shall look at some of these here.

The first is the phenomenon of runaway electrons, which involves a small fraction of the electrons in the plasma being accelerated to high energies in the toroidal electric field. This turned out to be of particular interest, not only because a large runaway current of over a megamp appeared, but also because a new mechanism for producing the runaway electrons was recognised, and because the implications for reactors are serious.

The second deals with the collisional interaction between the α-particles produced by fusion reactions and the plasma ions. It was found that in a small fraction of such collisions where there is a hard impact, very energetic plasma ions result and, following charge exchange, these have been detected.

The next investigation follows from the question - can we detect the radiation which the ions emit as a result of the acceleration involved in their Larmor orbits? A further subject is that of Alfvén waves, the natural waves of a plasma in a magnetic field. In a tokamak these waves are not so simple and can even be unstable. Consequently much careful theoretical and experimental attention has been given to their analysis.

Finally we shall look at the phenomenon cryptically called the “snake”. In reality this is a remarkable bifurcation of the plasma structure induced by the injection of a hydrogen pellet - raising several fundamental questions.

Runaway Electrons

When the toroidal electric field is applied to the plasma to drive the plasma current, the electrons take up a drift velocity at which the electric field force on them is balanced by the collisional drag with the ions, and this drift velocity determines the current density. However, although this describes the average behaviour of the electrons it is not correct for the fast electrons in the tail of the velocity distribution. The reason is that the drag on fast electrons falls rapidly as their velocity is increased. For electrons above a certain critical velocity the faster they move - the less the drag, and they “runaway” to high velocities, often close to the velocity of light.

Under normal circumstances the runaway electrons are small in number and present no problem, but following some disruptions in JET a circulating beam of relativistic runaway electrons carries a current of more than a megamp. Such a case is illustrated in Figure 13.1. In these disruptions the plasma has been cooled by the rapid influx of impurities, often to temperatures as low as a few eV. At first sight this would seem to prevent the runaway process because the collisional drag is much higher at low temperatures. However, this is more than compensated by

the increased electric field which, from Ohm's law, arises naturally to maintain the current in the now more resistive plasma. It is therefore quite understandable that runaway electrons are produced.

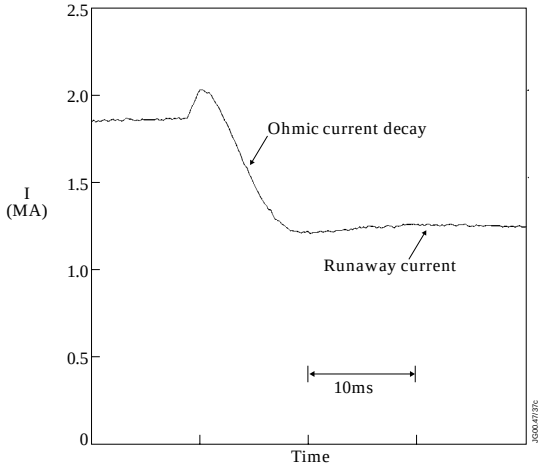

Figure 13.1. Following some disruptions the plasma current decays to leave a large current of runaway electrons which sometimes persists for several seconds.

This subject would probably only have been of minor interest but for the recognition, first of an alternative mechanism for creating runaway electrons, and second of the potential threat they present to a fusion reactor.

In the original runaway process electrons diffuse in velocity through multiple distant collisions with other electrons, and those which diffuse above the critical velocity then runaway. It was pointed out by Sokolov in 1979 that existing runaway electrons can knock slow electrons above the critical velocity in a single hard collision. In such a collision the fast electron typically comes within 10^{-14}m of the target electron, and the collision lasts about 10^{-22}s. Once knocked above the critical velocity such electrons runaway and are then able to create further runaways by the same process. For a fixed electric field this cascade would produce an exponential growth in the number of runaway electrons.

In tokamaks the runaway electrons soon become relativistic with a velocity very close to the velocity of light. The exponential growth in the number of runaways would therefore lead to an exponential growth in the current they carry. The runaway current which would be reached following a disruption depends on the electric field induced by the change of magnetic flux associated with the plasma current decay. For large tokamaks the available magnetic flux is large and for a tokamak reactor it was calculated that the cascade process would lead to a transfer of almost all of the plasma current to the runaway current. This would mean around 20MA of runaway electrons accelerated to energies of hundreds of MeV, a potential danger to surrounding surfaces when the runaway electrons are finally lost.

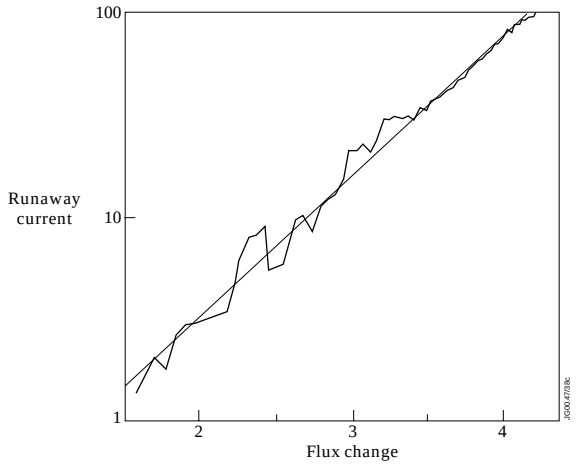

Figure 13.2. In some cases the runaway current grows exponentially, as expected if the electrons are produced by the cascade process. (The scales are in arbitrary units).

In an attempt to determine which runaway process was operative in JET both the growth and the decay of the runaway current were analysed. In some cases the growth of the current appeared to be exponential indicating the cascade process, and such a case is shown in Figure13.2. However other cases did not show this form. The current decay had the time dependence expected from an electron momentum distribution produced by the cascade process, but the measured decay of the energy of the electrons was inconsistent with this model. It is not, therefore, clear which mechanism dominates for the observed production of runaway electrons.

The account given above only sketches the physics involved in the runaway phenomenon and further subtleties remain to be explored in order to resolve the discrepancies. Since the issues are both important and interesting, it provides a good subject for future study.

α-Particle Knock-on Collisions

The principle of utilising the plasma ions which are neutralised by charge exchange and escape from the plasma as a diagnostic was described in Chapter 8. With deuterium-tritium plasmas the α-particles resulting from fusion reactions can also be studied in a similar way. Some of the α-particles undergo double charge exchange with impurity ions carrying electrons. This neutralises the α-particles which are then able to leave the plasma as neutral helium atoms which can then be examined by the neutral particle analyser to determine their energy. Since the α-particles slow down through collisions with the plasma particles, the measured energy spectrum is expected to give information about this slowing down.

When the energy spectrum was measured the results were surprising. Figure 13.3 gives the ratio of the expected flux based on collisional slowing of the α-particles to the measured

flux. It is seen that below about 1.2 MeV energy the measurement gives a flux of neutral particles an order of magnitude higher than expected.

The explanation is that the detected particles below 1.2 MeV are predominantly high energy *deuterium* atoms. These are not distinguished from the α-particles by the neutral particle analyser because deuterons and α-particles have the same charge-to-mass ratio. How could the plasma deuterons have acquired energies of MeV?

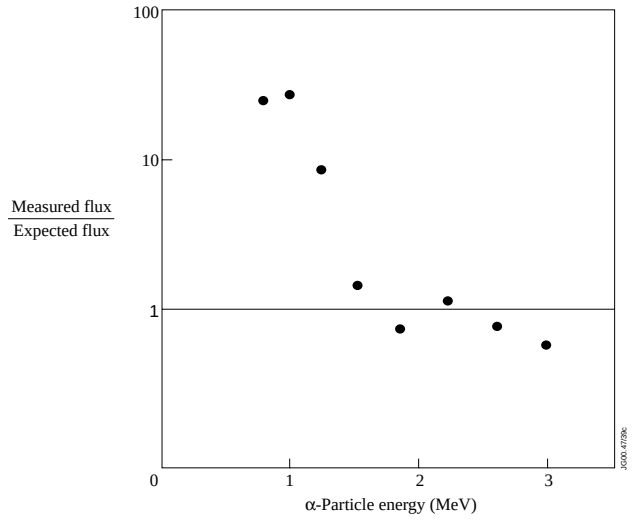

Figure 13.3. Ratio of the expected atomic flux arising from the fusion α-particles to the experimentally observed flux.

A head-on collision between a 3.5MeV α-particle produced by D-T fusion and a plasma deuteron kicks the deuteron to an energy of up to 3.1 MeV, and it is this knock-on process which has produced the fast deuterons. The deuterons have a spread in their energies due partly to the variable hardness of the collision and partly to the distribution of α-particle energies as they slow down.

This knock-on behaviour is similar to that of the electrons in the runaway cascade described earlier. Again the collisions are very brief, and during the collision the α-particles and the deuterons approach each other to a separation comparable with the nuclear size of the particles themselves.

Ion Cyclotron Emission

When charged particles are accelerated they emit radiation. In a magnetic field the particles undergo the continuous acceleration implied by their circular orbits and the resulting radiation is called cyclotron emission. Electron cyclotron emission is familiar through its use in measuring the electron temperature. Could the analogous ion cyclotron emission - I.C.E. - be detected?

The ions will emit radiation at harmonics of their gyrofrequency, typically tens of megahertz. Electromagnetic radiation of this frequency does not propagate in tokamak plasmas, but the radiated energy can propagate across the magnetic field as fast magnetosonic waves. This makes it possible to detect the ICE using the ion cyclotron heating antennas, which are designed to couple to fast waves to heat the plasma.

The initial idea was that of detecting the blackbody radiation from the thermal plasma ions. However, when the ICE spectra were measured they were not consistent with this expectation, having instead narrow equally-spaced emission lines, the spacing being proportional to the magnetic field, and intensities much larger than the blackbody level. The spectrum from a deuterium-tritium plasma is shown in Figure 13.4. The observed frequencies depend on the magnitude of the magnetic field at the location of the emission and, surprisingly, it was found that in JET this meant that the emission comes from the edge of the plasma in the outer mid-plane.

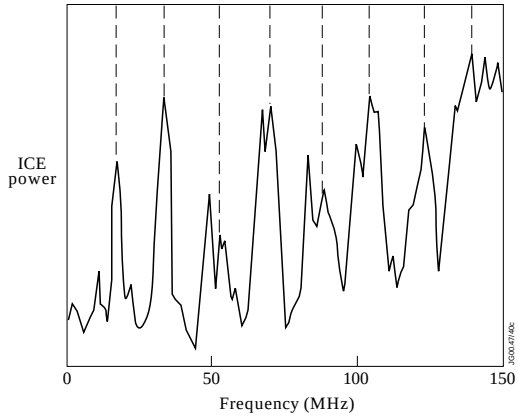

Figure 13.4. Spectrum of ion cyclotron emission power showing its equally spaced emission lines.

A further surprise was that the strength of the emission was strongly dependent on the fusion reaction rate. In otherwise similar plasmas, those with added tritium had many times the emission of those without, showing that the drive for the ICE mechanism comes, not from the deuterons, but from the energetic particles generated by fusion reactions. This is brought out more precisely in Figure 13.5 which shows the ion cyclotron emission to be almost proportional to the fusion reactivity over six decades.

It seems likely that the explanation of this behaviour is that some of the reaction products, α-particles and protons, born in the core of the plasma, have trapped orbits which take them into the plasma edge. The resulting velocity distribution of these particles can then be subject to an instability which excites waves at the ion cyclotron harmonics, and it is these waves which are observed.

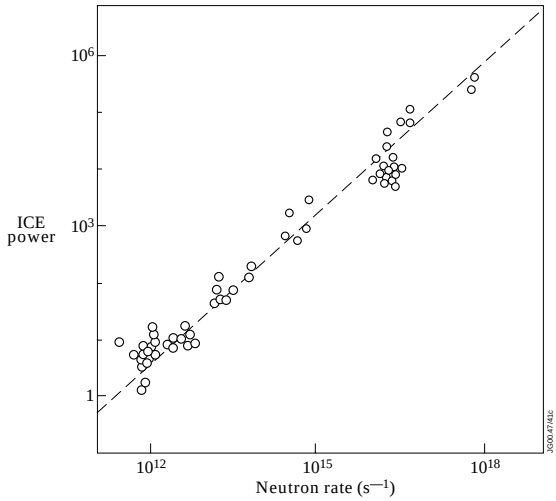

Figure 13.5. The ion cyclotron emission power is almost proprotional to the neutron rate over six decades. (The ICE power is in arbitrary units).

T.A.E.s

Highly conducting plasma in a magnetic field behaves as though the plasma is attached to the field lines. If the plasma is locally displaced it carries the magnetic field lines with it. The resulting bending of the magnetic field lines leads to an elastic restoring force. The combination of the elasticity of the magnetic field with the inertia of the plasma allows the propagation of waves, which are called Alfvén waves after their discoverer.

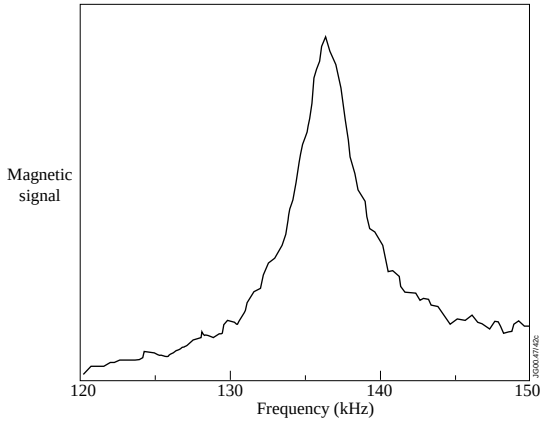

Figure 13.6. T.A.E. resonance excited by external coils and measured by the magnetic pick-up coils.

Alvén waves were first produced and examined in laboratory plasmas forty years ago. The so-called TAEs are a forbiddingly named variant - the Toroidal Alfvén Eigenmodes. These waves have been produced in JET and have been studied in depth - but first we need to know what they are.

The simple expectation would be that tokamak plasma would be able to carry Alfvén waves. However, in the approximation where the tokamak is regarded as a cylinder we do not find the discrete eigenmodes that we would expect from an elastic structure. Instead the spectrum is a continuum. When the toroidal nature of tokamaks is taken into account the continuum persists but with gaps, and inside each of these gaps there is a discrete mode. These are the toroidal Alfvén eigenmodes. Unlike the continuum they are not strongly damped and this means that they can be driven unstable by certain destabilising free energy sources - one of which is the distribution of α-particles resulting from fusion reactions.

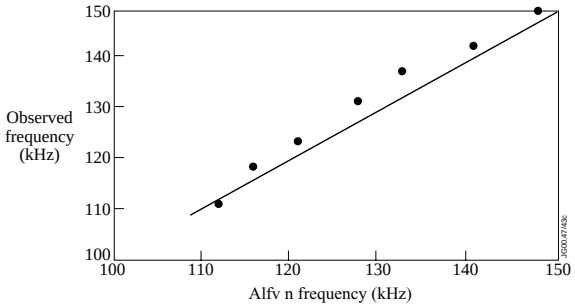

Figure 13.7. The Alfvén frequency was scanned by varying the toroidal magnetic field. The observed wave frequency is seen to vary in proportion to the magnetic field as expected from theory.

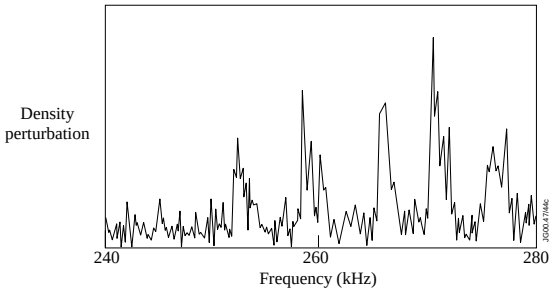

Figure 13.8. The multi-peak structure of the kinetic toroidal Alfvén resonance as observed in the density fluctuations.

The first experiment on JET utilised the set of “saddle coils” which had been mounted inside the vacuum vessel for the feedback control of instabilities. These coils could be used to generate the Alfvén waves. Figure 13.6 gives a plot of the amplitude of the wave against the applied frequency, and shows the resonance when the applied frequency is equal to the Alfvén

frequency for those waves. When the toroidal magnetic field was varied to scan the Alfvén frequencies the observed resonance frequency changed in proportion, as shown in Figure 13.7, verifying the identification of the waves.

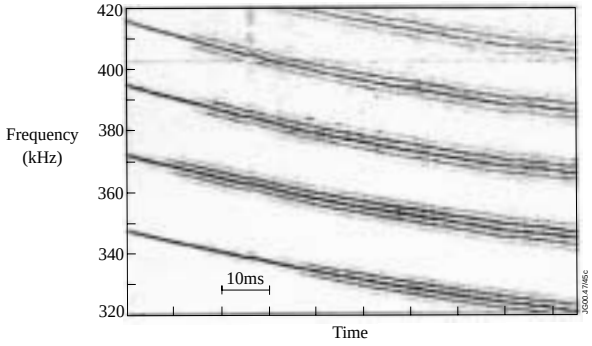

Figure 13.9. Splitting observed in the frequency of the toroidal Alfvén modes, followed in time.

There is a variant Alfvén wave called the Kinetic Toroidal Alfvén Eigenmode which actually derives from the continuous spectrum as a result of the “kinetic” thermal motions of the ions. The first observation of these modes was made on JET and Figure 13.8 shows the multi-peak structure of resonant frequencies observed on the density fluctuations.

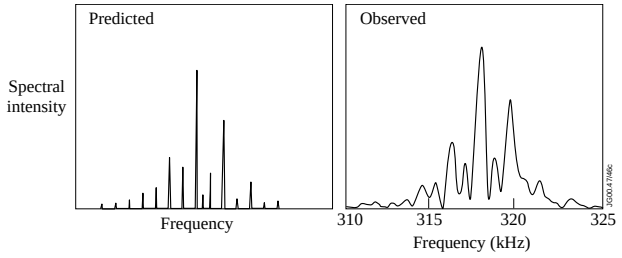

Figure 13.10. Comparison of the predicted and observed spectrum of the split toroidal Alfvén modes.

Another advance was the interpretation of the “splitting” of Alfvén eigenmodes observed in JET. These TAE modes occurred in plasmas with combined ion cyclotron and neutral beam heating, and the observed splitting is shown in Figure 13.9. The behaviour was explained in terms of the combined effect on the particle distribution of the TAE drive from the fast particles and a relaxation process, probably arising from particle diffusion in the ICRH wave field. The theory predicts a spectral structure, and a satisfactory comparison of the predictions with the experimental observations is made in Figure 13.10.

Snakes

The injection of pellets into the JET plasma led to a surprising discovery. As explained in Chapter 8 material evaporated from the pellet will generally spread over each magnetic surface as the pellet passes through it, but on surfaces with rational q the spreading is localised to a line. So around a rational surface with q = m/n, and particularly for low m, the pellet was expected to create a temporary high density along the field line through which it happened to pass.

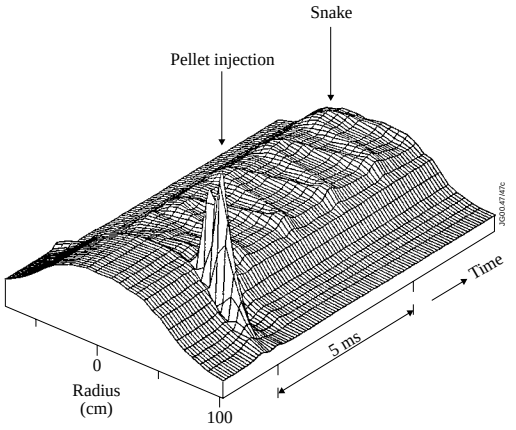

Figure 13.11. The snake-like pattern of the soft X-ray emission seen by the detector array.

Following pellet injection a localised increase in soft X-ray emission was indeed seen from the q = 1 surface. The structure of the emission had a poloidal mode number m = 1 and a toroidal mode number n = 1. This region of increased emission rotated round the torus and the detected signal moved backward and forward across the detector array producing a sinusoidal pattern as shown in Figure 13.11 - hence the name snake. For this m = 1, n = 1 structure the geometry of the emitting region is actually that of a tilted and displaced circle as shown in Figure 13.12. Atomo graphic reconstruction of a section through the plasma showing the enhanced density in the snake is shown in Figure 13.13.

Now although the appearance of the snake was not anticipated it was not really surprising - what *was* surprising was that it persisted and was effectively permanent. This implied that there could be a bifurcated state of the plasma, leading to fundamental questions about the properties the plasma must have for this to occur.

It was concluded that the localised cooling at the rational surface q = 1 must have led to the formation of a magnetic island, and calculation showed that pellet material would then be trapped inside the island. However, the cooling of the snake region was observed to be brief and so the problem of persistence, both of the magnetic island and the density increase within it, remained. With the general level of diffusivity observed in the plasma the density increase in the snake

would last for around a hundredth of a second. Even with only the basic collisional diffusion it should have decayed in about half a second. In the experiment the snake was observed for 2 seconds with practically no decay.

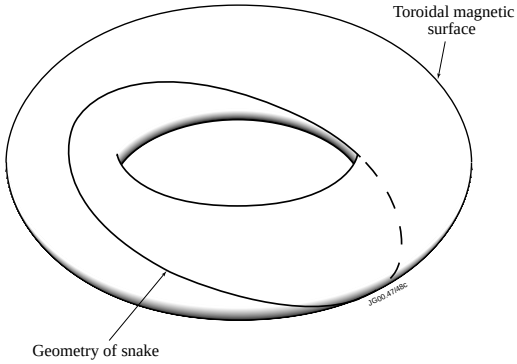

Figure 13.12. The source of the soft x-ray emission has the geometry of a tilted and displaced circle, and the snake-like pattern arises from the rotation of this structure around the torus.

It was determined from the soft X-ray emission that impurities are entrained within the snake, and the increased resistivity this implies explains the persistence of the magnetic island. Theory also offers an explanation of the enhanced impurity concentration in terms of a self-consistent electric field.

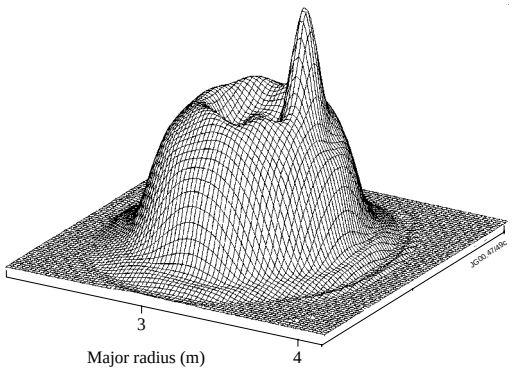

Figure 13.13. A tomographic reconstruction of the soft X-ray emission over the plasma cross-section shows the enhanced emission associated with the snake.

With regard to the persistence of the increased density there is no definitive explanation, but it might be a consequence of the so-called inward pinch. The radial flow of the plasma is basically an outward diffusion, but this is found to be modified by an additional mechanism which contributes a flow toward the axis - the inward pinch. The convergence of this inward

pinch provides a density source which in normal steady state would be balanced by the diffusive loss. If, in the modified magnetic structure of the snakes the diffusion is reduced, the source provided by inward pinch would lead to an enhanced density - as observed in the snake. Calculation shows that if this explanation is correct it implies a very high level of confinement within the snake's magnetic island. Whatever the final explanation of the persistence of the snake, its appearance shows that some unanticipated and fundamental physical processes are at work.

The basic physics described in this chapter has provided exciting insights into the nature of magnetic plasma, and illustrate the richness of the plasma behaviour found in tokamaks. It seems likely that other surprises await further research, with the potential for improving our understanding of the underlying physics.

Bibliography

Electron runaway resulting from hard collisions was described by

Sokolov, Yu. A. Multiplication of accelerated electrons in a tokamak, JETP Letters 29, 218 1979.

Two JET papers on the experimental observations are

Gill, R.D. Generation and loss of runaway electrons following disruptions in JET, Nuclear Fusion 33, 1613 (1993).

Gill, R.D., Alper, B., Edwards, A.W., and Johnson, M.F. Direct observations of runaway electrons following disruptions in the JET tokamak, Nuclear Fusion 40, 163 (2000).

The detection of deuteron knock-on collisions is reported in

Korotkov, A.A., Gondhalekar, A., and Akers, R.J. Observations of MeV energy deuterons produced by knock-on collisions between DT fusion α-particles and plasma fuel ions. Physics of Plasmas 7, 1 (2000).

The original ICE measurements were described in

Cottrell, G.A. and Dendy, R.O. Superthermal radiation from fusion products in JET. Physical Review Letters, 60, 33 (1988),

and further measurements with DT plasmas in

Cottrell, G.A., Bhatnagar, V.P., Da Costa, O., Dendy, R.O., Jacquinot, J., McClements, K.G., Mccune D.C., Nave, M.F.F., Smeulders, P., and Start, D.F.H. Ion cyclotron emission measurements during JET deuterium-tritium experiments. Nuclear Fusion 33, 1365 (1993).

The measurement of damping of TAEs excited by external antennas was reported in

Fasoli, A. et al. Direct measurement of the damping of toroidicity-induced Alfvén eigenmodes, Physical Review Letters, 75, 645 (1995),

and the observation of kinetic TAEs in

Fasoli, A. et al. Observations of multiple kinetic Alfvén eigenmodes. Physical Review Letters 76, 1067 (1996).

The non-linear splitting of TAEs in JET is described in

Fasoli, A., Breizman, B.N., Borba, D., Heeter, R.F., Pekker, M.S., and Sharapov, S.E. Nonlinear splittng of fast particle driven waves in a plasma: observation and theory. Physical Review Letters 81, 5564 (1998).

The papers dealing with snakes are

Weller, A., Cheetham, A.D., Edwards, A.W., Gill, R.D., Gondhalekar, A., Granetz, R.S., Snipes, J., and Wesson, J. Persistant density perturbations at rational-q surfaces following pellet injection in the Joint European Torus. Physical Review Letters 59, 2303 (1987).

Gill, R.D., Edwards, A.W., Pasini, D., and Weller, A. Snake-like density perturbations in JET, Nuclear Fusion 32, 723 (1992).

Wesson, J.A. Snakes, Plasma Physics and Controlled fusion 37, A337 (1995).

14. FUSION POWER

Over the first forty years of "fusion" research there was little contact with fusion power itself. The reason, of course, was that those years of development were needed to find the most promising confinement system - tokamaks - and to build a sufficiently large device with the heating power necessary to reach the temperature required for fusion. This meant that some scientists spent their whole careers in fusion research without needing to consider nuclear reactions at all.

The aim with JET was to reach conditions where the introduction of tritium, with its high cross-section for fusion reactions with deuterium, would produce a significant fusion power. It would take nine years to reach the preliminary experiments with tritium, and a further six years to obtain fusion power comparable with the input power.

During most of JET's operation the gas used was simply deuterium. This provided an intermediate stage where fusion reactions occur through deuterium-deuterium collisions but, because of the lower cross-section, the number of neutrons and the power produced were quite low. However, deuterium provided an extra diagnostic in that the neutrons could be counted, and this provided a measurement of the ion temperature. Using arrays of neutron detectors viewing collimated lines of sight the space dependence of the reaction rate could also be determined.

The use of tritium to produce megawatt powers involves two complications. Firstly, tritium is radioactive, undergoing β-decay, with a lifetime of 12 years. It has, therefore, to be treated with care and be under complete control. The second problem arises from the neutron flux resulting from the fusion reactions. These neutrons produce nuclear reactions in the vacuum vessel, leaving it radioactive. The level of radioactivity soon reaches a level which makes entry into the vessel impossible, and calls for remote handling to carry out modifications and repairs. The most troublesome radioactivity arises from the transmutation of nickel to cobalt 60 which emits γ-rays and has a half-life of 5 years.

Tritium

About 10 years was spent in developing a sophisticated system for handling the tritium. The mass of tritium involved was quite small, a total inventory of 20 grams, but this had to be supplied to the experiment and recovered with precise control.

Tritium was introduced into the plasma using some of the neutral beam injectors. The tritium leaving the plasma had to be extracted from the vacuum vessel, and an even larger amount had to be collected from the neutral beam injection system.

The tritium handling equipment system is located in a separate building and is connected to JET through a 100 metre line. The tritium, along with the other plasma components, is initially collected by a cryogenic pump with surfaces at four degrees above absolute zero. At a later stage the gases are transferred to a uranium bed where the hydrogen isotopes, including tritium are

held as uranium hydrides.

When the tritium is to be separated, the uranium bed is heated and the hydrogen isotopes evaporate. The separation of the tritium is then brought about using gas chromatography. The combined hydrogenic gases are passed over palladium covered spheres which absorb the lighter isotopes preferentially, allowing the tritium to be separated with a high degree of purity.

The Preliminary Tritium Experiment

As the time for using tritium approached it became necessary to identify the type of plasma to be used. Naturally, the aim was to use a plasma capable of a high fusion power. The chosen plasma was a hot ion H-mode of the type described in Chapter 11. Optimisation led to a plasma with a current of 3MA in a toroidal magnetic field of 2.8T. This plasma would be heated with 14MW of neutral beam heating. Trial experiments using deuterium beams showed that on the application of additional heating the plasma quickly entered the H-mode and the neutron yield rose steeply to 4×10^{16} neutrons per second. The apparently unavoidable problem with this discharge was that when the total plasma energy reached about 9MJ the neutron yield underwent a rather abrupt fall. As explained earlier this had initially been attributed to an influx of carbon into the plasma - the carbon bloom, but it was later realised that the fundamental problem was an unexplained abrupt loss of confinement. Whatever the explanation, it was unfortunate that such promising plasma was spoilt while the neutron yield was still rising rapidly. Anyway, these plasmas gave the best performance and would be used in the tritium experiments.

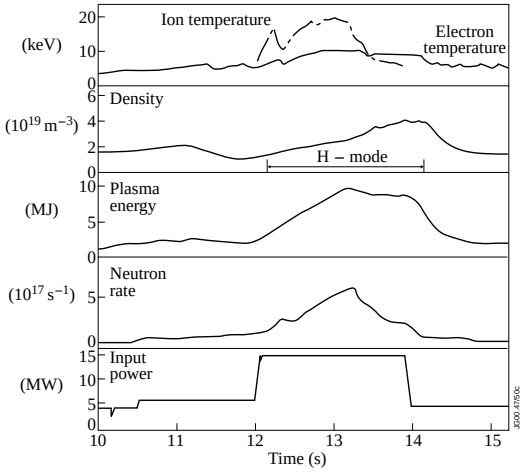

Figure 14.1. Time traces of a plasma with a 10% tritium concentration. The application 14 MW of heating for a period of 2 seconds produces H-mode confinement with an ion temperature of 19 keV.

The experiment carried out in November 1991 was called the Preliminary Tritium Experiment. Preliminary, because at this stage is was necessary to limit the neutron production so that the vessel activation would be low enough to allow the planned modifications to the divertor to take place. Instead of the 50% tritium / 50% deuterium mixture which would maximise the fusion yield the tritium content would be 10%.

Optimisation was carried out using a few shots with a tritium concentration of 1%, and then two pulses with the 10% concentration were produced. The two pulses were similar and both produced a fusion power of over 1.5MW.

The time traces of the basic parameters of one of the pulses are displayed in Figure 14.1. During the pulse the injected neutral beam power was raised to 14MW and with full power there was a transition to H-mode, and an ion temperature of 19keV was soon reached. The beam injection also raised the plasma density giving a steady increase in the plasma energy and the neutron yield. The traces in Figure 14.1 also show the sudden loss of performance, most obviously with the abrupt fall in the neutron production rate.

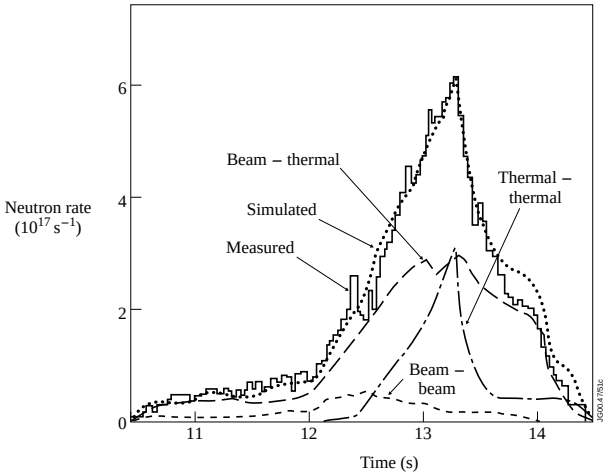

Figure 14.2. In addition to the neutrons from reactions between thermal particles, there are contributions from the injected beam particles. The total neutron rate is compared with that calculated using the measured plasma parameters.

The neutron production was not simply that of the heated plasma ions. When the neutral beam particles are ionised in the plasma they have their injection energy. The ions from the beam then slow down over about a tenth of a second to join the thermal distribution of the plasma ions. This means that in addition to the neutron production from the thermal ions there are neutrons produced by fusion reactions between beam ions and plasma ions. There is also a small number of reactions from collisions between beam ions. To disentangle these contributions a numerical simulation of the plasma was carried out using the measured experimental data. The resulting neutron rates are shown in Figure 14.2.

This experiment, using tritium for the first time, was a landmark in fusion research. It could of course be said that all that had been done was to replace ten percent of the deuterons by tritons. But the purpose of *all* the previous developments in fusion research had been to produce plasmas in which the introduction of tritium would produce significant fusion power. Whereas in deuterium plasmas the fusion power had typically been less than 1% of the input power, even this preliminary tritium experiment had raised this figure to more than 10%.

Record Fusion Power

The decision as to when to use tritium in JET plasmas inevitably involved an assessment of the price to be paid in terms of reduced access to the inside of the machine once the radioactivity of the vessel had been raised by the high neutron bombardment involved.

The optimum time for a full fusion power experiment arrived in the autumn of 1997. The programme called for replacement of the divertor after this experiment, but by this time the remote handling system was ready to carry out the task, entirely without human entry into the vessel.

In the six years since JET's preliminary tritium experiment the TFTR tokamak at Princeton had been used for tritium experiments, and had produced 9MW of fusion power. It was natural to hope that the new JET experiments would exceed this power, and there was gratification when a record fusion power of 16MW was achieved.

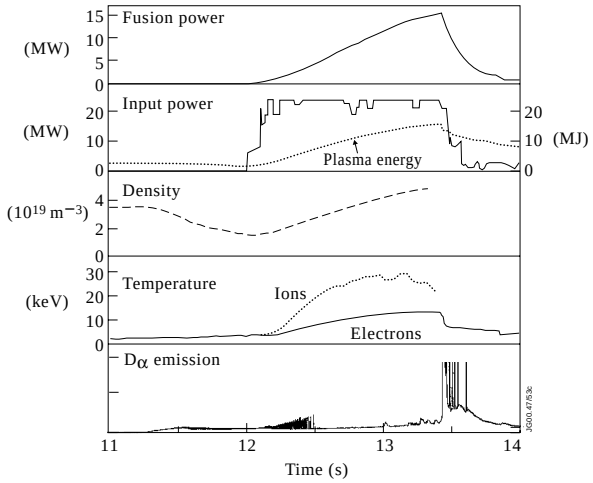

Figure 14.3. Traces for the plasma in which record fusion power of 16 MW was reached

The plasma used in this record case was similar to that of the preliminary tritium experiment, a hot ion H-mode plasma. The main difference, of course, was the use of 50% tritium, but the plasma current and toroidal magnetic field were also raised, to 4.2MA and 3.8T, increases of

40% and 36% respectively. The time traces of the main parameters are shown in Figure14.3. A neutral beam heating power of 22MW was applied with an additional 3MW of ion cyclotron heating. The ion temperature rose to 30keV and the electron density to $5 \times 10^{19} m^{-3}$.

As with the preliminary tritium experiment the increase in fusion power halted with an abrupt loss of confinement. The onset of pulses of D_α radiation seen at this time is an indicator that the ELM instability was occurring, contributing to, and possibly triggering, the deterioration in confinement.

Scientists in fusion research had always looked forward to the day when the fusion power in experiments would be measured in respectable units - megawatts. An obvious milestone was that the fusion power produced would be equal to the heating power supplied. A natural “quality factor” Q is just the ratio of these two powers - power produced divided by power supplied.

The earliest toroidal fusion experiments were in the pinch devices of the 1950s. Deuterium was used in these experiments and the heating was the ohmic heating of the plasma current. The resulting Q value was around 10^{-12} . What was the Q-value in JET? In the record discharge Q was 0.6 - a creditable advance, with Q now “of order one”. In fact there is a subtlety, which should be allowed for, which gives a somewhat higher value of Q. The point of the correction is that, at the time of maximum Q, the temperature and density were rising. This means that part of the power supplied was used in *increasing* the energy of the plasma. We could imagine the “thought experiment” in which the plasma was maintained with its energy in steady state with a somewhat reduced power. If we allow ourselves this correction Q turns out to be 0.9 - close enough to 1.0 when compared to 10^{-12}!

Steady State Fusion Power

In the record fusion power experiment the plasma was produced in a “hot ion H-mode”. This is achieved by starting with a low density, the low frequency of collisions decoupling the ion and electron temperatures, and by having a more triangular plasma, which stabilises the surface against ELMs. The unfortunate feature of such plasmas is the abrupt loss of confinement.

It had been found that the way to produce a steady-state plasma was to reduce the triangularity and increase the starting density. At this density collisions between ions and electrons hold the temperatures almost equal. In this type of plasma regular but smaller ELMs occur and, although still in H-mode, the confinement is somewhat reduced.

Figure 14.4 shows the traces for the best of these plasmas. A fusion power of around 4MW was maintained for 4 seconds, and a fusion energy of more than 20MJ was produced - another record.

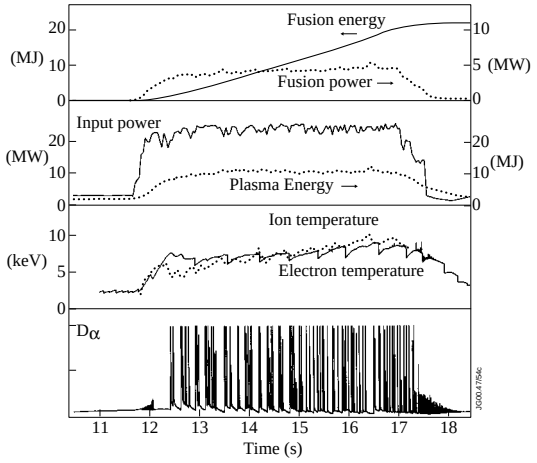

Figure 14.4. Fusion power of around 4 MW was maintained for 4 seconds. The plasma energy is constant during this time and the temperature almost so. The plasma was in H-mode with repetitive ELMs as seen from the D_α radiation signal.

α-Particle Heating

The achievement of significant amounts of fusion power clearly moves fusion research into a new era. For decades those involved have been principally concerned with the physics of non-reacting plasmas. Now attention will move to take account of the effects of the fusion reactions. The principal effect within the plasma is due to the α-particles released in the nuclear reactions.

α-particles are simply the nuclei of helium atoms, and are therefore positively charged. So when they are produced they are trapped by the magnetic field. In JET their orbits are much smaller than the minor radius of the plasma, and this gives them time to transfer their energy to the plasma before they are lost. As the α-particles collide with the plasma particles they slow down and the energy they lose heats the plasma, a process providing a crucial form of heating in a fusion reactor. In close collisions the energy is transferred preferentially to ions, but distant collisions dominate and this results in most of the α-particle energy being transferred to the electrons. Can we detect this electron heating in the experiment?

The ratio of tritium to deuterium was varied in a set of otherwise similar discharges. The total fusion power can be calculated from the measured neutron yield, and since the α-particle power is 20% of the total the α-particle heating power is known for each discharge. Figure14.5(a) gives a plot of the measured electron temperature against this α-particle heating. The effect of α-particle heating is clear. The optimal case, with 60% tritium, has an electron temperature 2keV higher than the baseline case with no tritium.

The rise in electron temperatures with α-particle heating can also be compared to the rise obtained in discharges with no tritium but with ion cyclotron heating in the same range. In

Figure 14.5(b) two such cases are added to the graph, showing a temperature rise consistent with the α-particle heated discharges.

Transport with Tritium

The introduction of tritium into the JET plasmas allowed two further investigations into the transport behaviour. In the first the dependence of the energy confinement on the ion mass was explored. Having discharges with various amounts of hydrogen, deuterium and tritium, with masses in the ratio 1:2:3, the mass dependence of confinement could be explored more fully. The other investigation used the measured neutron emission from deuterium-tritium reactions to follow the tritium profiles of a trace of tritium puffed into a deuterium plasma. Once ionised the tritium diffuses in the plasma, and analysis of the profiles allows a calculation of the diffusion coefficient across the plasma radius.

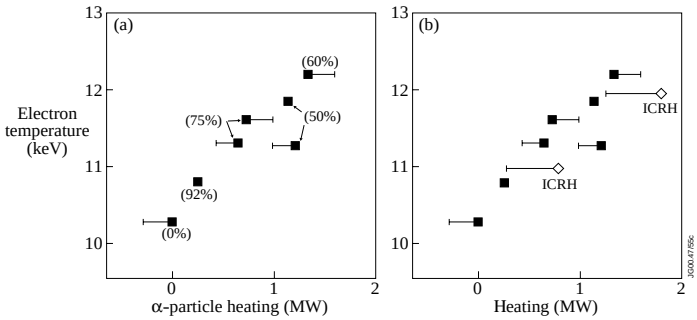

Figure 14.5(a). The fusion α-particles heat the plasma and the resulting increase in electron temperature is clear from the graph, the tritium fractions being shown in brackets. (b) Showing that the α-particle heating is similar to that achieved by comparable ion cyclotron heating of deuterium plasmas.

The mass dependence of the energy confinement is important partly because it is necessary to extrapolate present data with hydrogen and deuterium to the deuterium-tritium mixture which would be used in a reactor. It is also important for the constraint which it imposes on possible theories of anomalous transport. If we knew the exact experimental mass dependence, any theory giving a different dependence could be dismissed. Unfortunately it's not like that. Experiments on other tokamaks have given results varying between no mass dependence and an almost proportional dependence.

The measurements using all the hydrogen isotopes on JET gave a very weak mass dependence, and in H-mode discharges with repetitive ELMs there was virtually no dependence. However, although it would be good to have a simple and clear result, more detailed analysis indicated that perhaps the zero mass dependence was a coincidence.

The confinement in H-mode discharges is partly dependent on the transport properties in the bulk core of the plasma and partly on the enhanced confinement of a transport barrier at the plasma edge. Separating the mass dependence of confinement into these two parts it was found that core confinement deteriorated with higher mass whereas the edge contribution to confinement showed an improvement with increasing mass. The combinations of these effects gives the weak overall mass dependence observed.

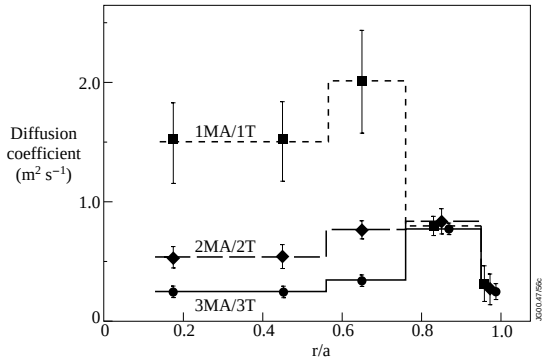

Figure 14.6. Radial dependence of the tritium diffusion coefficient determined from the trace tritium experiments carried out with three different levels of magnetic field, the plasma current being held in constant ratio to the field.

Results on the diffusion of tritium from the trace tritium experiments are shown in Figure14.6. The tritium diffusion coefficient is plotted over the plasma radius for three cases having similar magnetic field structures but with three different magnitudes of the field. This is achieved by increasing the plasma current in proportion to the toroidal magnetic field. Thus we have 1MA/1T, 2MA/2T and 3MA/3T. The plasmas also have similar values of other parameters, leaving the ion temperature and the magnetic field as the basic variables. In the core of the plasma the diffusion coefficient is consistent with the scaling called gyro-Bohm which is proportional to both the Bohm diffusion coefficient which varies as the ratio of temperature and magnetic field, T/B, and to the ratio of the Larmor radius to the plasma size, ρ/a. However, as seen from the figure, the magnetic field dependence disappears at the edge of the plasma, again revealing a more complex situation.

We have now examined the important aspects of the plasma behaviour in the JET fusion experiments but, before concluding, mention must be made of the outstanding work on the remote handling system which became a necessary requirement once the vacuum vessel was radioactive.

Remote Handling

It has already been commented that for decades fusion research involved no significant level of

nuclear reactions. With the D-T experiments this was changed and the neutrons from the fusion reactions soon made the interior of the vacuum vessel radioactive - so radioactive that it was no longer possible for workers to enter the vessel.

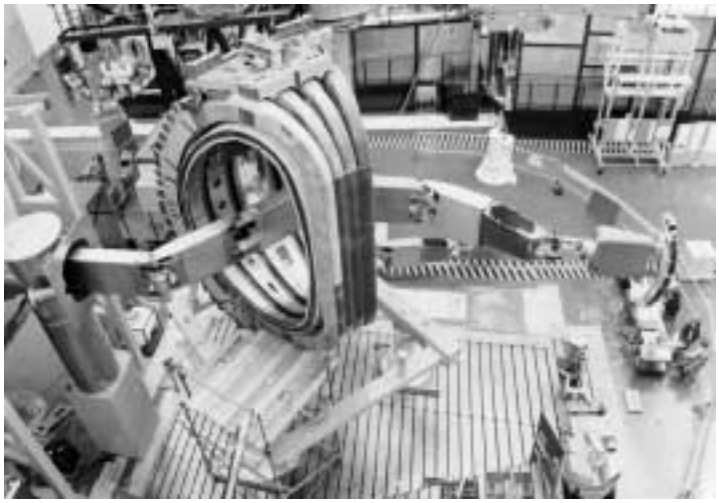

Figure 14.7. The remote handling boom being used to place an ICRH antenna in a Òmock-upÓ layout.

This was, of course, foreseen from the outset of JET, and over the years from the construction of JET a sophisticated system of remote handling had been designed and built. This system is remarkable.

Figure 14.8. The mascot at the end of the boom placing a tile support for the divertor.

The “handling” had to be precise and delicate. For example it had to be able to remove and replace any tile, and ultimately it was used to replace a complete divertor. Because of the size of JET the handling tools had to be carried on a flexible boom with a very large reach - its length is 10m and it can carry up to half a tonne. Figure 14.7 shows the boom being used to place an ICRH antenna using a partial replication of the actual configuration. Figure 14.8 is a photograph of the “mascot” on the end of the boom placing a tile support for the divertor inside the torus.

In principle it would have been possible to design a system which following “the press of a button” would carry out its task. For the JET design it was decided to include “a man in the loop”, the operation of the tools being under the constant control of an operator. In the resulting system the forces on the tool are re-created at the hand of the operator who can also see what is happening on several screens providing different viewing angles. He even hears what is happening through a microphone on the boom. Figure 14.9 is a photograph of an operator in a remote control room using the visual display to manipulate the tools inside the vessel.

Figure 14.9. The operator in a room remote from the torus using the Òhands-onÓ system of remote control.

Separate tools were designed for specific tasks, and the operators practised the planned tasks outside the vessel. A large number of unplanned tasks were also performed, involving the replacement, repair and cleaning of various components.

The wide range of experience gained with the JET remote handling system provides a basis for the more comprehensive requirements of a fusion reactor.

Bibliography

The first JET tritium experiment was reported and described in a Nuclear Fusion article entitled “Fusion energy production from a deuterium-tritium plasma in the JET tokamak” (Vol. 32, 187, 1992). The authorship is the “JET Team” which is listed as

Rebut, P.H., Gibson, A., and Huguet, M., plus more than 300 other authors.

The technological contributions were presented in a Topical Issue of Fusion Engineering and Design (Vol. 19, 1992) dedicated to the first tritium experiments. Papers included are:

Huguet, M., et al. Technical aspects of the first JET tritium experiment.

Saibene, G., Sartori, R., Andrew, P., Hone, J., King, Q., and Peacock, A.T. Tritium accounting during the first tritium experiment at JET.

Hemmerich, J.L., Lässer, R., and Winkel, T. Gas recovery system for the first JET tritium experiment.

The high fusion power experiments of 1997 are described in a JET team paper,

Keilhacker, M., Gibson, A., Gormezano, C., Lomas, P.J., Thomas, P.R., Watkins, M.L., et al. High fusion performance from deuterium-tritium plasmas in JET. Nuclear Fusion, 39, 209 (1999).

An “Overview of ITER physics deuterium-tritium experiments in JET” is given by

Jacquinot, J., et al., for the JET Team in Nuclear Fusion, 39, 235 (1999).

The steady state experiments are described in

Horton, L.D., Sartori, R., et al. High fusion power steady state operation in JET DT plasmas. Nuclear Fusion, 39, 993 (1999).

The March 1999 (Vol. 39) issue of Nuclear Fusion was devoted to the JET D-T experiments, the ten papers included being

Cordey, J.G., et al. Plasma confinement in JET H-mode plasmas with H, D, DT and T isotopes, p301.

Righi, E., et al. Isotope scaling of the H-mode power threshold in JET, p309.

Start, D.F.H. et al., Bulk ion heating with ICRH in JET plasmas, p321.

Eriksson, L.-G., Mantsinen, M.J., et al. Theoretical analysis of ICRF heating in JET DT plasmas, p327.

Bhatnagar, V.P., Lingertat, J., et al. Edge localised modes and edge pedestal in NBI and ICRF heated H, D and T plasmas in JET, p353.

Parail, V.V., Guo, H.Y., and Lingertat, J. Fast particles and the edge transport barriers, p369.

Sharapov, S.E., et al. Stability of alpha particle driven Alfvén eigenmodes in high performance JET DT plasmas, p373.

Cottrell, G.A., et al. Approach to steady state high performance in DD and DT plasmas with optimised shear in JET, p407.

Parail, V.V., et al. Predictive modelling of JET optimised shear discharges, p429.

Further papers on the D-T experiments are

Thomas, P.R., et al. Observation of alpha heating in JET DT plasmas. Physical Review Letters 80, 5548 (1998)

Maggi, C.F., Monk, R.D., Horton, L.D., Borrass, K., Corrigan, G., Ingesson, L.C., König, R.W.T., Saibene, G., Smith, R.J., and Stamp, M.F. The isotope effect on the L-mode density limit in JET hydrogen, deuterium and tritium divertor plasmas. Nuclear Fusion 39, 979 (1999).

Saibene, G., Horton, L.D., Sartori, R., et al. The influence of isotope mass, edge magnetic shear and input power on high density ELMy H-modes in JET. Nuclear Fusion 39, 1157 (1999).

15. SUCCESS

It is now time to assess the JET experiment. We shall first review the achievements in terms of the stated aims of JET listed in Chapter 4 and then take a broader view. We shall see that the enormous advance in understanding that has been made over the years, both by JET and the world's other tokamaks, means that practically every area of the subject now involves issues which were not even contemplated when the JET aims were specified.

First we look at the original aims of JET in turn, starting with the scaling of the plasma behaviour with parameters approaching the reactor range.

Scaling of Plasma Behaviour

The central issue here was, and is, the energy-confinement time. The best tokamak in operation when JET was proposed had a confinement time of tens of milliseconds. The step up to JET was so large that JET's confinement time was an open question, a very wide range of outcomes being possible. It was then conceivable that the confinement time could be close to the neoclassical value with the energy loss being determined simply by collisions - giving the best possible confinement. In the other direction there was almost no limit to how bad the confinement might turn out to be.

In the absence of knowledge, the simplest assumption was that confinement is determined by a diffusive process and that the diffusion coefficients would be unchanged. The confinement time would then scale as the cross-sectional area of the plasma. This assumption gave a confinement time for JET of around one second. Given the enormous range of uncertainty this estimate was remarkably good, the best confinement time in JET turning out to be 1.8 seconds.

However, one of the principal aims of JET was to replace such "back of envelope" estimates by as much precision as could be extracted from the experiments. It is obvious that to obtain the most reliable scaling law, results from as many tokamaks as possible should be included in the analysis. This was carried out as an international collaborative effort, with the results from JET, being the tokamak nearest to a reactor, playing a crucial role in the procedure. The results of this massive endeavour were described in Chapter 11. Over the years the situation has been transformed to one in which quite detailed features of the scaling laws are now debated.

Another role of JET has been to determine the scaling of the threshold power required for transition to H-mode confinement. Since it is envisaged that a reactor will operate in H-mode it is clearly important to know how much power would be needed to reach this mode. The existence of H-mode confinement was unknown when the aims of JET were specified, this area of research has been one of many which were unforeseen when JET was designed.

It is the reward of imaginative projects such as JET that they allow the exploration of such unanticipated discoveries. Attention has now turned to the nature of the improved core confinement

which seems to be created by modifying the magnetic shear in the plasma, as described in Chapter 11. This investigation clearly needs an accurate measurement of the magnetic field to determine the magnetic shear and this has led to another development, the installation of a system to measure the field using the motional Stark effect.

Plasma-Wall Interaction

The fact that this part of JET's aims is given the name plasma-*wall* interaction indicates the way the problem was seen during the design phase. The plasma would be bounded by limiters, and there would be recycling of neutral particles between the plasma and the wall. The problem would be to limit the influx of impurities arising from these interactions.

The actual outcome was that JET would dispense with limiters and concentrate on the development of divertors. It should be mentioned, however, that even in the JET design report of 1975 it was intended that the effect of a divertor would be examined at some stage.

During the early phase of JET, studies with limiter discharges led to an understanding of the scaling of the edge density and temperature with the plasma density in ohmically-heated discharges. Studies were also made of the erosion and redisposition of the limiter surface material and of the adsorbed deuterium.

The persistence of impurities in plasmas with limiters led to the conclusion that the flow of particles and energy out of the plasma must be led to a surface more remote from the plasma, where the impurities would be better controlled. There followed several years of divertor research and development, during which a much deeper understanding of the requirements, and options, for a reactor became clear.

The increasing level of understanding gave rise to three successive divertors in JET as described in Chapter 12. The design finally settled on a divertor structure which confined the neutral gas and impurities, and used the neutral gas to radiate the power flowing from the plasma, preventing localised deposition of the heat. This meant that the heat load requirements on the material surfaces was much reduced, making this a possible design for a reactor.

A crucial question raised in the original JET design report was the choice of materials for the plasma facing surfaces. The metal beryllium offered the lowest possible nuclear charge Z. Beryllium atoms have only four electrons, with the potential advantage of minimising the dilution of the plasma. However, researchers had shied away from beryllium, largely because of its toxicity. Nevertheless, such difficulties were overcome and beryllium was introduced into JET both as tile material and by evaporation onto the other non-beryllium surfaces. The hoped for improvement in the average Z value of the plasma was found, but surface melting of the beryllium was also observed.

The other low-Z competitor was carbon. Carbon sublines rather than melts, and so the problem of melting does not arise. It was possible to consider using carbon in a reactor if the problem of releasing atoms from its surface under bombardment from the plasma could be

overcome. Two difficulties arose.

The divertor design which radiates the energy, and produces a low temperature at the divertor's surfaces, successfully reduces the physical sputtering of carbon. However, it was realised that there is another form of sputtering which is not similarly reduced. This is chemical sputtering in which hydrogen atoms arriving at the carbon surface undergo a chemical reaction to form modules, such as CH_4, which then escape from the surface to become potential impurities for the main plasma.

The second problem comes from the observation that, even when the divertor is operating correctly, there is a larger than expected release of impurities from the plasma facing wall of the vessel itself.

Most of the advances in our understanding of "plasma-wall interactions" summarised above were unanticipated when JET was designed, and are the outcome of careful analysis of experiments over many years.

Plasma Heating

When the JET design team started their endeavours in 1973 tokamaks were ohmically heated, and the information about additional heating was scant indeed. Both neutral beam heating and ion cyclotron heating were just being tried at a low level in several experiments. By the end of 1974 tokamaks had been heated by both schemes with powers of hundreds of kilowatts.

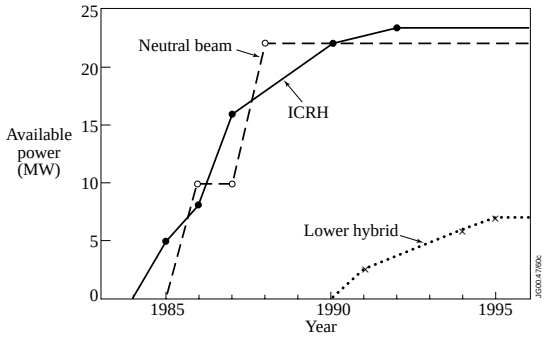

Figure 15.1. The available ion cyclotron and neutral beam heating increased rapidly, both reaching powers of over 20MW. The lower hybrid resonance heating was added later.

The uncertainties about confinement left the question of the required heating power a matter for speculation and, furthermore, multi-megawatt heating systems had yet to be developed.

Four methods of heating were envisaged - adiabatic compression, neutral beam injection, and wave heating at the lower hybrid resonance and at harmonics of the ion cyclotron frequency. In the design report the aim was stated to be a study of "their efficiency in heating the plasma into the reactor domain".

The experiments on compression heating were unfruitful, and significant lower-hybrid heating was only introduced after ten years of JET operation. The development of the other two schemes - neutral beam injection and ion cyclotron heating - was very successful, the power available increasing rapidly. The first heating was 5 megawatts by ICRH in 1985 and 10 megawatts of neutral beam heating in 1986. By 1988 both systems could supply about 20 megawatts. A graph showing how the available power developed is given in Figure 15.1.

In addition to providing powerful heating, the ion cyclotron system led to the discovery of fast particle stabilisation of the sawtooth instability. Its capability to drive plasma current, and to do this in a controlled way, also allowed sawtooth stabilisation by local modification of the current profile. The ability to control the location of the deposition with ion cyclotron heating is one of its assets. However, the requirement of achieving efficient coupling to the plasma makes it less flexible than neutral beam injection.

The neutral beam heating system turned out to be extremely reliable, and it became the basic work-horse of plasma heating. The system achieved an unanticipated success when it was used to inject the tritium in the two sets of deuterium - tritium experiments.

The heating systems transformed plasmas with ion temperatures of a few keV to plasmas producing megawatts of thermonuclear power at temperatures up to 30keV. Because their development went so well this achievement tends to be taken for granted. We must remember that success was not guaranteed, and depended on the solution of many complex design problems.

α-particle Production, Confinement and Plasma Heating

The studies of the behaviour of α-particles produced by fusion reactions in JET mark the early steps in the understanding of this crucial aspect of fusion reactors.

The rate of α-particle production in the deuterium - tritium experiments is easily measured by counting the 14 MeV neutrons which are produced at the same rate. Calculation of the expected rate is, however, more complex. The injected fast ions undergo fusion reactions before they are thermalised and so, in addition to the neutrons from the thermal plasma, there are neutrons from reactions between the fast ions and the plasma, and from reactions between the fast ions themselves.

Calculations taking account of the ion temperature, the beam injection and the beam slowing are found to give a neutron, and therefore α-particle, production rate which is consistent with that measured. A time trace of the calculated and observed neutron rate for a discharge with peak fusion power of 16MW is shown in Figure 15.2.

In the high fusion power plasmas, heating of the plasma by the α-particles was observed as described in Chapter 14. The level of heating is not accurately known but comparison with similar discharges using deuterium alone, with ion cyclotron heating substituted for α-particle heating, indicated that the energy of the α-particles is transferred mainly to the plasma. This is encouraging because it implies that the α-particles are confined for a time at least long enough

for the energy transfer to take place, and there is no evidence that the α-particles generate any instability causing them to be lost.

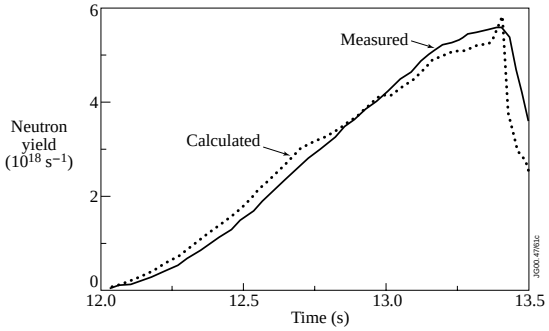

Figure 15.2. Time development of the neutron yield in the highest fusion power experiment. The measured yield is compared with expected yield calculated using the plasma parameters.

The studies of the behaviour of α-particles produced by fusion reactions in JET mark the early steps in the understanding of this crucial aspect of fusion reactors.

So, What are the Achievements?

We do not know when a useful fusion reactor will be produced, but it is certain that the JET experiment will be seen as an enormous stride toward that goal. The progress in fusion research has clearly been the result of a worldwide effort and of international collaboration, but JET has been widely recognised as the leading experiment. Its contribution can be placed in five categories.

Firstly, there is the extension of tokamak operation into new realms. The plasma current of 7MA achieved in 1988 was an order of magnitude advance over the currents in tokamaks existing when JET was designed, and was several times larger than the current in the tokamaks operating when JET was built. JET's size gave it a special place in scaling studies, and the wide range of continuously available diagnostics allowed a comprehensive analysis of the plasma behaviour, particularly of the powerfully heated plasmas. The development of a tritium handling system, and the system for the remote installation and maintenance of components inside the vacuum vessel, are both achievements in their own right, and put in place technologies essential for development of fusion reactors.

The second area has been the practical developments unforeseen at the outset. In particular the achievement of H-mode confinement by introducing a separatrix into the magnetic geometry, and the subsequent construction and study of three divertor systems. The divertor programme led to experiments in which the material surfaces were protected from the intense heat load by a shield of radiating plasma. Another development was the use of beryllium surfaces for comparison with carbon, with the resulting reduction of the effective impurity level. More recently the

appearance of regions of high confinement within the plasma under conditions of low magnitude shear has led to a massive and continuing effort, both to understand and to utilise this unexpected good fortune.

The third area is perhaps best described as "learning by doing". The most dramatic example was the discovery of the effect of the loss of control of the so-called vertical instability. The plasma is normally held rigidly in place by a feedback system, but when this system was fooled by the instability a force of hundreds of tons was unleashed, and a complex of new problems had to be resolved. A careful study was also made of the pattern and mechanism of the disruptive instability, demonstrating the role of radiation in producing an unstable configuration. The most severe collapse of the plasma current in disruptions was shown to be due, not to plasma turbulence as had been previously assumed but rather to the, more mundane, sudden influx of impurities. Another, somewhat surprising, cause of disruptions was the presence of very small "errors" in the magnetic field arising from slight asymmetries in the field coils. All of these discoveries have implications for reactors, and it was important that they be uncovered at this stage.

The fourth category of achievements consists of the many experimental results which were unexpected and which have a clear scientific content. Among these results, those connected with the confinement and transport of plasma energy are quite mysterious and unexplained. One example is the H-mode onset, which was thought to occur through the sudden appearance of a transport barrier at the plasma edge. The discovery that, at the onset, the transport can be affected simultaneously over a large part of the plasma was unexpected and still not explained. Another unexplained phenomenon is the sudden change in the thermal conductivity by a factor three over the whole plasma at the time of the "X-event". The careful analysis of sawtooth oscillations on JET has transformed our understanding of the subject. The measured soft X-ray emission has shown that the geometry of the instability and its growth rate are quite different from those expected. The observation that the suddenness of the onset of the sawtooth collapse, as with the ELM instability, was completely contrary to existing theory has led to the recognition of this "trigger problem" as a fundamental challenge to plasma theory. The discovery of the motional Stark effect in the spectrum emitted from JET led to its use in measuring the magnetic field, and the analysis of neutral particles leaving the plasma led to the identification of highly energetic deuterons produced in collisions with fusion α-particles. These examples are just some of the highlights of scientific study of the JET plasmas which has been pursued in parallel with the performance oriented programme.

Finally the major success has been the fulfilment of the stated aim of obtaining and studying plasma in conditions and dimensions approaching those needed in a thermonuclear reactor - as summarised above under the headings 'scaling of plasma behaviour', 'plasma-wall interaction', 'plasma heating', and 'α-particle production, confinement, and plasma heating'. This work, with the achievement of plasma conditions which produce fusion power comparable to the heating power, has enabled us to envisage what at reactor would be like and how it would behave.

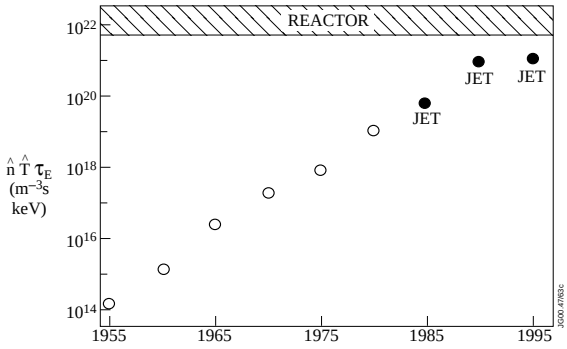

Figure 15.3. Showing JET's contribution in advancing the figure of merit $nT\tau_E$ toward the value required in a reactor.

To end, let us return to the figure of merit $nT\tau_E$ which measures the proximity to reactor conditions. In Chapter 9 the improvement on $nT\tau_E$ was plotted up to 1975. Figure 15.3 brings the graph up-to-date and shows how the JET contribution has brought us within sight of a reactor.

Future progress calls for the level of commitment, skill and originality which has been shown by those who designed, built, operated and studied JET with great success and worldwide acclaim.

APPENDIX I

THE CHRONOLOGY OF JET

1973 Design team starts work with Paul-Henri Rebut as Head.

1975 JET-R5 Report outlines the objectives and the design.

1977 Culham site chosen.

1978 Hans-Otto Wüster - first director.

1979 Site work began.

1983 (25 June) Operation began.

Plasma current 3MA. Electron temperature, with ohmic heating, 2 keV.

1984 (19 April) Official opening ceremony performed by Queen Elizabeth in the presence of Francois Mitterand, President of France.

1984 Pulse 1947 - vertical instability leads to force of over 200 tonnes on the vacuum vessel, calling for new vessel supports.

1985 Paul-Henri Rebut becomes director on the death of Hans-Otto Wüster.

Plasma current of 5MA.

Ion cyclotron heating introduced - 6MW of power. Confinement degradation observed. Electron temperature 5keV.

X-point operation demonstrated.

Radiation induced collapse in density limit disruptions observed.

Rapid sawtooth collapse inconsistent with Kadomtsev model.

1986 Neutral beam heating introduced - 10MW of power, ion temperature 12keV.

X-point operation gives H-mode confinement.

Sawtooth instability stabilised with additional heating producing so-called monster sawteeth.

Single pellet injection - peak density $2.5 \times 10^{20} m^{-3}$.

1987 Plasma current of 6MA, exceeding the design specification.

Electron temperature 10keV.

q = 2 disruption limit verified.

Experiments with multi-pellet injection system.

LIDAR system installed.

1988 Plasma current of 7MA.

Neutral beam injection reaches full power 21MW - ion temperature 20keV.

With combined neutral beam and ion cyclotron heating a total heating power of 35MW achieved.

Pellet enhanced performance (PEP) - first internal transport barrier observed.

Confinement time of 1 second in ohmically heated plasma.

1989 Introduction of beryllium tiles and beryllium evaporation.

Plasma temperature and neutron yield observed to collapse at “carbon bloom”.

Ion temperature exceeds 20keV.

1990 Ion cyclotron heating up-graded to 21MW.

Prototype lower-hybrid current drive introduced - current drive up to 1MA.

1991 (9 November) Preliminary tritium experiment - 1.7MW peak fusion power, 2MJ fusion energy.

Problem of sudden loss of performance - the X-event - recognised. Possible implication of “carbon bloom”.

Ion cyclotron current drive demonstrated, leading to sawtooth stabilisation by current profile modification.

AC operation demonstrated.

Plasma maintained for 1 minute.

Confinement time of 1.8 seconds in ohmically heated plasma.

Steady state H-modes for 18 seconds.

1992 Martin Keilhacker becomes director when Paul-Henri Rebut leaves to become director of ITER.

Toroidal field ripple experiments.

Shut-down for installation of divertor.

1993 Installation of mark I divertor.

1994 Plasma detachment in divertor.

New target tile arrangement eliminates carbon bloom, but sudden loss of performance in high performance plasmas remains.

7MW of lower-hybrid power.

Saddle coils used for TAE experiments.

Steady-state ELMy H-modes (20secs) with density and impurity control achieved with mark I divertor.

1995 Installation of mark II divertor.

Closed geometry raises divertor neutral pressure and so particle exhaust.

H-modes at 6MA.

1996 Recognition that abrupt change of global of confinement state underlies the X-event.

Optimised shear plasmas developed with internal transport barriers.

Study of dimensionless scaling of confinement.

Ion temperature exceeds 30keV.

1997 The deuterium-tritium experiments - 16MW of fusion power, 13.8MJ fusion energy, α-particle heating demonstrated, steady fusion power of 4MW maintained for 4seconds, ion temperature 40keV.

1998 Divertor replaced by gas-box divertor using fully remote handling.

1999 Jean Jacquinot becomes director on the retirement of Martin Keilhacker.

Study of physics of internal transport barriers.

Inside-launch pellet injector installed and enhanced fuelling demonstrated.

Joint Undertaking ends - JET to continue.

APPENDIX II

The success of JET was the result of the dedicated efforts of a large number of scientists and engineers. Many of their names appear in the bibliographies of the various chapters, but often the author lists were too long and required truncation. To put this right three complete lists of the JET team are appended below. They are taken from particularly significant papers published by the team at different stages of the project. The first is the list from the London IAEA Conference of 1984, the first such conference after JET came into operation. The second is from the Nuclear Fusion article (Vol. 32, p187, 1992) reporting the first tritium experiment. The third is the team list from the Nuclear Fusion article (Vol. 39, p209, 1999) describing the record high fusion power experiments.

1984 - THE FIRST EXPERIMENTS IN JET

P.-H.REBUT, D.V.BARTLETT, G.BÄUMEL, K.BEHRINGER, R.BEHRISCH[1], E.BERTOLINI, C.BEST, R.J.BICKERTON, F.BOMBI, J.L.BONNERUE, A.BOSCHI, G.BRACCO[2], M.L.BROWNE, M.BRUSATI, A.BULLIARD, D.J.CAMPBELL, P.G.CAROLAN[3], J.CHRISTIANSEN, P.CHUILON, J.G.CORDEY, S.CORTI, A.E.COSTLEY, G.DECKER[4], K.J.DIETZ, D.F.DUCHS, G.DUESING, R.K.F.EMERY, W.W.ENGELHARDT , T.ERIKSSON, J.FESSEY, M.J.FORREST[3], C.FROGER, K.FULLARD, M.GADEBERG[5], A.GIBSON, R.GILL, A.GONDHALEKAR, C.GOWERS, B.J.GREEN, G.GROSSO[6], N.C.HAWKES[3], J.HEMMERICH, M.HUART, A.HUBBARD[7], C.A.HUGENHOLTZ[8], M.HUGUET, 0.N.JARVIS, B.E.JENSEN, E.M.JONES, G.E.KÄLLNE, J.C.KÄLLNE, L.de KOCK, H.KRAUSE[1], P.KUPSCHUS, J.R.LAST, E.LAZZARO, P.LOMAS, G.M.McCRACKEN[3], G.MAGYAR, F.K.MAST[1], M.MEAD , P.L.MONDINO, P.MORGAN, A.W.MORRIS[3], L.NICKESSON, H.NIEDERMEYER[1], P.NIELSEN, P.NOLL, J.PAILLÈRE, N.J.PEACOCK[3], M.PICK, J.P.POFFÉ, R.PRENTICE, C.RAYMOND, D.C.ROBINSON[3], R.ROSS, G.SADLER, J.SAFFERT, V.SCHMIDT, F.C.SCHÜLLER, K.SONNENBERG, M.F.STAMP. C.A.STEED, A.STELLA, P.E.STOTT, D.SUMMERS. A.TANGA, P.R.THOMAS, G.TONETTI[9], E.USSELMANN. P.VANBELLE, H.VANDERBEKEN , J.E.VANMONTFOORT, M.L.WATKINS. J.A.WESSON, T.WINKEL, V.ZANZA[2], J.ZWART.

1. Euratom-IPP Association, Institut für Plasmaphysik, Garching, Federal Republic of Germany.
2. Euratom-ENEA Association, Centro di Frascati. Italy.
3. Euratom-UKAEA Association, Culham Laboratory, Abingdon, Oxfordshire, UnitedKingdom.
4. University of Düsseldorf, Düsseldorf, Federal Republic of Germany.
5. Euratom-Riso Association, Riso National Laboratory, Roskilde, Denmark.
6. Euratom-CNR Associaion, Istituto di Fisica del Plasma, Milan, Italy.
7. Imperial College of Science and Technology, University of London, London,
8. Euratom-FOM Association. FOM Instituut voor Plasmafysica, Nieuwegein, Netherlands.
9. Euratom-Suisse Association, Centre de Recherches en Physique des Plasmas, Lausanne, Switzerland.

1992 - FUSION ENERGY PRODUCTION FROM A DEUTERIUM-TRITIUM PLASMA IN THE JET TOKAMAK

P.-H.REBUT, A.GIBSON, M.HUGUET, J.M.ADAMS[1], B.ALPER. H.ALTMANN, A.ANDERSEN[2], P.ANDREW[3], M.ANGELONE[4], S.ALI-ARSHAD, P.BAIGGER, W.BAILEY,B .BALET, P.BARABASCHI, P.BARKER, R.BARNSLEY[5], M.BARONIAN, D.V.BARTLETT, L.BAYLOR[6], A.C.BELL, G.BENALI, P.BERTOLDI, E.BERTOLINI, V.BHATNAGAR, A.J.BICKLEY, D.BINDER, H.BINDSLEV[2], T.BONICELLI, S.J.BOOTH, G.BOSIA, M.BOTMAN, D.BOUCHER, P.BOUCQUEY, P.BREGER, H.BRELEN, H.BRINKSCHULTE, D.BROOKS, A.BROWN, T.BROWN, M.BRUSATI, S.BR YAN, J.BRZOZOWSKI[7], R.BUCHSE[22], T.BUDD, M.BURES, T.BUSINARO, P.B UTCHER, H.BUTTGEREIT, C.CALDWELL-NICHOLS, D.J.CAMPBELL, P.CARD, G.CELENTANO, C.D.CHALLIS, A.V.CHANKIN[8], A.CHERUBINI, D.CHIRON, J.P.CHRISTIANSEN, P.CHUILON, R.CLAESEN, S.CLEMENT, E.CLIPSHAM, J.P.COAD, I.H.COFFEY[9], A.COLTON, M.COMISKEY[10], S.CONROY, M.COOKE, D.COOPER, S.COOPER, J.G.CORDEY, W.CORE, G.CORRIGAN, S.CORTI, A.E.COSTLEY, G.COTTRELL, M.COX[11], P.CRIPWELL[12], 0.Da COSTA, J.DAVIES, N.D AVIES, H.de BLANK, H.deESCH, L.deK OCK, E.DEKSNIS, F.DELVART, G.B.DENNE-HINNOV, G.DESCHAMPS, W.J.DICKSON[13], K.J.DIETZ, S.L.DMITRENKO, M.DMITRIEVA[14], J.DOBBING, A.DOGLIO, N.DOLGETTA, S.E.DORLING. P.G.DOYLE, D.F.DOCHS, H.DUQUENOY, A.EDWARDS, J.EHRENBERG, A.EKEDAHL, T.ELEVANT[7], S.K.ERENTS [11], L.-G.ERIKSSON, H.FAJEMIROKUN[12], H.FALTER, J.FREILING[15], F.FREVILLE, C.FROGER, P.FROISSARD, K.FULLARD, M.GADEBERG, A.GALETSAS, T.GALLAGHER, D.GAMBIER, M.GARRIBBA, P.GAZE, R.GIANNELLA, R.D.GILL, A.GIRARD, A.GONDHALEKAR, D.GOODALL[11], C.GORMEZANO, N.A.GOTTARDI, C.GOWERS, B.J.GREEN, B.GRIEVSON, R.HAANGE, A.HAIGH, C.J.HANCOCK, P.J.HARBOUR, T.HARTRAMPF, N.C.HAWKES[11], P.HAYNES[11], L.L.HEMMERICH, T.HENDER[11], J.HOEKZEMA, D.HOLLAND, M.HONE, L.HORTON, J.HOW, M.HUART, I.HUGHES, T.P.HUGHES[10], M.HUGON, Y.HUO[16], K.IDA[17], B.INGRAM, M.IRVING, J.JACQUINOT, H.JAECKEL, L.F.JAEGER, G.JANESCHITZ, Z.JANKOVICZ[18], 0.N.JARVIS, F.JENSEN, E.M.JONES, H.D.JONES, L.P.D.F.JONES, S.JONES[19], T.T.C.JONES, LF .JUNGER, F.JUNIQUE, A.KAYE, B.E.KEEN, M.KEILHACKER, G.J.KELLY, W.KERNER, A.KHUDOLEEV[21], R.KONIG, A.KONSTANTELLOS, M.KOVANEN[20], G.KRAMER[15], P.KUPSCHUS, R.LASSER, J.R.LAST, B.LAUNDY, L.LAURO-TARONI, M.LAVEYRY, K.LAWSON[11], M.LENNHOLM, J.LINGERTAT[22], R.N.LITUNOVSKI, A.LOARTE, R.LOBEL, PLOMAS , MLOUGHLIN , C.LOWRY, JLUPO , A.C.MAAS[15], J.MACHUZAC[19], B.MACKLIN, G.MADDISON[11], C.F.MAGGI[23], G.MAGYAR, W.MANDL[22], V.MARCHESE, G.MARCON, F.MARCUS, J.MART, D.MARTIN, E.MARTIN, R.MARTIN-SOLIS[24], P.MASSMANN, G.MATTHEWS, H.McBRYAN, G.McCRACKEN[11], J.McKIVITT, P.MERIGUET, P.MIELE, A.MILLER, J.MILLS, S.F.MILLS, P.MILLWARD, P.MILVERTON, E.MINARDI[4], R.MOHANT1[21], P.L.MONDINO, D.MONTGOMERY[26], A.MONTVAI[27], P.MORGAN, H.MORSI, D.MUIR, G.MURPHY, R.MYRNAS[28], F.NAVE, G.NEWBERT, M.NEWMAN, P.NIELSEN, P.NOLL, W.OBERT, D.O'BRIEN, J.ORCHARD, J.W.ROURKE, R.OSTROM, M.OTTAVIANI, M.PAIN, F.PAOLETTI, S.PAPASTERGIOU, W.PARSONS, D.PASINI, D.PATEL, A.PEACOCK, N.PEACOCK[11], R.LM.PEARCE, D.PEARSON[12], J.F.PENG[16], R.PEPEDESIL VA, G.PERINIC, C.PERRY, M.PETROV[21],

M.A.PICK, J.PLANCOULAINE, J-P.POFFÉ, R.PÖHLCHEN, F.PORCELLI, L.PORTE[13], R.PRENTICE, S.PUPPIN, S.PUTVINSKI[8], G.RADFORD[30], T.RAIMONDI, M.C.RAMOSDEANDRADE, R.REICHLE, J.REID, S.RICHARDS, E.RIGHI, F.RIMINI, D.ROBINSON[11], A.ROLFE, R.T.ROSS, L.ROSSI, R.RUSS, P.RUTTER, H.C.SACK, G.SADLER, G.SAIBENE, L.L.SALANAVE, G.SANAZZARO, A.SANTAGIUSTINA, R.SARTORI, C.SBORCHIA, P.SCHILD, M.SCHMID, G.SCHMIDT[31], B.SCHUNKE, S.M.SCOTT, LSERIO , A.SIBLEY, R.SIMONINI, A.C.C.SIPS, P.SMEULDERS, R.SMITH, R.STAGG, M.STAMP, P.STANGEBY[3], R.STANKIEWICZ[32], D.F.START, C.A.STEED, D.STORK, P.E.STOTT, P.STUBBERFIELD, D.SUMMERS, H.SUMMERS[13], L.SVENSSON, J.A.TAGLE[33], M.TALBOT, A.TANGA, A.TARONI, C.TERELLA, A.TERRINGTON, A.TESINI, P.R.THOMAS, E.THOMPSON, K.THOMSEN, F.TIBONE, A.TISCORNIA, P.TREVALION, B.TUBBING, P.VANBELLE, H.VANDERBEKEN , G.VLASES, M.VONHELLERMANN , T.WADE, C.WALKER, R.WALTON[31], D.WARD, M.L.WATKINS, N.WATKINS, J.WATSON, S.WEBER[34], J.WESSON, T.J.WUNANDS, J.WILKS, D.WILSON, T.WINKEL, R.WOLF, D.WONG, C.WOODWARD, Y.WU[35], M.WYKES, D.YOUNG, I.D.YOUNG, L.ZANNELLI, A.ZOLFAGHARI[19], W.ZWINGMANN.

1. Harwell Laboratory, UKAEA, Harwell, Didcot, Oxfordshire, UK.
2. Riso National Laboratory, Roskilde, Denmark.
3. Institute for Aerospace Studies, University of Toronto, Downsview, Ontario, Canada.
4. ENEA Frascati Energy Research Centre, Frascati, Rome, Italy.
5. University of Leicester, Leicester, UK.
6. Oak Ridge National Laboratory, Oak Ridge, TN, USA.
7. Royal Institute of Technology, Stockholm, Sweden.
8. I.V. Kurchatov Institute of Atomic Energy, Moscow, Russian Federation.
9. Queens University, Belfast, UK.
10. University of Essex, Colchester, UK.
11. Culham Laboratory, UKAEA, Abingdon, Oxfordshire, UK.
12. Imperial College of Science, Technology and Medicine, University of London, London, UK.
13. University of Strathclyde, Glasgow, UK.
14. Keldysh Institute of Applied Mathematics, Moscow, Russian Federation.
15. FOM-Institute for Plasma Physics “Rijnhuizen”, Nieuwegein, Netherlands.
16. Institute of Plasma Physics, Academia Sinica, Hefei, Anhui Province, China.
17. National Institute for Fusion Science, Nagoya, Japan.
18. Soltan Institute for Nuclear Studies, Otwock/Swierk, Poland.
19. Plasma Fusion Center, Massachusetts Institute of Technology, Boston, MA, USA.
20. Nuclear Engineering Laboratory, Lappeenranta University, Finland.
21. A.F. Ioffe Physico-Technical Institute, St. Petersburg, Russian Federation.
22. Max-PlanckInstitut ffir Plasmaphysik, Garching, Germany.
23. Department of Physics, University of Milan, Milan, Italy.
24. Universidad Complutense de Madrid, Madrid, Spain.

25. North Carolina State University, Raleigh. NC, USA.
26. Dartmouth College, Hanover, NH, USA.
27. Central Research Institute for Physics, Budapest, Hungary.
28. University of Lund, Lund, Sweden.
29. Laboratorio Nacional de Engenharia e Tecnologia Industrial, Sacavem, Portugal.
30. Institute of Mathematics, University of Oxford, Oxford, UK.
31. Princeton Plasma Physics Laboratory, Princeton University, Princeton, NJ, USA.
32. RCC Cyfronet, Otwock/Swierk, Poland,
33. Centro de Investigaciones Energdticas, Medioambientales y Tecnologicas, Madrid, Spain.
34. Freie Universitat. Berlin. Germany.
35. Insitute for Mechanics, Academia Sinica. Beijing, China.

1999 - HIGH FUSION PERFORMANCE FROM DEUTERIUM - TRITIUM PLASMAS IN JET.

S.ARSHAD, D.BAILEV, N.BAINBRIDGE., B.BALET. Y.BARANOV[4], P.BARKER, R.BARNSLEY[5], M.BARONIAN, D.V.BARTLETT, A.C.BELL, L.BERTALOT, E.BERTOLINI, V.BHATNAGAR, A.J.BICKLEY, H.BINDSLEV, K.BLACKLER, D.BOND, T.BONICELLI, D.BORBA[7], M.BRANDON, P.BREGER, H.BRELEN, P.BRENNAN, W.J.BREWERTON, M.L.BROWNE, T.BUDD, R.V.BUDNY[8], A.BURT, T.BUSINARO, M.BUZIO, C.CALDWELL-NICHOLS, D.CAMPLING, P.CARD, C.D.CHALLIS, A.V.CHANKIN, D.CHIRON. J.P.CHRISTIANSEN, P.CHUILON, D.CIRIC, R.CLAESEN, H.E.CLARKE, S.CLEMENT, I.COFFEY[9], S.CONROY[10], G.CONWAY[11], S.COOPER, J.G.CORDEY, G.CORRIGAN, G.COTTRELL, M.COX[9], S.J.COX, R.CUSACK, N.DAVIES, S.J.DAVIES, J.J.DAVIS, M.DEBENEDETTI. H.DEESCH, J.DEHAAS , E.DEKSNIS, N.DELIANAKIS, A.DINES, S.L.DMITRENKO, J.DOBBING. N.DOLETTA. S.E.DORLING. P.G.DOYLE, H.DUQUENOY, A.M.EDWARDS[9] A.W.EDWARDS, J.EGEDAL, J.EHRENBERG, A.EKEDAHL[12], T.ELEVANT[12], J.ELLIS, M.ENDLER[13], S.K.ERENTS[9], G.ERICSSON[10], L.-G.ERIKSSON, B ESPOSITO[6], HFAL TER, J.FARTHING, M.FICHTMÜLLER, G.M.FISHPOOL, K.FULLARD, M.GADEBER, L.GALBIATI, A.GIBSON, R.D.GILL, D.GODDEN, A.GONDHALEKAR, D.GOODALL[9], C.GORMEZANO, C.GOWERS, M.GROTH[14], K.GUENTHER, H.GUO, A.HAIGH, B.HAIST[15], C.J.HANCOCK, P.J.HARBOUR, N.C.HAWKES[9], N.P.HAWKES[1], J.L.HEMMERICH, T.HENDER[9], J.HOEKZEMA, L.HORTON, A.HOWMAN, M.HUART, T.P.HUGHES, F.HURD, G.T.A.HUYSMANS, C.INGESSON[16], B.INRAM, M.IRVING, J.JACQUINOT, H.JAECKEL, J.F.JAEGER, 0.N.JARVIS, M.JOHNSON, E.M.JONES, T.T.C.JONES, J.-F.JUNGER, F.JUNIQUE, C.JUPEN, J.KALLNE[10], A.KAYE, B.E.KEEN, M.KEILHACKER, W.KERNER, N.G.KIDD, S.KNIPE, R.KONIG, A.KOROTKOV, A.KRASILNIK OV[2], J.G.KROM, P.KUPSCHUS , R.LÄSSER, J.R.LAST, L.LAURO-TARONI, K.LAWSON[9], M.LENNHOLM, J.LINGERTAT, X.LITAUDON[17], T.LOARER, P.J.LOMAS, M.LOUGHLIN, C.LOWRY, A.C.MAAS[16], B.MACKLIN, C.F.MAGGI, M.MANTSINEN[18], V.MARCHESE, F.MARCUS, J.MART, D.MARTIN, G.MATTHEWS, H.McBRYAN, G.McCRACKEN,

P.A.McCULLEN, A.MEIGS, R.MIDDLETON, P.MIELE, F.MILANI, J.MILLS, R.MOHANTI, R.MONK, P.MORGAN, G.MURPHY, M.F.NAVE[7], G.NEWBERT, P.NIELSEN, P.NOLL, W.OBERT, D.O'BRIEN, M.O'MULLANE, E.OORD, R.OSTROM, S.PAPASTERGIOU, V.V.PARAIL, R.PARKINSON, W.PARSONS, B.PATEL, A.PAYNTER, A.PEACOCK, R.J.H.PEARCE, A.PEREVERENTSEV, M.A.PICK, J.PLANCOULAINE, 0.POGUTSE, R.PRENTICE, S.PUPPIN, G.RADFORD[19], R.REICHLE, V.RICCARDO, F.G.RIMINI, F.ROCHARD[17], A.ROLFE, A.L.ROQUEMORE[8], R.T.ROSS, A.ROSSI, G.SADLER, G.SAIBENE, A.SANTAGIUSTINA, R.SARTORI, R.SAUDERS, P.SCHILD, M.SCHMID, V.SCHMIDT, B.SCHOKKER[16], B.SCHUNKE, S.M.SCOTT, S.SHARAPOV, A.SIBLEY, M.SIMON, R.SIMONINI, A.C.C.SIPS, P.SMEULDERS, P.SMITH, R.SMITH, F.SÖLDNER, J.SPENCE, E.SPRINGMANN, R.STAGG, M.STAMP, P.STANGEBY[20], D.F.START, D.STORK, P.E.STOTT, J.D.STRACHAN[8], P.STUBBERFIELD, D.SUMMERS, L.SVENSSON, P.SVENSSON, A.TABASSO[3], M.TABELLINI, J.TAIT, A.TANGA, A.TARONI, C.TERELLA, P.R.THOMAS, K.THOMSEN, E.TRANEUS[10], B.TUBBING, P.TWYMAN, A.VADGAMA, P.VANBELLE, G.C.VLASES, M.VON HELLERMANN, T.WADE, R.WALTON, D.WARD, M.L.WATKINS, N.WATKINS, M.J.WATSON, M.WHEATLEY, D.WILSON, T.WINKEL, D.YOUNG, I.D.YOUNG, Q.YU[21], K.-D.ZASTROW, W.ZWINGMANN.

1. UKAEA. Harwell. Didcot. Oxfordshire. UK.
2. TRINITI, Troitsk. Moscow, Russian Federation.
3. Imperial College, University of London, UK.
4. A.F. loffe Institute, St. Petersburg, Russian Federation.
5. University of Leicester, Leicester. UK.
6. ENEA, CRE Frascati, Rome, Italy.
7. IST, Centro de Fusao Nuclear, Lisbon, Portugal.
8. Princeton Plasma Physics Laboratory, Princeton, New Jersey, USA.
9. UKAEA Culham Laboratory, Abingdon, Oxfordshire, UK.
10. Department of Neutron Research, Uppsala University, Sweden.
11. University of Saskatchewan, Saskatoon, Canada.
12. Royal Institute of Technology, Stockholm, Sweden.
13. Max-Planck-Institut für Plasmaphysik, Garching, Germany.
14. University of Manchester Institute of Science and Technology, Manchester, Lancashire, UK.
15. FZ, Jullich, Germany.
16. FOM Instituut voor Plasmafysica, Nieuwegein, Netherlands.
17. CEA Cadarache, St. Paul-lez-Durance, France.
18. Helsinki University of Technology, Espoo, Finland.
19. Institute of Theoretical Physics, University of Oxford, Oxfordshire, UK.
20. Institute for Aerospace Studies, University of Toronto, Ontario, Canada.
21. Institute of Plasma Physics, Hefei, China.